THE EFFECT OF POLYMER CHAIN MOBILITY ON PROTEIN ADSORPTION AND SUBSEQUENT CELL BEHAVIOR

by

Moira Catherine Vyner

A thesis submitted to the Graduate Program in Chemical Engineering

in conformity with the requirements for

the Degree of Doctor of Philosophy

Queen's University

Kingston, Ontario, Canada

(November, 2015)

Abstract

Many cell types are known to respond to the stiffness of polymeric biomaterial substrates. However, the mechanism by which cells sense this stiffness is still under investigation. Cell response to a material is believed to be mediated by the composition and/or configuration of the protein layers that adsorb to the biomaterial surfaces prior to cell contact. It is, therefore, hypothesized that polymer stiffness, and specifically, the flexibility of the polymer chains at the polymer-aqueous interface, affects the composition and configuration of the adsorbed protein layer, which is responsible for influencing cell response. In this thesis, two biomaterials known to induce stiffness dependent cell responses are used as model systems to determine whether polymer chain flexibility influences cell behavior via differences in the protein adsorption. The first is an elastomer formed from an acrylated *star*-poly(D,L-lactide-co-ϵ-caprolactone) (ELAS) which has been shown to support higher NIH3T3 fibroblast proliferation on a less stiff version of the elastomer despite minimal differences in surface chemistry. The second is poly(trimethylene carbonate) (PTMC) which has been shown to degrade *in vivo* via macrophage mediated erosion at molecular weights higher than 100 kg/mol, but does not degrade at molecular weights of less than 70 kg/mol, despite no difference in surface chemistry. Quantity and viscoelastic properties of protein layers adsorbed from individual solutions of albumin, immunoglobulin G, fibronectin and vitronectin, as well as fetal serum and adult plasma supplemented environments were compared on different stiffnesses of these materials to determine whether polymer chain flexibility affects protein adsorption. Polymer stiffness was found to affect quantity and conformation of individually adsorbed protein layers as well as the composition of protein layers adsorbed from serum and plasma

supplemented media. Surface adsorbed fetuin A and vitronectin were identified and proposed to be responsible for influencing fibroblast proliferation and macrophage behavior, respectively. It was concluded that the flexibility of the polymer chains at the polymer-aqueous interface affects the arrangement of water molecules at the interface and alters the entropic gain associated with protein adsorption, thus favoring the adsorption of different types and adsorbed conformation of proteins which influences the subsequent cell response to the biomaterial.

Acknowledgements

Firstly, I would like to thank Dr. Brian Amsden who has guided my research throughout this PhD. You have improved my skills as a both researcher and as a writer. Thank you for your endless support and patience.

My heartfelt gratitude goes to my parents, Liz and Stan. You have been my constant support throughout this PhD and throughout my life. Nothing have done or will do would have been possible without you. Thank you.

Thank you to Julian Chesterman, my oldest friend as a graduate student. We started together, attended classes together, researched together, and have watched many other students, as well as a decent part of our lives, pass us by. Without a doubt, I would not be the person I am, nor the researcher I am, had I not met you.

And finally, thank you to the all the students past and present who have passed through the Amsdenlab. Thank you for your friendship, for brightening my day, and for helping me with my research. Special thanks go to Dale Marecak, who never left an item unordered or a group meeting unscheduled. My research has benefitted from your invaluable expertise. Thanks also to Roshni, Fiona, Sara, Shadi, Fei, Stuart, Nick and Ginger and my undergrad students Anne and Anand. This experience would not have been as enjoyable or as memorable without you. I will remember all of you.

Table of Contents

Abstract ii
Acknowledgements iv
Table of Contents v
List of Figures x
List of Tables xiii
List of Abbreviations xiv
Chapter 1 Introduction 1
1.1 The Research Problem – Cell Response to Material Stiffness 1
1.2 Biomaterial-Cell Interactions 2
1.2.1 Tissue Cell Attachment Mechanisms 2
1.2.2 Monocyte/macrophage Adhesion and Activation 4
1.3 Protein Adsorption to Polymeric Biomaterial Surfaces 5
1.3.1 The Polymer-Water Interface 5
1.3.2 Protein Adsorption 7
1.4 Material Stiffness, Protein Adsorption and Cell Response 8
Chapter 2 Literature Review 10
2.1 Introduction 10
2.2 Mechanisms By Which Cells Sense Biomaterial Stiffness 11
2.2.1 Sensing of Biomaterial Stiffness via Direct Attachment 11
2.2.2 Sensing Stiffness via the Adsorbed Protein Layer 13
2.3 The Effect of Polymer Chain Mobility on Protein Adsorption 16
2.4 Introduction to the Thesis Project 18
2.5 The Effect of ELAS Stiffness on Cell Proliferation 18
2.5.1 Elastomers Formed from Acrylated *Star* Poly(D,L-lactide-*co*-ε-caprolactone) 19
2.5.2 NIH3T3 Fibroblasts 21
2.5.3 RAW 264.7 Macrophages 22
2.6 The Effect of PTMC Stiffness on RAW 264.7 Macrophage Mediated Erosion 23
2.7 Summary 24
Chapter 3 Scope 25
3.1 Hypotheses 25
3.2 Objectives 26

3.2.1 Objective 1: The Influence of Polymer Chain Flexibility of ELAS on Individual Protein Adsorption 26
3.2.2 Objective 2: The Influence of Polymer Chain Flexibility of ELAS on Competitive Protein Adsorption 27
3.2.3 Objective 3: The Influence of PTMC Polymer Chain Flexibility on Macrophage Behavior and Enzymatic Adsorption and Conformation. 27
3.2.4 Objective 4: The Influence of Protein Adsorption and Subsequent Macrophage Activity on PTMC and ELAS surfaces 28
Chapter 4 The Effect of Elastomer Chain Flexibility on Protein Adsorption 29
4.1 Completed Objectives 29
4.2 Introduction 30
4.3 Materials and Methods 32
4.3.1 Elastomer Fabrication 32
4.3.2 Contact Angle Measurements 33
4.3.3 Glass Transition Temperature Measurements 33
4.3.4 Water Absorption Measurement 34
4.3.5 Atomic Force Microscopy 34
4.3.6 Mechanical Testing 34
4.3.7 Culture of NIH3T3 Fibroblasts 35
4.3.8 Radiolabeled Protein Adsorption 36
4.3.9 QCM-D Sensor Coating 36
4.3.10 QCM-D Protein Adsorption 37
4.3.11 Surface Plasmon Resonance 38
4.3.12 ATR-FTIR 39
4.3.13 Statistics 40
4.4 Results and Discussion 40
4.4.1 Fibroblast Attachment and Proliferation 42
4.4.2 Protein Adsorption 43
4.5 Conclusion 53
Chapter 5 Polymer Chain Flexibility-Induced Differences in In Fetuin A Adsorption and its Implications for Cell Attachment and Proliferation 54
5.1 Objectives Completed 54
5.2 Introduction 55
5.3 Materials and Methods 58

5.3.1 Microsphere Preparation 59
5.3.2 Protein Adsorption 59
5.3.3 Protein Identification and Quantitation 60
5.3.4 QCM-D Sensor Coating 62
5.3.5 QCM-D Measurements 63
5.3.6 Surface Plasmon Resonance 64
5.3.7 Cell culture 65
5.4 Statistics 66
5.5 Results 67
5.5.1 NIH3T3 fibroblast culture with FBS and adult bovine plasma 67
5.5.2 Quantitative Proteomics 68
5.5.3 Fetuin Adsorption 71
5.5.4 Fetuin supplemented fibroblast culture 73
5.6 Discussion 76
5.7 Conclusions 81
Chapter 6 The Effect of Poly(trimethylene carbonate) Molecular Weight on Macrophage Behavior and Enzyme Adsorption and Conformation 82
6.1 Objectives Completed 82
6.2 Introduction 83
6.3 Materials and Methods 85
6.3.1 PTMC Synthesis 85
6.3.2 Contact Angle Measurements 86
6.3.3 Glass Transition Temperature Measurements 86
6.3.4 Water Uptake Measurement 87
6.3.5 Enzymatic Degradation of pTMC 87
6.3.6 Macrophage Culture 88
6.3.7 Macrophage Culture Analysis 88
6.3.8 Scanning Electron Microscopy 89
6.3.9 QCM-D Sensor Coating 89
6.3.10 QCM-D Protein Adsorption 90
6.3.11 Surface Plasmon Resonance 90
6.3.12 ATR-FTIR 91
6.3.13 Atomic Force Microscopy 91
6.3.14 Dual Indentation Testing 92

6.3.15 Nanoindentation Testing 92
6.3.16 Statistics 93
6.4 Results and Discussion 93
6.4.1 Polymer Characterization 93
6.4.2 Macrophage Behavior 95
6.4.3 Enzymatic Degradation 97
6.4.4 Enzyme Adsorption 98
6.4.5 Surface Water Absorption 102
6.5 Conclusion 104
Chapter 7 The Effect of Protein Adsorption and Subsequent Macrophage Activity on Acryl *star*-Poly(D,L lactide-co-ϵ-caprolactone) Elastomer and Poly(trimethylene carbonate) Degradation 106
7.1 Completed Objectives 106
7.2 Introduction 107
7.3 Materials and Methods 110
7.3.1 Polymer Fabrication 110
7.3.2 Nanoindentation of ELAS 5000 111
7.3.3 Scanning Electron Microscopy 112
7.3.4 Macrophage Adhesion and Activity on 100PTMC and ELAS 5000 113
7.3.5 Enzymatic and Oxidative Degradation 114
7.3.6 Proteomics 114
7.3.6.1 Microsphere fabrication 115
7.3.6.2 Plasma Adsorption to Microspheres 115
7.3.6.3 Proteomics Analysis 116
7.3.7 Statistics 117
7.4 Results 117
7.4.1 Surface Characterization 117
7.4.2 Scanning Electron Microscopy 118
7.4.3 Oxidative and Enzymatic Degradation of 100PTMC and ELAS 5000 119
7.4.4 Macrophage Adhesion and Activity on 100PTMC and ELAS 5000 120
7.4.5 Protein Adsorption to 100PTMC and ELAS 5000 121
7.5 Discussion 123
7.5.1 Degradation of 100PTMC and ELAS 5000 123
7.5.2 Protein Adsorption to 100PTMC and ELAS 5000 124
7.6 Conclusion 127

Chapter 8 Conclusions and Recommendations for Future Work 128
8.1 Conclusions 128
8.1.1 The Effect of Polymer Chain Flexibility on Protein Adsorption 128
8.1.2 The Effect of Polymer Chain Flexibility on Water Adsorption/Absorption 129
8.1.3 Polymer Chain Flexibility, Fetuin A Adsorption and Subsequent Cell Behavior 130
8.1.4 Individual and Competitive Protein Adsorption and the Non-Physiologic Nature of FBS 131
8.1.5 Conflicts in RAW 264.7 Macrophage Results 132
8.2 Recommendations for Future Work 134
8.2.1 Improvements on Relative Quantitation Proteomics 134
8.2.2 Other Uses of Relative Quantitation Proteomics for Analysis of Cell Response 135
8.2.2.1 Cellular Modification of Biomaterial Surfaces 135
8.2.2.2 Relative Quantitation Proteomics for Analysis of Cell Response 135
8.2.3 Additional Adsorbed Protein Conformation Studies 136
8.2.4 Macrophage Activation by Biomaterial Surfaces 137
8.2.5 Macrophage Cell Lines vs. Primary Cells 138
References 141
Appendix Supplemental Data and Figures 157
A.1 Representative NMR Spectra: 157
A.1.1 Acrylated *star* poly(D,L lactide-*co*-ϵ-caprolactone) (ASCP) 157
A.1.2 Poly(trimethylene carbonate) 159
A.2 Atomic Force Microscopy Nano-indentation 160
A.3 SEM Micrographs of microspheres fabricated from ELAS 2000, ELAS 5000, and 100PTMC 162

List of Figures

Figure 1.1: Differences in polymer stiffness and polymer chain flexibility may affect the organization of water molecules at the polymer-aqueous interface. Differences in water molecule organization affect the release of water molecules as a protein adsorbs. 6

Figure 2.1: A: Cells may be able to respond to substrate stiffness directly by unfolding proteins and exerting traction forces on the polymer surface. B: Material stiffness may influence the characteristics of the adsorbed protein layer which in turn influences cell response. 14

Figure 2.2: Molecular structure of acrylated star poly (D,L lactide-co-ϵ-caprolactone) (ASCP) with repeating units m = D,L-lactide and n = ϵ-caprolactone. 20

Figure 2.3: Molecular structure of poly(trimethylene carbonate) (PTMC) 21

Figure 4.1: Top: Representative curves of QCM-D data. ΔFrequency and ΔDissipation at the 5th, 7th and 9th overtone for albumin adsorption to ELAS 5000 over 12 hours. Bottom: Representative curves of SPR response data from 4 flowcells (Fc) for serum adsorption to ELAS 5000 over 4000 seconds. 39

Figure 4.2: Fibroblast attachment and proliferation on ELAS 2000, ELAS 5000, and TCPS surfaces over 14 days. *p<0.05 compared to ELAS 2000 surface. **p<0.05 compared to both elastomer surfaces. Confluence was reached on TCPS surfaces by 7 days (n=6) 43

Figure 4.3: A: Mass of protein adsorbed to ELAS 2000 and ELAS 5000 surfaces; B: Thickness of protein layers adsorbed to ELAS 2000 and ELAS 5000 surfaces; C: Shear modulus of protein layers adsorbed to ELAS 2000 and ELAS 5000 surfaces; D: Shear viscosity of protein adsorbed to ELAS 2000 and ELAS 5000 surfaces.*p<0.05 compared to ELAS 2000, (n=3). 45

Figure 4.4: Possible configurations of fibronectin (see Table 4.3) adsorbed to the elastomer surfaces. Top: "On end" adsorption of fibronectin on ELAS 5000 allows for more protein as well as a less stiff protein layer. Bottom: Adsorption of fibronectin on ELAS 2000 in a flattened orientation restricts available space and forms a more rigid layer. 48

Figure 4.5: ATR-FTIR scans of ELAS 2000 and ELAS 5000 incubated in water for 0, 1, 4, and 24 hours. Top: full spectrum; Lower left: expansion of water peak at 3350 cm-1 (stretching); Lower right: expansion of water peak at 1650 cm-1 (bending) 50

Figure 5.1: NIH3T3 fibroblast number when cultured on E2 and E5 surfaces over 14 days in (A) 10% FBS supplemented DMEM (reprinted with permission from Elsevier from Vyner *et al.*, 2013 [80]) and (B) 10% adult bovine plasma supplemented DMEM. *p < 0.05 compared to E2 surface. **p < 0.05 compared to both E2 and E5 surfaces (n=6) 67

Figure 5.2: Mass and viscoelastic properties of the fetuin A layer adsorbed to the E2 and E5 surfaces from solutions of 2 mg/mL and 20 mg/mL fetuin A in PBS. (A) Fetuin A layer mass, (B) thickness, (C) shear modulus, and (D) viscosity. *p < 0.05 compared to E2 surface, (n=5). 72

Figure 5.3: NIH3T3 fibroblast number when cultured over 14 days on the E2 and E5 surfaces in DMEM supplemented with (A) 10% plasma, 2 mg/mL fetuin A and (B) 2 mg/mL fetuin A, only. *p < 0.05 compared to non-fetuin A group, **p < 0.05 compared to E2 surface, (n=6)..... 73

Figure 5.4: NIH3T3 cell number when cultured over 14 days on the E2 and E5 surfaces in DMEM supplemented with (A) fetuin A (2 mg/mL), FGF-2 (37 pg/mL) and 10% plasma or (B) fetuin A (2 mg/mL) and FGF-2 (37 pg/mL), only. *p < 0.05 compared to E2 surface, **p < 0.05 compared to E5 + FGF + P and E5 + P, (n=6). 75

Figure 6.1: SEM images of 60PTMC and 100PTMC at days 1 and 14 with macrophages removed. No degradation is observed on the 60PTMC surface at day 14, while significant degradation is observed on the 100PTMC surface, evidenced by the presence of cavities on the surface..... 95

Figure 6.2: Macrophage attachment and proliferation (A), superoxide anion secretion per cell (B), Reactive oxygen species secretion per cell (C), and esterase secretion per cell (D) over 14 days on 60PTMC, 100PTMC and TCPS. *p<0.05, (n=6). 96

Figure 6.3: Degradation of 60PTMC and 100PTMC by cholesterol esterase (CE) and lipase (L), (n=3)..... 97

Figure 6.4: QCM-D frequency (F5) and dissipation (D5) data (5^{th} overtone) for the adsorption of cholesterol esterase over 96 h (A) and 30 min (C) and lipase over 24 h (B) and 30 min (D) on 60PTMC and 100PTMC. 99

Figure 6.5: Mass (A), thickness (B), shear modulus (C) and viscosity (D) of cholesterol esterase and lipase adsorbed to 60PTMC and 100PTMC surfaces. *p<0.05, (n=3). 101

Figure 6.6: ATR-FTIR scans of 60PTMC (top group) and 100PTMC (bottom group) incubated in water for 0 min, 15 min, 30 min, 1 h, 2.5 h, 6 h, 24 h, 5 days and 7 days (lines top to bottom)..... 102

Figure 7.1: RAW 264.7 monocyte-macrophage degradation of 100PTMC and ELAS 5000 over 14 days of plasma supplemented culture (scalebar = 50 μm). 119

Figure 7.2: A: Oxidative degradation of 100PTMC and ELAS 5000. B: Enzymatic degradation of 100PTMC and ELAS 5000 by cholesterol esterase and lipase, (n=3)..... 119

Figure 7.3: Number and degradative species secretion of RAW 264.7 cells cultured on 100PTMC, ELAS 5000 and tissue culture polystyrene (TCPS) surfaces. A: Cell number. B: Reactive oxygen species (excluding superoxide anion) secretion per cell. C: Superoxide anion secretion per cell. D: Esterase secretion per cell. *p<0.05 compared to 100PTMC, **p<0.05 compared to 100PTMC and ELAS 5000, (n=6). 121

Figure 7.4: Proposed schematic for the influence of polymer chain flexibility and surface hydration on protein adsorption. Polymer chain flexibility influences the organization of water molecules bound to and around the polymer chains. This difference in organization affects the amount of bound water freed from the surface upon protein adsorption, affecting the preferred adsorbed conformation of the adsorbed protein. 126

Figure A.1: Representative NMR spectrum of star poly(D,L lactide-co-ϵ-caprolactone) (SCP) in dDMSO 157

Figure A.2: Representative NMR spectrum of acrylated *star* poly(D,L lactide-*co*-ϵ-caprolactone) (ASCP) in dDMSO with peak assignments 158

Figure A.3: Representative NMR spectrum of poly(trimethylene carbonate) in $CDCl_3$ 159

Figure A.4: Representative force-displacement curve for nanoindentation of PTMC 160

Figure A.5: Representative force-displacement curve for nanoindentation of ELAS 160

Figure A.6: SEM micrographs of ELAS 2000 microspheres 162

Figure A.7: SEM micrograph of ELAS 5000 microspheres 163

Figure A.8: SEM micrograph of 100PTMC microspheres 163

List of Tables

Table 4.1: Summary of elastomer sample preparation methods and preconditioning 41

Table 4.2: Bulk and surface properties of dry and wet ELAS 2000 and ELAS 5000..... 41

Table 4.3: Physical properties of the proteins examined 43

Table 5.1: Media supplementation for cell culture experiments..... 65

Table 5.2: Ratios (E5:E2) of proteins that adsorbed from FBS supplemented media 68

Table 5.3: Ratios (E5:E2) of proteins that adsorbed from adult bovine plasma suppl. media..... 69

Table 6.1: Bulk and surface properties of dry and wet 60PTMC and 100PTMC..... 94

Table 7.1: Surface and bulk material properties of 100PTMC and ELAS 5000 118

Table 7.2: Ratio of protein adsorbed from plasma suppl. media to ELAS 5000 : 100PTMC 122

Table A.1: Bulk and surface moduli of dry and hydrated ELAS and PTMC 161

List of Abbreviations

M1	Classically activated macrophages
M2	Alternatively activated macrophages
ASCP	Acrylated *star* poly(D,L lactide-*co*-ϵ-caprolactone
ELAS 2000	Elastomer fabricated from ASCP of 2000 g/mol
ELAS 5000	Elastomer fabricated from ASCP of 5000 g/mol
E2	ELAS 2000
E5	ELAS 5000
PTMC	Poly(trimethylene carbonate)
60PTMC	Poly(trimethylene carbonate) of 60 kg/mol
100PTMC	Poly(trimethylene carbonate) of 100 kg/mol
ECM	Extra-cellular matrix
LPS	Lipopolysaccharide
ROS	Reactive oxygen species
FBGC	Foreign body giant cell
PEG	Poly(ethylene glycol)
MSC	Mesenchymal stem cell
PLGA	Poly(lactide-*co*-glycolide)
PCL	Poly(caprolactone)
RGD	Arginine-glycine-aspartic acid
T_g	Glass transition temperature (midpoint)
PDMS	Poly(dimethylsiloxane)
DSC	Differential scanning calorimetry
AFM	Atomic force microscopy
SPR	Surface plasmon resonance

QCM-D	Quartz crystal microbalance with dissipation
ATR-FTIR	Attenuated total reflectance-fourier transform infrared spectroscopy
DMPA	2,2-dimethoxy-2-phenyl-acetophenone
UV	Ultraviolet light
DMEM	Dulbecco's modified Eagle medium
PBS	Phosphate buffered saline
FBS	Fetal bovine serum
TCPS	Tissue culture polystyrene
IgG	Immunoglobulin G
LC-MS/MS	Liquid chromatography – tandem mass spectrometry
FGF-2	Basic fibroblast growth factor
DMAP	Dimethylaminopyridine
H^1-NMR	Proton nuclear magnetic resonance
SEM	Scanning electron microscopy
SDS	Sodium dodecyl sulphate
HPLC	High performance liquid chromatography
IGF	Insulin-like growth factor
TGF-β1	Transforming growth factor – beta 1
PEC	Poly(ethylene carbonate)
DCM	Dichloromethane
pNP	Para-nitrophenol
pNPA	Para-nitrophenyl Acetate
R_q	Mean roughness
MMPs	Matrix metalloproteinases
IL	Interleukin

TEA	Triethylamine
THF	Tetrahydrofuran
M_n	Number average molecular weight

Chapter 1

Introduction

1.1 The Research Problem – Cell Response to Material Stiffness

Biodegradable, elastomeric polymers are currently being investigated as materials for tissue engineering scaffolds. They are considered promising materials for this purpose due to their chemical and mechanical properties, which can be modified to approximate those of many soft tissues [1,2]. A functional biomaterial scaffold should provide structural support (if needed) at the site of injury while supporting cellular growth, minimizing inflammation, and directing cellular behavior towards healing and restoring natural function to the injured site [3]. Therefore, the investigation of the chemical and mechanical properties of biomaterial polymers with respect to their ability to direct cellular response is the subject of continued study.

The behavior of many types of cells including tissue cells [4], monocytes/macrophages [5–8], and stem cells [9] is known to depend on the stiffness of the substrate on which they are grown [10], despite minimal differences in surface chemistry affected by properties such as crosslink density or crystallinity. Such behaviors include differences in attachment [4] and proliferation [11], cytoskeleton organization [12], motility [13], and differentiation [9]. The means by which cells sense and/or respond to material stiffness, however, is still under investigation.

Cellular behavior in response to an implanted biomaterial is believed to be influenced by the proteins that adsorb to the biomaterial surface [14,15]. Protein adsorption is considered to be the first biological event that occurs after biomaterial implantation, reaching equilibrium before cells make contact with the implant and effectively "shielding" the material from direct cellular interaction [16]. The composition and configuration of the adsorbed protein layer is, in turn, influenced by the surface properties of the biomaterial [17,18], which impacts which proteins adsorb to the surface and their respective conformations and effectively, the surface to which the cells respond [14].

Since material stiffness is able to influence cellular response, and cellular response is believed to be mediated by the adsorbed protein layer, the central hypothesis of this thesis is that material stiffness, itself, influences the composition or configuration of the adsorbed protein layer. There are few studies that investigate the connection between polymer stiffness and protein adsorption, or possible mechanisms therein, primarily due to the challenge of fabricating materials of varying stiffness while still maintaining similar surface chemistries. A better understanding of how material stiffness affects protein adsorption and subsequent cell behavior may allow for the design or modification of biomaterials to better direct cellular behavior, tissue integration and healing.

1.2 Biomaterial-Cell Interactions

1.2.1 Tissue Cell Attachment Mechanisms

Most tissue cells (e.g. fibroblasts, smooth muscle cells, etc.) are anchorage dependent and require secure attachment to their substrate in order to live, proliferate and function [10].

Tissue cells attach to biomaterial substrates primarily via integrin binding mechanisms [11]. Integrins are heterodimeric transmembrane receptors found in cells, which bind to specific peptide sequences found in proteins that comprise the extracellular matrix (ECM) (e.g. fibronectin, laminin) [19]. Integrins function synergistically with syndecans, cell membrane receptors that possess long glycosaminoglycan chains that act as receptors for both ECM proteins and growth factors [20]. The binding of multiple integrin attachments triggers a signaling cascade, which induces the formation of focal adhesions [21], large attachment structures capable of mechanotransduction between the ECM and the cell [22]. Beyond integrins, cells also possess other membrane receptors that bind to ECM proteins and regulate cell adhesion and signaling such as collagen receptors (discoidin domain receptors) [23], laminin receptors [24], and annexins [25].

Surfaces of implanted biomaterials, however, usually possess no such peptide sequences until proteins adsorb from the surrounding environment (plasma, serum supplemented media, and so on). Specifically, cellular attachment to biomaterials is believed to be mediated by the quantity of adsorbed proteins that contain sequences for integrin binding, such as fibrinogen, fibronectin and vitronectin [19]. Because integrins attach to specific peptide sequences within these adsorbed proteins, proteins must be adsorbed to surfaces in conformations such that their integrin binding peptide sequences are exposed and available to the receptors of an approaching cell [26]. Materials that adsorb very little protein (e.g. polyethylene glycol (PEG)) are known to resist cell attachment and induce a muted biological response [24].

1.2.2 Monocyte/macrophage Adhesion and Activation

Macrophages are white blood cells that form part of the innate immune system. Macrophages are primarily derived from monocytes which circulate in the blood before migrating into surrounding tissues in response to inflammatory signals where they differentiate into macrophages [27], though some macrophages reside permanently in various tissues including the liver, lung, spleen and bone marrow [28]. Macrophages fulfill multiple functions; classically activated macrophages (M1) are phagocytic cells whose function is to engulf and destroy particulates (e.g. microbes, cellular debris, biomaterials), whereas alternatively activated macrophages (M2) are associated with wound healing and tissue remodeling [29]. Macrophages may be classically activated by stimulant molecules such as lipopolysaccharide (LPS), found in the membrane of gram negative bacteria, [30] or by the complement activation pathway, where particulate surfaces are opsonized by complement or immunoglobulin molecules, inducing a phagocytotic response from the macrophages [31]. The macrophages then degrade the engulfed particles by secreting reactive oxygen species (ROS) and degradative enzymes [29]. When an implanted material is too large for a macrophage to engulf, frustrated phagocytosis occurs; adherent macrophages may fuse into foreign body giant cells (FBGC) [27] and release degradative species into the space between the cell membrane and the material [32] in an attempt to degrade the material.

Monocytes/macrophage response to biomaterials is believed to be mediated by proteins adsorbed to the biomaterial surface, which may affect monocyte adhesion and differentiation [33]. Monocyte/macrophage adhesion to biomaterials is mediated by integrins (e.g. Mac-1) and Fc receptors [34], which bind to adsorbed fibronectin, complement C3 and immunoglobulins [27]. Evidence of macrophage activation including chemokine secretion [35]

and FBGC formation [36] have been shown to differ based on the type and conformation [37] of the protein present on the material surface.

1.3 Protein Adsorption to Polymeric Biomaterial Surfaces

1.3.1 The Polymer-Water Interface

The first event after implantation of a polymeric biomaterial into an aqueous environment (i.e. *in vivo* or *in vitro* culture), is the adsorption and absorption of water molecules onto and into the material surface [14]. Due to the continuous mobility of polymer chains at the surface, water both adsorbs to and around the chains forming an interphase region at the biomaterial surface, hypothesized by Vogler to be "comprised of continuously changing component concentrations" and "a zone of solute/solvent enrichment near to but not bound to the surface" [38] (Figure 1.1).

The organization of the water molecules within this interphase region depends on both the presence of hydrophilic functionalities within the polymer structure and the flexibility of the polymer chains. If numerous functional groups capable of forming hydrogen bonds exist and the polymer has flexible polymer chains, as is the case with PEG, water molecules will form strong bonds with the polymer chains, and the polymer chains will possess a high mobility and extend far into the aqueous medium [39]. Highly hydrophilic crosslinked materials such as PEG will form hydrogels, where water molecules penetrate the material and associate with the polymer chains throughout the bulk of the material. Hydrophobic polymers have fewer hydrophilic functionalities. Therefore, fewer water molecules will directly

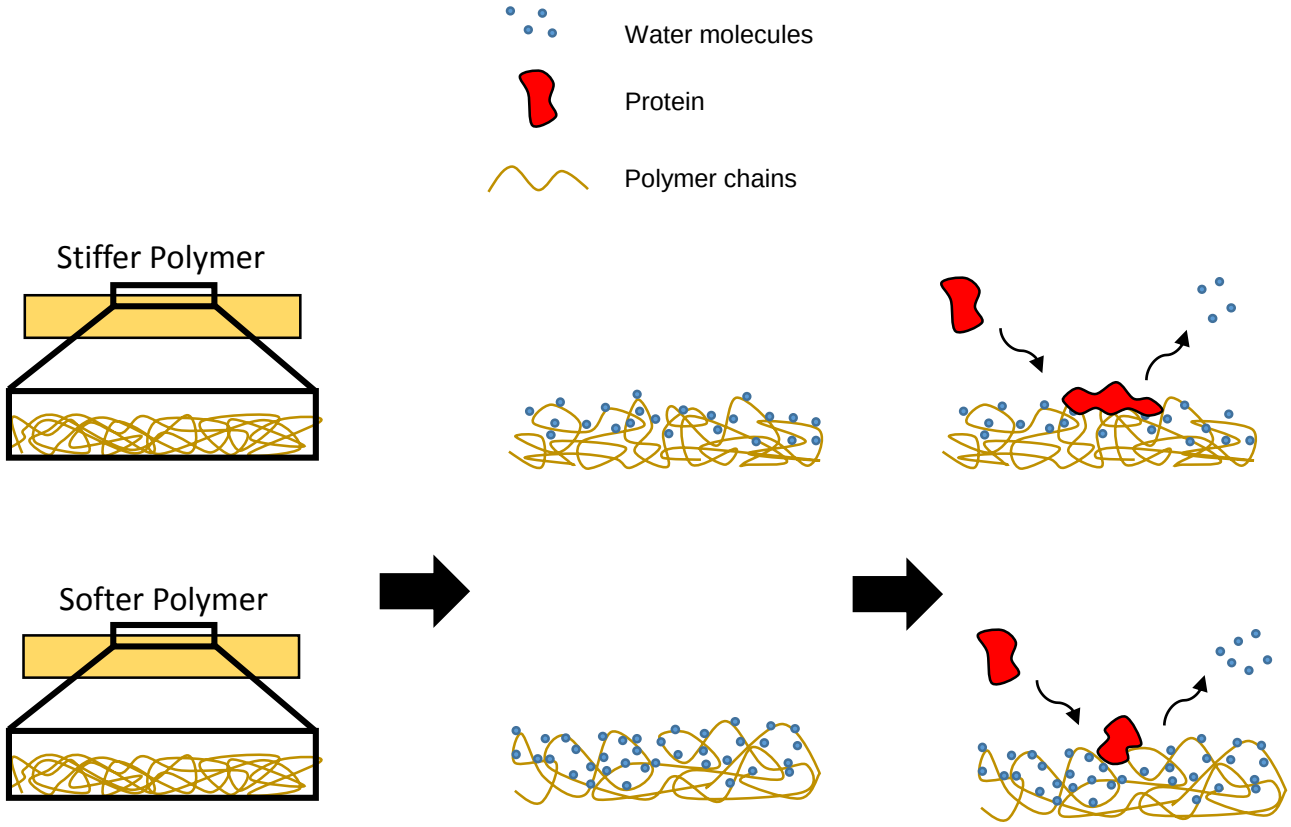

Figure 1.1: Differences in polymer stiffness and polymer chain flexibility may affect the organization of water molecules at the polymer-aqueous interface. Differences in water molecule organization affect the release of water molecules as a protein adsorbs.

associate with the polymer chains and the depth of water penetration at the surface will be shallow. However, if the polymer chains are mobile (i.e. the material is above its glass transition temperature) there will exist some region at the material-aqueous interface where polymer chains protrude into the aqueous media and water molecules will penetrate the polymer surface, forming a super-hydrated zone. Even very hydrophobic surfaces such as poly(dimethyl siloxane) (PDMS) [40] have been shown to adsorb some water in aqueous environments. Similarly, crosslinked or semi-crystalline materials will have lower polymer chain mobility's when compared with the same material when it is uncrosslinked. The crosslinks/crystals effectively either covalently or physically bind polymer chains to each other

and restrict the polymer chain's movement at the crosslink/crystal site. However, the polymer chains at the interface between such crosslinks will still protrude into the aqueous media, and develop an interphase, superhydrated layer.

1.3.2 Protein Adsorption

The formation of the biomaterial-water surface interphase region may influence protein adsorption from the surrounding environment to the biomaterial surface [41]. Protein adsorption is primarily an entropically driven phenomenon [18]. The adsorption of protein at the biomaterial-water interface displaces water molecules both bound to the protein and present at the biomaterial surface, thereby increasing the entropy of the system. Hydrophilic polymers, which tend to form strong hydrogen bonds with water molecules (e.g. PEG, hydrogels), also resist protein adsorption due to the unfavorable energy penalty of breaking the hydrogen bonds and freeing the bound water [16].

Proteins are amphiphilic, asymmetrical molecules. In aqueous solution, they exist in a roughly globular shape in which the protein's hydrophilic sections are exposed to the aqueous environment and its hydrophobic sections are concealed within the center of the structure. As a protein approaches a surface it may unfold and adsorb in a particular orientation or conformation that depends on the potential entropy gain and reduction in interfacial energy at the polymer-water interface [18]. In systems where the environment is comprised of multiple proteins, such as *in vivo* or in a serum or plasma supplemented *in vitro* culture, proteins will adsorb and rearrange/replace each other as described by the Vroman effect [17,42]. The first proteins to arrive at the biomaterial surface are highly abundant proteins and small proteins that diffuse to the surface quickly. These proteins are later replaced by larger, slower diffusing

proteins that have greater affinity for the surface and which resist replacement. After equilibrium is reached, the material surface is covered with a layer of multiple types, orientations and conformations of proteins.

The affinity that a protein has for and the conformation in which the protein will adsorb to a biomaterial surface is influenced by the chemical and mechanical properties of the biomaterial. In general, hydrophobic surfaces adsorb more proteins than hydrophilic surfaces, due to both a favorable decrease in the interfacial energy of a biomaterial during protein adsorption and because the water molecules associated with a hydrophobic surface are easier to displace [14]. Additionally, because the driving force for protein adsorption is the release of bound water from the superhydrated interphase region, any material properties that affect the arrangement of the water molecules at the polymer-aqueous interface could potentially affect a protein's affinity for the surface and the preferred adsorbed conformation of that protein.

1.4 Material Stiffness, Protein Adsorption and Cell Response

Cells are known to respond to the stiffness of polymeric biomaterial substrates. Because protein adsorption occurs before cell attachment and response, cells are thought to be responding to the protein layer that is adsorbed to the material surface. Therefore, if material stiffness is capable of affecting cell response, either cells are able to perceive the stiffness of the material directly via force transduction transmitted through the protein layer, or the cells do not perceive "stiffness" of the material at all, rather material stiffness, or rather, the polymer chain flexibility at the material surface, impacts the composition/configuration of the adsorbed protein layer to which the cells subsequently respond. Due to the complicated nature of cell-

protein and cell-material interactions, cell response to material stiffness may be driven by a combination of these mechanisms.

Few studies have examined the impact of polymer stiffness or polymer chain flexibility/mobility on protein adsorption. This is due partly to the challenge of isolating stiffness as a material property without modifying the other surface properties of the materials. An examination of how polymer stiffness impacts protein adsorption and subsequent cell behavior would improve the understanding of cell responses to biomaterial properties and could lead to future methods able to influence cell behavior with polymeric biomaterials.

Chapter 2

Literature Review

2.1 Introduction

The mechanical properties of the underlying substrate upon which cells are grown have been shown to influence cell behaviors including adhesion [21,43], spreading [4,44], cytoskeleton organization [45,46] and stiffness [47], differentiation [48], and migration [13], and is therefore, an important parameter to be considered in the design of new biomaterials. *In vivo*, cells are attached directly to peptide sequences found in the proteins that comprise the surrounding extracellular matrix primarily via integrins [10,22], heterodimeric cell surface receptors that are connected to the cytoskeleton of the cell and serve as mechanotransducers. Cells then probe matrix stiffness by applying traction forces to their substrates via cytoskeleton contractility. The resistance of the substrate to the applied force is transmitted back the cell via the integrin attachments, which stimulates a cascade of chemical reactions that determines cellular response [49].

Cells also respond to the stiffness of synthetic biomaterial substrates. Unlike native extracellular matrix, synthetic biomaterial surfaces may not include peptide sequences to which integrins and other attachment receptors may bind. Furthermore, synthetic biomaterials are prone to protein adsorption at their surfaces, which shields the biomaterial surface from direct contact with the cells [14]. Finally, even if cells are able to adhere strongly to the biomaterial, the stiffness of many biomaterials is beyond that which a cell can generate to probe the surface [50]. For this reason, it has been hypothesized that cells may sense and interpret the stiffness of biomaterial substrates by a different mechanism than they do native

extracellular matrix [10]. However, this mechanism is currently under investigation, and has generated two possible explanations: 1) that, as with native extracellular matrix, cells sense stiffness directly by applying force to their substrates, and 2) that cells do not sense biomaterial stiffness directly, but rather are responding to stiffness via some intermediate, usually thought to be an adsorbed protein layer. More specifically, biomaterial stiffness influences the characteristics of the protein layer adsorbed to the substrate surface which then are responsible for influencing cellular response [16]. It is also possible that cells are able to respond to material stiffness via both of these mechanisms; which mechanism dominates likely depends on the nature of the biomaterial substrate.

2.2 Mechanisms By Which Cells Sense Biomaterial Stiffness

2.2.1 Sensing of Biomaterial Stiffness via Direct Attachment

In general, cells strengthen their attachment structures and applied traction forces in response to stiff surfaces. Integrin clustering [51,52], focal adhesion formation [21], cytoskeleton organization [53,54], strengthening of integrin-cytoskeleton connections [46] and strength of applied traction force [13,45,50] have all been found to be influenced by substrate stiffness. Additionally, many cell responses [9,55] to substrate stiffness as well as stiffness induced signaling pathways [56,57] suggest that cells are able to directly and accurately determine the stiffness of their substrates. A table reviewing the responses of various cell types to ECM-like substrates of different stiffness is found in Levental, *et al.*, 2007 [58].

Famously, mesenchymal stem cells (MSCs), which can differentiate into neurons, myocytes or osteoblasts, expressed markers belonging to cells from "stiffer" tissues when

grown on stiffer matrices [9,59]. Fibroblasts grown on fibronectin coated polyacrylamide gels of varying stiffnesses adjust their area and cytoskeletal stiffness according to the stiffness of the substrate on which they are grown [55]. Cell area and cytoskeleton stiffness were closely correlated with substrate stiffness, with the stiffness of the cell's cytoskeleton always remaining slightly below the stiffness of the substrate.

Cells maintain a basal level of tension on their substrates, constantly probing substrate stiffness [56] and are believed to sense substrate stiffness through an "inside-outside-in" feedback process [49]. The cell forms integrin attachments/focal adhesions and uses the contractility of its cytoskeleton to apply traction forces to its substrate [10]. Substrate resistance mediates signaling processes within the cell [11,52] and results in the cell reorganizing its focal adhesions and cytoskeleton, which increases the traction forces the cell generates on a substrate. It is possible that this feedback mechanism exists to prevent cells from tearing and damaging their substrate.

Cells clearly possess the ability and sensitivity to attach and directly sense the stiffness of some biomaterials as they do with extracellular matrix. However, a cell's ability to sense a biomaterial's surface is limited by the availability/adhesion of integrin binding sites and the strength of the traction forces that the cell can exert on the biomaterial. Cells grown on materials with no or poorly attached integrin binding sites cannot form strong focal adhesions, or the cells may remove the integrin binding sites during probing [50]. Materials of stiffness beyond what a cell can probe (approximately 20 kPa [50]) may be only sensed as "stiff" surfaces, and the cells will not be able to discriminate between materials stiffer than that maximum [60].

With these specifications in mind, in order for a cell to be able to sense the stiffness of a biomaterial directly, the biomaterial must possess covalently (or otherwise strongly) attached integrin binding peptide sequences and the modulus of the substrate must be in the range that cells can probe. A low modulus and high availability of integrin binding sites are common in hydrogel biomaterials that utilize native extracellular matrix (e.g. collagen gels or coatings) or that graft integrin binding sequences to synthetic gels [61–63]. However, they are uncommon in more hydrophobic, non-hydrogel biomaterials (e.g. poly(lactide-*co*-glycolide) (PLGA)). Both of these issues limit the mechanism by which cells can sense the stiffness of these biomaterials.

2.2.2 Sensing Stiffness via the Adsorbed Protein Layer

Synthetic biodegradable polymers (poly(trimethylene carbonate) (PTMC), PLGA, poly(ε-caprolactone) (PCL), and so on) are currently being investigated as materials for tissue repair, due to their adjustable mechanical properties that approximate those of many tissues [3] and their history of acceptable biocompatibility in humans [1]. Compared to hydrogel substrates, these polymers are relatively hydrophobic and their surfaces are prone to protein adsorption from protein-rich biological systems [18], which effectively prevents direct interaction between the material surface with the attaching cells [14]. Cells that attach to the biomaterial via adsorbed proteins are not directly attached to their substrates as with native ECM or native ECM-mimicking matrices. Despite lack of direct attachment, cell behavior has been observed to be influenced by the stiffness of these synthetic polymers [64–67].

The ability of cells to respond to polymer stiffness through an adsorbed protein layer suggests two possible mechanisms for response to stiffness: either the cell is able to directly probe the substrate by unfolding the adsorbed protein enough to exert direct traction forces on the substrate (Figure 2.1A), or the cell is not "sensing" stiffness at all, rather polymer stiffness is influencing the characteristics of the adsorbed protein layer (e.g. conformation, composition) to which the cell is attached (Figure 2.1B). These differences in adsorbed proteins activate different cellular pathways and drive the observed differences in cellular response, which are

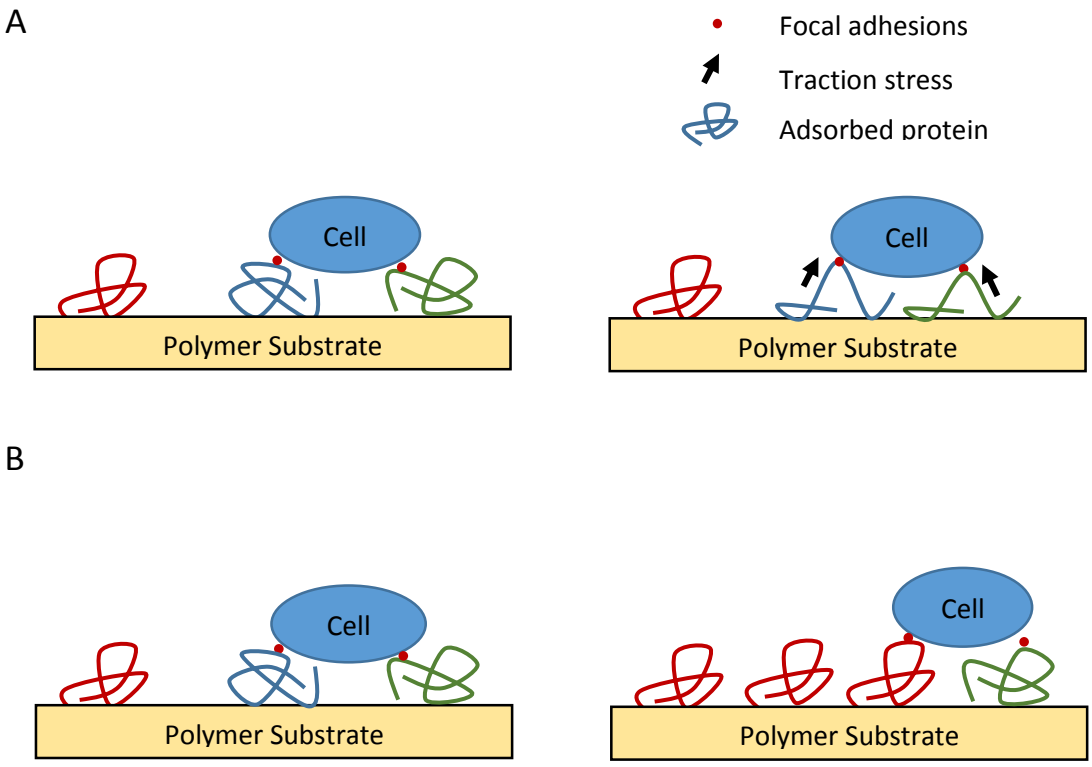

Figure 2.1: A: Cells may be able to respond to substrate stiffness directly by unfolding proteins and exerting traction forces on the polymer surface. B: Material stiffness may influence the characteristics of the adsorbed protein layer which in turn influences cell response.

not necessarily reflective of the true stiffness of the material.

Cells are able to unfold the proteins that comprise the extracellular matrix [68]. However, it is unlikely that cells are able to probe substrate stiffness directly by unfolding

adsorbed proteins (Figure 2.1A), since the stiffness of many polymers is beyond the maximum adhesion force of the protein or traction force that cells are capable of exerting. The maximum traction force/stress that a cell can generate varies by cell type [69]. Maximal traction stress generated by NIH3T3 fibroblasts was found to be 0.4 kPa [50] whereas C2.7 myoblasts were found to generate a maximum traction force of approximately 300 nN [70]. On the other hand, protein adhesion force to a substrate varies by both the substrate and the type of proteins adsorbed. Approximately 50 nN is required to remove an adsorbed fibronectin molecule from glass [71] and more than 220 nN to remove it from polystyrene [72]. Depending on the cell type, traction stresses have the potential to remove adsorbed proteins [50], artificially decreasing the perceived stiffness of the material. If a cell were able to exert enough traction force to unfold a protein and "pull" on a material surface with a relatively high modulus, the adsorbed protein would likely be removed before the surface was even slightly deformed. Moderately stiff materials, including the synthetic polymers described here, would merely be perceived as a "stiff surface" [60]. That cells have been observed to respond differently to materials with stiffnesses orders of magnitude greater than the measured cell traction force suggests cells respond to substrate stiffness through a mechanism other than direct probing.

Instead of directly sensing material stiffness, cells may be responding to stiffness induced differences in the type or conformation of proteins that adsorb to the biomaterial surface, which have been hypothesized to mediate cell response to a material [16,27]. A difference in the concentration of available integrin binding sequences in proteins adsorbed to the surfaces (ligand density) has been shown to impact cell adhesion and other responses associated with stiffer materials [73]. Beyond proteins that provide integrin binding sites, the presence of other proteins may have effects on cell behavior. For example, differences in the

amount of complement or immunoglobulin can affect attachment and differentiation of monocytes/macrophages and subsequently the immune response to the material [74]. If material stiffness can influence the type of proteins that are present on the material surface, material stiffness may influence cell behavior via this adsorbed protein layer.

2.3 The Effect of Polymer Chain Mobility on Protein Adsorption

Any material property that is capable of affecting protein adsorption can potentially influence cell behavior; however, it is still under investigation as to whether differences in material stiffness are sufficient to influence the type or conformation of adsorbed proteins. Because protein adsorption is an interfacial phenomenon, material bulk stiffness does not influence protein adsorption as much as interfacial (surface) stiffness. At the molecular level, the substrate-aqueous interface consists of mobile polymer chains and bound and free water molecules [38]. The mobility/flexibility of these interfacial polymer chains is related to the material bulk stiffness and may drive a difference in protein adsorption at the material surface.

Few studies have investigated the effect of biomaterial stiffness or polymer chain flexibility on protein adsorption, partly due to the difficulty of modifying material stiffness while maintaining polymer surface chemistry [58,67]. The flexibility of surface vinyl methacrylate chains was found to affect the adsorbed quantity and conformation of fibrinogen [75] and fibronectin, which subsequently influenced MSC adhesion and osteogenic differentiation [60]. Similarly, poly(dimethylsiloxane) stiffness was found to influence the conformation of adsorbed fibronectin, specifically the exposure of the adsorbed fibronectin's arg-gly-asp (RGD) cell binding motif, which then affected NIH3T3 fibroblast adhesion [66].

The influence of material stiffness and polymer chain flexibility on protein adsorption has been hypothesized to be due to differences in the arrangement of water at the material surface [76]. Yang *et al*. found that fibrinogen adsorption to polyurethanes had a quadratic dependence on water adsorption [77]. Guiseppe-Elie *et al*. found that lower modulus hydrogels have a higher bulk to bound water ratio that correlated with increased fibroblast adhesion, hypothesized to be due to a difference in the adsorption of serum proteins to the surfaces [67]. Interestingly, material stiffness also impacted protein adsorption in materials below their glass transition temperatures where the chains in the polymer bulk are immobile, which was hypothesized to be due to differences in water penetration at the surfaces [78].

Differences in polymer chain mobility and water absorption may influence protein adsorption by changing the entropy of the system. Protein adsorption is driven primarily by the entropy increase associated with the release of bound water molecules from the material surface and the adsorbing protein molecule [18]. The polymer-aqueous interface is believed to exist as a superhydrated gel-like "interphase" region where water penetrates into the polymer surface and the polymer chains protrude into the aqueous media [4] (Figure 1.1).

A difference in polymer chain mobility effects the thickness of this interphase region; that is, the depth of water penetration, the protrusion of the polymer chains into the aqueous media and the arrangement of the water molecules bound to the polymer chains. Differences in arrangement of water molecules in the interphase region may influence the number of water molecules released during adsorption, affecting the likelihood that certain proteins or conformations of proteins adsorb [67].

2.4 Introduction to the Thesis Project

The objective of this thesis was to determine whether material stiffness/polymer chain mobility influences cellular response by affecting the nature of the adsorbed protein layer. Two types of polymer biomaterials, an elastomer formed from crosslinking an acrylated *star* poly(D,L-lactide-*co*-ε-caprolactone) pre-polymer (ELAS) and high molecular weight PTMC, have been shown to induce different cellular responses depending on their stiffness. For these two polymers, varying polymer stiffness does not significantly alter surface chemistry.. These two polymers and their respective cell behaviors, therefore, were chosen as model systems to examine the effect of material stiffness on protein adsorption and subsequent cell response.

2.5 The Effect of ELAS Stiffness on Cell Proliferation

The stiffness of ELAS is determined by the molecular weight of the pre-polymer prior to crosslinking, with lower molecular weight pre-polymers possessing a higher number of acrylate crosslinking groups per volume and, thus, yielding stiffer (higher crosslink density) elastomers. Previously, both bovine coronary smooth muscle cells [79] and NIH3T3 murine fibroblasts [80] were shown to proliferate more on an ELAS surface prepared from 5000 g/mol pre-polymer (ELAS 5000) compared to a 2000 g/mol pre-polymer (ELAS 2000). The elastomer surfaces are chemically identical and differ only in stiffness/polymer chain mobility.

2.5.1 Elastomers Formed from Acrylated *Star* Poly(D,L-lactide-*co*-ε-caprolactone)

Star-poly(D,L-lactide-*co*-ε-caprolactone) is synthesized by the ring opening melt polymerization of D,L-lactide and ε-caprolactone monomers, initiated by glycerol. The resulting polyester is a random co-polymer consisting of a 1:1 ratio of D,L-lactide to caprolactone. The terminal hydroxyl groups are subsequently acrylated resulting in the pre-polymer (ASCP) (Figure 2.2) that can be crosslinked by UV or visible light. The molecular weight of the pre-polymer determines the crosslink density, and thus the bulk stiffness and flexibility of the polymer chains of the elastomer, of the resulting elastomer [80].

For these elastomers, a lower molecular weight pre-polymer results in a stiffer elastomer. ELAS 2000, formed from pre-polymer of molecular weight 2000 g/mol, possesses a modulus of approximately 8 MPa and a glass transition temperature midpoint (T_g) of 0 ± 0.1 °C, while ELAS 5000, formed from a pre-polymer of 5000 g/mol has a Young's modulus of 1 MPa and a T_g of -7 ± 1 °C. ELAS is fairly hydrophobic with a contact angle of 83°, which does not vary with crosslink density [80]. In aqueous environments, ELAS experiences virtually no swelling and very little water adsorption. Contact angle measurements and attenuated total reflectance Fourier transform infrared spectrometry surface analysis show no difference in surface chemistry or chain/functional group rearrangement upon conditioning in aqueous environments, beyond the presence of water at the surface. As with most polyesters, ELAS degrades via bulk hydrolytic degradation at the ester bonds in the polymer backbone, which are hydrolyzed into carboxylic acids. While, in the long term, the degradation of the ELAS surface may alter the surface and modulus of the polymer, no significant degradation is reported for up to 10 weeks in an aqueous environment [80], much longer than the time frame of the observed cellular responses.

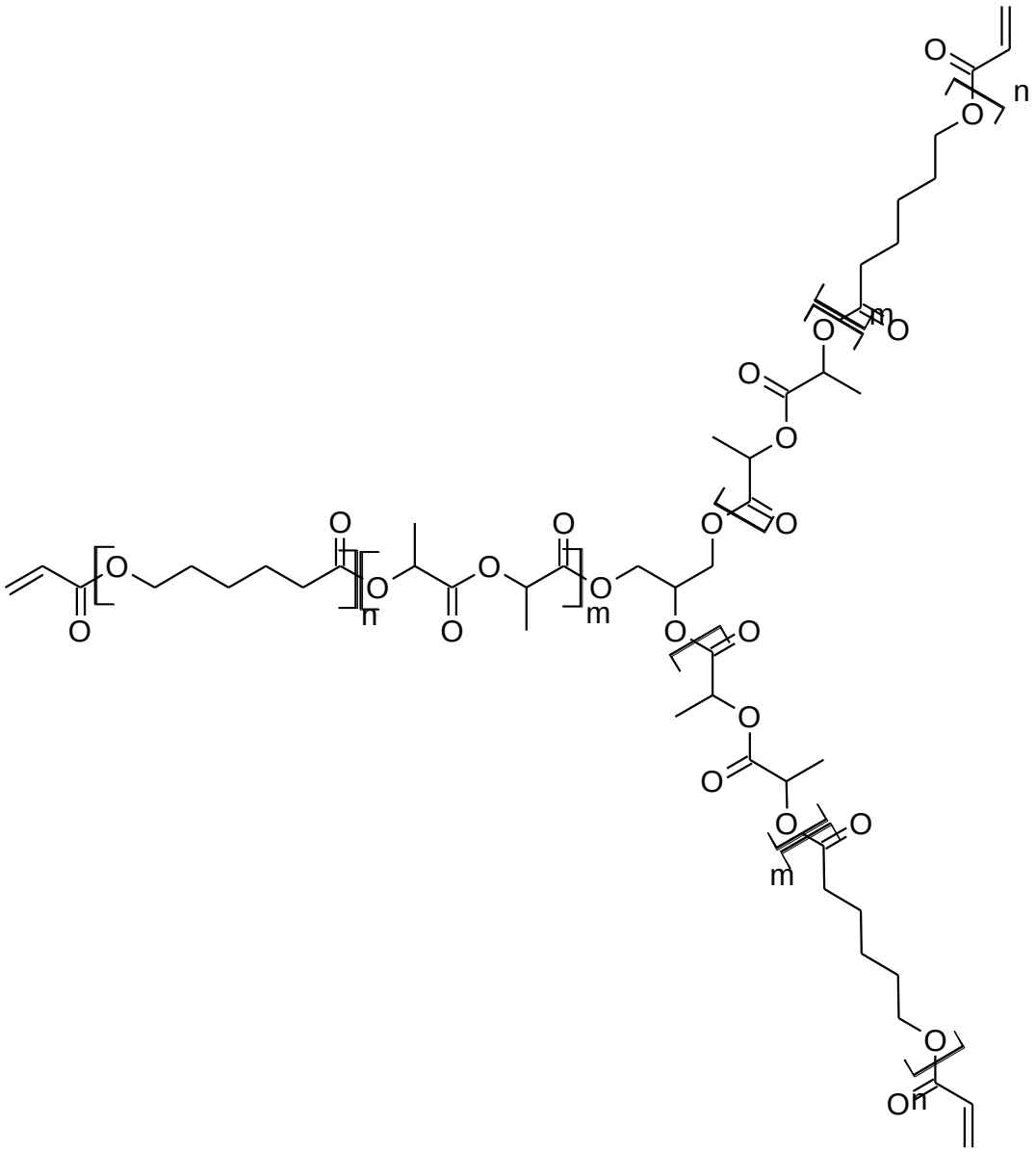

Figure 2.2: Molecular structure of acrylated star poly (D,L lactide-co-ϵ-caprolactone) (ASCP) with repeating units m = D,L-lactide and n = ϵ-caprolactone.

Poly(trimethylene carbonate) is formed from ring-opening melt polymerization of trimethylene carbonate (Figure 2.3) and is currently being investigated for several biomedical applications [1,81], in part because of its unique degradation properties. PTMC is not

susceptible to hydrolytic degradation, rather *in vivo* PTMC is degraded by macrophage mediated enzymatic and oxidative surface erosion and produces no acidic degradation products [82,83].

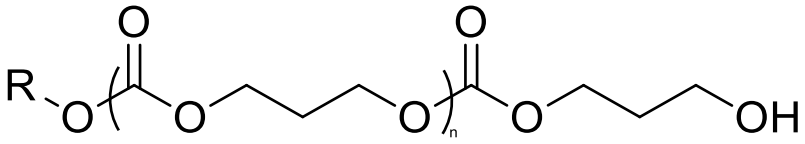

Figure 2.3: Molecular structure of poly(trimethylene carbonate) (PTMC)

Very high molecular weight (>100 kg/mol) PTMC is not covalently crosslinked, however, due to highly entangled polymer chains, PTMC is rubbery and deforms elastically at low strains. Due to its low glass transition temperature (-16 °C [84]), the polymer chains of PTMC are flexible and mobile at physiological temperature. PTMC is relatively hydrophobic with a contact angle of approximately 75, which does not vary with molecular weight, and undergoes very little bulk swelling in aqueous environments (approximately 3% [84]). No change in contact angle is observed between dry and aqueous conditioned pTMC and ATR-FTIR analysis shows no polymer chain/functional group reorientation at the surface during aqueous conditioning over 7 days.

2.5.2 NIH3T3 Fibroblasts

NIH3T3 is an immortalized murine fibroblast cell line commonly used in biomaterials research. NIH3T3 cells are anchorage dependent [85] and adhere to extracellular matrix/adsorbed serum and plasma proteins primarily through integrin binding mechanisms

[86,87]. They are thought to adhere particularly to fibronectin [88], vitronectin [12] and other sources of the RGD integrin binding motif [89]. NIH3T3 cells attach and spread more when grown on hydrophilic (wettable) surfaces [12,90] hypothesized to be due to a preferentially higher adsorption of fibronectin on hydrophilic materials [88].

3T3 cells respond to the stiffness of both hydrogel [13,21,91] and non-hydrogel [64,66] polymeric biomaterials. NIH3T3 cells show increased spreading and more stable focal adhesions [21], more organized cytoskeletons and stress fibers [92], higher growth and lower levels of apoptosis [93] when grown on stiffer hydrogel substrates. NIH3T3 response to the stiffness of non-hydrogel substrates appears to vary by material [64]. NIH3T3 cells have been observed to migrate towards stiffer regions on PDMS, which was correlated with increased ECM remodeling [94]; however, when grown on PCL films, NIH3T3 cells proliferated more on the less stiff surface [64]. These material-specific responses may reflect the variance in surface chemistry between polymers and different levels of protein adsorption, which also influences cell behavior. NIH3T3 adhesion to PDMS of different stiffnesses did not directly correlate with bulk stiffness, but was correlated to the concentration of exposed RGD integrin binding sites in adsorbed proteins [66].

2.5.3 RAW 264.7 Macrophages

RAW 264.7 cells are an immortalized murine monocyte-macrophage line commonly used to model macrophage activation. They are naturally adherent and do not require the addition of stimulant, such as LPS, to differentiate into an adherent phenotype [30]. RAW 264.7 monocyte-macrophages adhere to biomaterial surfaces via integrin binding (Mac-1 and

VAL-4) and Fc receptor binding [8,30] to serum proteins, especially fibrinogen, fibronectin, immunoglobulins [95] and complement [96]. When activated by a biomaterial such as polycarbonate [97], RAW 264.7 cells secrete degradative species [98] and inflammatory cytokines [99] in an attempt to degrade the material.

RAW 264.7 monocyte-macrophages have also been shown to have stiffness dependent responses. Classically activated cells (i.e. via LPS) exhibited a decreased immune response to less stiff hydrogels [8,100,101]. The mechanism for uptake of nanoparticles by RAW 264.7 cells was dependent on the stiffness of the nanoparticles [102]. Additionally, it has been hypothesized that both polymer chain flexibility as measured by glass transition temperature could affect the behavior of RAW 264.7 cells grown on aliphatic polyesters such as PCL [96].

2.6 The Effect of PTMC Stiffness on RAW 264.7 Macrophage Mediated Erosion

High molecular weight PTMC degrades *in vivo* via macrophage mediated enzymatic and oxidative surface erosion mechanisms. PTMC of molecular weight greater than 100 kg/mol degrades *in vivo* [103] and in *vitro* macrophage culture, whereas PTMC of molecular weight less than 70 kg/mol undergoes no such degradation [65]. Due to the low saturation of end groups, 100 kg/mol PTMC and 60 kg/mol PTMC have almost identical surface chemistries. These PTMC have similar bulk stiffness, but different surface stiffness, when hydrated [84]. No studies have been performed specifically examining the behavior of RAW 264.7 cells when cultured on different stiffnesses of PTMC; however, a similar monocyte-macrophage cell line (J774A cells) degraded crosslinked PTMC at rate dependent on the crosslink density of the PTMC [65].

2.7 Summary

The method by which cells sense or respond to the stiffness of polymeric biomaterial substrates is incompletely understood, due to the complex connections between polymer surface properties, protein adsorption and cell response. Additionally, the effect of polymer stiffness on protein adsorption and cell response as an isolated property has been seldom investigated, due to the challenge of modifying polymer stiffness without altering surface chemistry. Elastomers formed from acrylated *star* poly(D,L-lactide-*co*-ε-caprolactone) pre-polymers of different crosslink densities and PTMC of different molecular weights induce differences in fibroblast proliferation and monocyte/macrophage degradation, respectively, while still maintaining similar surface chemistries, and thus are ideal model systems to examine the effect of polymer stiffness and polymer chain flexibility on protein adsorption and subsequent cell response.

Chapter 3

Scope

3.1 Hypotheses

The over-arching hypothesis of this project is that the mobility of the polymer chains at the polymer-aqueous interface affects cell behavior by influencing the quantity and/or conformation of the proteins that adsorb to the polymer surface. The polymer chain mobility affects the composition of the adsorbed protein layers, leading to differences in the quantity or conformations of proteins, which in turn influences the respective cell behavior. Within the context of this main hypothesis, two main sub-hypotheses were formulated, specific to each polymer being examined (hypotheses 1 and 2). Based on results obtained during the fulfillment of hypothesis 2, a third hypothesis was generated:

1. It is hypothesized that the ELAS 5000 surface, which induces higher NIH3T3 fibroblast proliferation, will adsorb greater quantities or different conformations of proteins associated with cell attachment compared to the ELAS 2000 surface.

2. 100PTMC undergoes faster macrophage mediated degradation by RAW 264.7 murine monocyte derived macrophages compared to 60PTMC. It is hypothesized that the faster degradation of 100PTMC is due to increased levels of macrophage attachment or activity at the 100PTMC surface, driven by differences in quantities of proteins that induce macrophage response (e.g. complement proteins and immunoglobulin) or due to greater adsorption of degradative enzymes compared to the 60PTMC surface.

3. The results from the fulfillment of hypothesis 2 (objective 3) showed that 100PTMC is degraded faster than 60PTMC by murine monocyte derived macrophages due to a difference in the enzymatic activity at their surfaces, and not due to a difference in macrophage activity driven by differences in protein adsorption. However, 100PTMC also undergoes faster macrophage mediated degradation by RAW 264.7 monocyte/macrophages compared to ELAS 5000 despite similar rates of enzymatic degradation. It is hypothesized that, due to differences in surface chemistry and polymer chain flexibility, the 100PTMC surface adsorbs greater quantities of proteins that induce macrophage attachment and activity (e.g. complement proteins and immunoglobulin) compared to the ELAS 5000 surface.

3.2 Objectives

With respect to Hypothesis 1, the following objectives were established:

3.2.1 Objective 1: The Influence of Polymer Chain Flexibility of ELAS on Individual Protein Adsorption

Determine if polymer chain mobility influences the quantity or conformation of proteins adsorbed from solutions of individual proteins. Elastomer hydrophilicity, bulk modulus, glass transition temperature, and roughness will be determined by water contact angle, double indentation test, differential scanning calorimetry (DSC) and atomic force microscopy (AFM), respectively. Adsorbed protein layer mass will be measured from

individual protein solutions and FBS supplemented cell culture media using radiolabelling and surface plasmon resonance (SPR), respectively. Viscoelastic properties of the adsorbed protein layers will be measured by quartz crystal microbalance with dissipation (QCM-D) and viscoelastic modeling.

3.2.2 Objective 2: The Influence of Polymer Chain Flexibility of ELAS on Competitive Protein Adsorption

Determine if polymer chain mobility influences the quantity or conformation of proteins adsorbed from a serum supplemented (competitive adsorption) environment. Additionally, determine which adsorbed protein(s) may be influencing fibroblast proliferation on the elastomer surfaces. Fetal bovine serum supplemented cell culture media will be adsorbed to ELAS 2000 and ELAS 5000 surfaces, with adult bovine plasma (in which cells do not grow) as a control. Protein identity will be determined by relative quantitation proteomics [104]. Following the identification of a protein believed to influence fibroblast behavior, that protein will be used as a serum free media supplement to determine its effect on fibroblast proliferation on the ELAS surfaces.

3.2.3 Objective 3: The Influence of PTMC Polymer Chain Flexibility on Macrophage Behavior and Enzymatic Adsorption and Conformation.

With respect to Hypothesis 2, the following objective was formulated:

Determine if differences in degradation rate between 100PTMC and 60PTMC (via macrophage mediated degradation) are due to differences in macrophage behavior (i.e. macrophage attachment, or macrophage secretion of ROS or degradative enzymes). Macrophage number, ROS and esterase secretion will be quantified. Additionally, the degradation rate of 100PTMC and 60PTMC in solutions of cholesterol esterase and lipase will be determined, as well as the adsorption quantities and viscoelastic properties of those proteins on the PTMC surfaces.

3.2.4 Objective 4: The Influence of Protein Adsorption and Subsequent Macrophage Activity on PTMC and ELAS surfaces

With respect to Hypothesis 3, the following objective was formulated:

100PTMC surfaces are eroded by macrophage-mediated degradation at a faster rate than ELAS 5000 surfaces despite similar susceptibility to enzymatic degradation. Determine if differences in the macrophage mediated degradation rate of 100PTMC and ELAS 5000 are due to differences in the protein layer that adsorbs from adult bovine plasma supplemented cell culture media. Protein layers will be adsorbed to 100PTMC and ELAS 5000 surfaces from adult bovine plasma supplemented media and protein identity and relative quantity will be determined by relative quantitation proteomics.

Chapter 4

The Effect of Elastomer Chain Flexibility on Protein Adsorption

4.1 Completed Objectives

The following chapter describes the completion of Objective 1, which was to determine if polymer chain mobility influences the quantity or conformation of proteins adsorbed from solutions of individual proteins. It was hypothesized that the previously observed stiffness dependent difference in NIH3T3 fibroblast proliferation was due to a difference in the amount or conformation of proteins that adsorbed to the different stiffnesses of elastomers fabricated from acrylated *star*-poly(D,L-lactide-co-ϵ-caprolactone) (ASCP). Elastomer hydrophilicity, bulk modulus, glass transition temperature, and roughness were determined by water contact angle, double indentation test, DSC and AFM, respectively. NIH3T3 fibroblasts were grown on two stiffnesses of elastomer (ELAS) (fabricated from 2000 g/mol and 5000 g/mol ASCP) and proliferate more on the less stiff surface (ELAS 5000). Solutions of individual proteins albumin, immunoglobulin G, fibronectin and vitronectin as well as serum supplemented cell culture media were adsorbed to the ELAS 2000 and ELAS 5000 surfaces and protein layer mass and viscoelastic properties (thickness, shear modulus, and viscosity) were measured by radiolabelling/SPR and quartz crystal microbalance with dissipation (QCM-D). Finally, surface water content of the hydrated elastomer surfaces was measured using attenuated total reflectance Fourier transform infrared spectroscopy (ATR-FTIR), showing significantly more surface water absorption on the ELAS 5000 surface.

Chapter 4 was published in *Biomaterials* Sept 11, 2013. All experiments described herein were designed and completed by me with the exception of the radiolabelling and adsorption of radiolabelled protein, which was completed by Lina Liu in Dr. Heather Sheardown's lab at McMaster University, Hamilton, ON. SPR experiments were performed by me in the Protein Function Discovery Facility, Queen's University. I am the first author of the manuscript, followed by Lina Liu and Dr. Heather Sheardown.

4.2 Introduction

Biodegradable elastomers are currently under considerable investigation for their utility as tissue engineering scaffolds, as their mechanical properties approximate those of many soft tissues[2,105]. We have previously found that smooth muscle cell response to elastomers formed from acrylated *star*-poly(D,L lactide-co-ϵ-caprolactone) (ASCP) varied depending on the elastomer crosslink density. Specifically, the smooth muscle cells proliferated faster on elastomer surfaces of lower crosslink density, despite crosslink density having no effect on the degree of smooth muscle cell attachment [79]. One proposed explanation for this finding was that the difference in this cell response was due to differences in protein adsorption to the elastomers.

Protein adsorption is the precursor to cellular-biomaterial interactions, and is considered to be the first event that occurs following biomaterial implantation [14,106]. The composition and configuration of the adsorbed protein layer depends on the material properties of the substrate and is believed to determine cellular response [18]. However, protein adsorption and its influence on cellular behavior is still incompletely understood due to the

multitude of factors, such as protein layer composition, protein orientation and configuration [16], which may be influenced by the surface properties of the material. We hypothesized that the smooth muscle cell response to the elastomer surfaces was a result of the differences in the amount, composition, and configuration of proteins adsorbed to these elastomer surfaces and that these differences arose due to the dissimilar polymer chain mobility at the surface of the elastomers as a result of their different crosslink densities.

Few studies have examined the effect of crosslink density on protein adsorption. At the medium-elastomer interface, the crosslink density affects polymer chain mobility, which in turn influences the structure of the hydrated interface region [1,17,107]. Typically, materials that strongly bind water molecules experience lower amounts of protein adsorption and reduced conformational changes in the proteins that adsorb [107,108], due to the steric hindrance provided by the water molecules and the unfavorable energy cost of displacing the bound water with protein [109]. Polymer chain mobility at the surface has previously been hypothesized to affect cell behavior [67] and protein conformation [60,75,66] due to the increased entropy associated with more mobile polymer chains. In this study we examine the influence of ASCP elastomer crosslink density, and thus polymer chain mobility, on protein adsorption quantity and on the viscoelastic properties of the adsorbed protein layer. Proteins were adsorbed from solutions of individual proteins and serum supplemented culture media at physiological conditions. Protein radiolabelling, surface plasmon resonance (SPR) and quartz crystal microbalance with dissipation (QCM-D) were used to determine protein quantity and viscoelastic properties of the protein layer including thickness, shear viscosity and shear modulus. Finally, infrared spectroscopy (ATR-FTIR) was used to determine differences in absorbed interfacial water at the elastomer surfaces.

4.3 Materials and Methods

4.3.1 Elastomer Fabrication

Elastomers were prepared from 2000 g/mol and 5000 g/mol acrylated *star*-poly(D,L lactide-co-ϵ-caprolactone) according to the procedure described in Amsden *et al*. [110]. These molecular weights were chosen because they have been previously shown to support different degrees of smooth muscle cell attachment and proliferation [79]. Briefly, a 1:1 molar ratio of D,L lactide (Purac, The Netherlands) and ε-caprolactone (Fluka, Switzerland), glycerol (Fisher, Canada) as the initiator, and tin (II) 2-ethylhexanoate (Sigma, Canada) as a catalyst were sealed under vacuum in a flame dried glass ampoule and reacted for 24 h at 130°C. The resulting polymer was dissolved in dichloromethane (Fisher, Canada) dried over 3Å molecular sieves (Acros, USA) and acrylated by the drop-wise addition of acryloyl chloride (Sigma, Canada), in the presence of triethylamine (Sigma, Canada) and dimethylaminopyridine (Sigma, Canada) as a catalyst. The degree of acrylation was greater than 98 % for both molecular weights of polymer. The resulting acrylated star copolymer prepolymer (ASCP) was purified by precipitation in isopropanol (Fisher, Canada) at -20°C. Molecular weights were confirmed by gel permeation chromatography (Waters, USA). The ASCP prepolymers were crosslinked in the absence of solvent with 2,2 dimethoxy-2-phenyl-acetophenone (DMPA) (Sigma, Canada) as a photoinitiator. The photoinitiator was dissolved in a minimal quantity of ethyl acetate (Fisher, Canada), mixed with the ASCP and the ethyl acetate allowed to evaporate overnight prior to crosslinking. The ASCP was irradiated in a glass mold with long-wave UV light (300-400 nm) (Lightningcure LC8, Hamamatsu) at an intensity of 30 mW/cm^2 for 5 min on each side. Elastomers fabricated from 2000 g/mol and 5000 g/mol ASCP will be referred

to as ELAS 2000 and ELAS 5000, respectively. ATR-FTIR scans indicate no differences in percent vinyl group conversion between ELAS 2000 and ELAS 5000 materials. For these elastomers, cross-link density increases as the molecular weight of the prepolymer decreases [110].

4.3.2 Contact Angle Measurements

Sessile drop water contact angles were measured on ELAS 2000 and ELAS 5000 films. Glass coverslips (Fisher, Canada) were coated in ASCP prepolymer with minimal ethyl acetate and photoinitiator. The coated coverslips were incubated at room temperature overnight, protected from light, to remove the ethyl acetate and level the polymer surface before crosslinking. Level surfaces were confirmed by caliper measurement of the edge thickness of the coated coverslips. The coating thickness was approximately 1 mm. 1 μL of distilled water was deposited on the surface of the flat coated coverslip. As protein adsorption occurs in an aqueous environment, contact angles were measured for both dry samples and samples that had been soaked overnight in distilled water (VCA Optima XE, AST Products Inc.). Measurements were taken after 30 seconds of equilibration. Contact angles are reported as the average of 3 samples with 5 drops per sample.

4.3.3 Glass Transition Temperature Measurements

The glass transition temperatures (T_g) of ELAS 2000 and ELAS 5000 were measured using differential scanning calorimetry (DSC 1, Mettler Toledo). The samples were run by first

cooling from ambient to -45ºC, then using a heating-cooling-heating cycle from -45 to 25°C. Glass transition temperatures were determined for both dry samples and samples which had been conditioned in distilled water for 24 h. The glass transition temperature was measured from the second heating cycle (n=2).

4.3.4 Water Absorption Measurement

Percent water absorption was determined by gravimetric analysis. Dry samples (n=2) of ELAS 2000 and ELAS 5000 elastomers were weighed, conditioned in distilled water for 24 h, blotted dry, then weighed a second time to determine water content.

4.3.5 Atomic Force Microscopy

The surface roughness of ELAS slabs (n=3) and spin-coated sensors (n=1) was determined by atomic force microscopy. ELAS 2000 or ELAS 5000 was prepared in slabs or spin coated onto gold QCM-D sensors as described above. A Veeco Multimode Microscope equipped with a Nanoscope IIIa Controller with a Veeco Probes TESP AFM tip was operated in tapping mode. RMS roughness (Rq) was quantified using the NanoScope V6.13 Software (Veeco, USA).

4.3.6 Mechanical Testing

Elastomer bulk moduli were measured in uniaxial compression using a single indentation. Previous double indentation measurements have determined a Poisson ratio of

approximately 0.5, common for elastomers[111]. The indentation measurement was performed on a 25x25x1.5 mm square slab using a circular indenter with a 2 mm diameter, and a deformation rate of 0.03 mm/sec (TA.XT *plus* Texture Analyzer, Stable Micro Systems). The modulus was determined from the slope of the linear regression of the applied stress vs. applied strain between 5% and 20% strain (n=2).

4.3.7 Culture of NIH3T3 Fibroblasts

Differences in cellular attachment and proliferation on different crosslink densities of elastomer were confirmed by culturing NIH3T3 murine fibroblasts on ELAS 2000 and ELAS 5000 surfaces with tissue culture polystyrene as a comparison surface. The prepolymers were dissolved in ethyl acetate in a 50% w/v solution with a minimal amount of DMPA. The wells of 96 well tissue culture polystyrene plates (Corning) were coated with 50 μL of the prepolymer solutions. The plates were incubated overnight to allow the solvent to evaporate then irradiated with 30 mW/cm^2 UV light. The coated well plates were sterilized under low intensity (40 μW/cm^2) UV light for 30 min then incubated in DMEM (Sigma) at 37°C for 24 h prior to cell seeding. Frozen NIH3T3 immortalized murine fibroblasts were thawed and expanded in T-175 flasks for 1 week prior to seeding. The cells were passaged with 10X trypsin (Sigma), centrifuged and re-suspended at a concentration of 50,000 cells/mL. The cells were seeded at a density of 10,000 cells per well and cultured for 14 days in DMEM supplemented with 10% fetal bovine serum (FBS, Sigma) and 1% anti-mycotic (Hyclone). At days 1, 3, 7, 10 and 14 cell number was quantified using a fluorescent DNA binding assay (Quantifluor, Promega, n=6).

4.3.8 Radiolabeled Protein Adsorption

Iodine radiolabeled proteins were used to measure mass of protein adsorbed to the elastomer surfaces. Albumin and IgG were labeled with I^{125} using the iodine monochloride method[112] and purified by twice passing through an AG 1-X4 packed column. Fibronectin and vitronectin were labeled using the iodogen method[113]. Approximately 1 mm thick sheets of ELAS 2000, ELAS 5000 and poly(dimethylsiloxane) (PDMS) were punched into 0.635 cm diameter discs (n=4) and conditioned overnight in PBS. Protein solutions were used at their physiological concentrations in adult human plasma. Solutions of human serum albumin (44 mg/mL[114], 2.5% labeled), immunoglobulin G (10.5 mg/mL[115], 2.5% labeled, Sigma), fibronectin (0.325 mg/mL[116], 2% labeled, Sigma) or vitronectin (0.225 mg/mL[117], 2% labeled, Cedarlane) in PBS were prepared and incubated with the discs for 12 h. Following adsorption, the elastomer discs were rinsed 3 times for 5 min each in PBS and blotted dry. Radioactivity was determined using a Wizard 3 1480 Automatic Gamma Counter (Perkin Elmer); radioactivity was converted to a protein mass using a standard curve.

4.3.9 QCM-D Sensor Coating

Thickness, modulus and viscosity of protein layers adsorbed to ELAS 2000 and ELAS 5000 were quantified using a quartz crystal microbalance with dissipation (QCM-D E1, Q-Sense). Gold QCM-D sensors (4.95 MHz, 14 mm diameter, Q-Sense) were spin-coated (WS-400, Laurell Technologies) with a 1% solution of ELAS 2000 or ELAS 5000 pre-polymer in ethyl acetate with a minimal amount of DMPA photoinitiator. 1 mL of the solution was pipetted drop-wise onto the spinning sensor (4000 rpm, 5 min). Coated sensors were crosslinked under

UV radiation (30 mW/cm^2, 5 min). The coated sensors were dried overnight at room temperature and stored in a desiccator when not in use. The thickness of the elastomer coating and surface roughness were determined using QCM-D measurements and atomic force microscopy, respectively.

4.3.10 QCM-D Protein Adsorption

Dry ELAS coated sensors were inserted into the QCM-D chamber. Phosphate buffered saline (Sigma) was then flowed over the sensor (50 μL/min) for 8 h until stable frequency and dissipation baselines were measured. A protein solution was then flowed into the sensor chamber (50 μL/min) for 10 min until the chamber was filled. The flow of the protein solution was then halted and the protein allowed to adsorb statically for 12 h, approximating the adsorption that takes place in an *in vitro* cell culture (n=3) (Figure 4.1). Solutions of individual proteins were used at physiological concentrations and included human serum albumin (44 mg/mL, Sigma), immunoglobulin G (10.5 mg/mL) (Sigma), fibronectin (0.325 mg/mL, Sigma) or vitronectin (0.225 mg/mL, Cedarlane) in pH 7.4 phosphate buffered saline (PBS). To examine the viscoelastic properties of layers that adsorb during cell culture, protein adsorption was also measured using the supplemented *in vitro* cell culture medium (10% FBS in DMEM). For media adsorption measurements, the coated sensors were baselined using unsupplemented DMEM and DMEM supplemented with 10% FBS was used as the protein solution. Protein layer thickness, viscosity, and shear moduli were calculated using a Voigt viscoelastic model[118], assuming a protein density of 1400 kg/m^3 [119].

4.3.11 Surface Plasmon Resonance

Surface plasmon resonance (SPR) was used to quantify the mass of protein adsorbed from a serum solution. Plain gold SPR sensor chips (Au, Biacore) were coated in ASCP prepolymer. Briefly, 20 μL of a 0.1 mg/mL solution of ASCP in acetone with a minimal amount of photoinitiator was pipetted onto the surface of a SPR sensor. The acetone was allowed to evaporate before the coated sensor was cross-linked under long-wave UV light (30 seconds, 30 mW/cm^2). The coated SPR sensors were dried for 8 h before the experiment. The sensors were inserted into the SPR (Biacore 3000, Biacore, Sweden) and unsupplemented DMEM was flowed over the sensor until a baseline measurement was achieved (400 seconds). 330 μL of DMEM supplemented with 10% fetal bovine serum was then injected into the flow cell at 10 μL/min). The coated sensor was exposed to the protein solution for 30 min. Following adsorption, unsupplemented DMEM was injected into the flow cell as a rinse step. Adsorbed protein mass was measured as the difference in signal between the stabilized post rinse data (4000 s) and the baseline (500 s) (Figure 4.2).

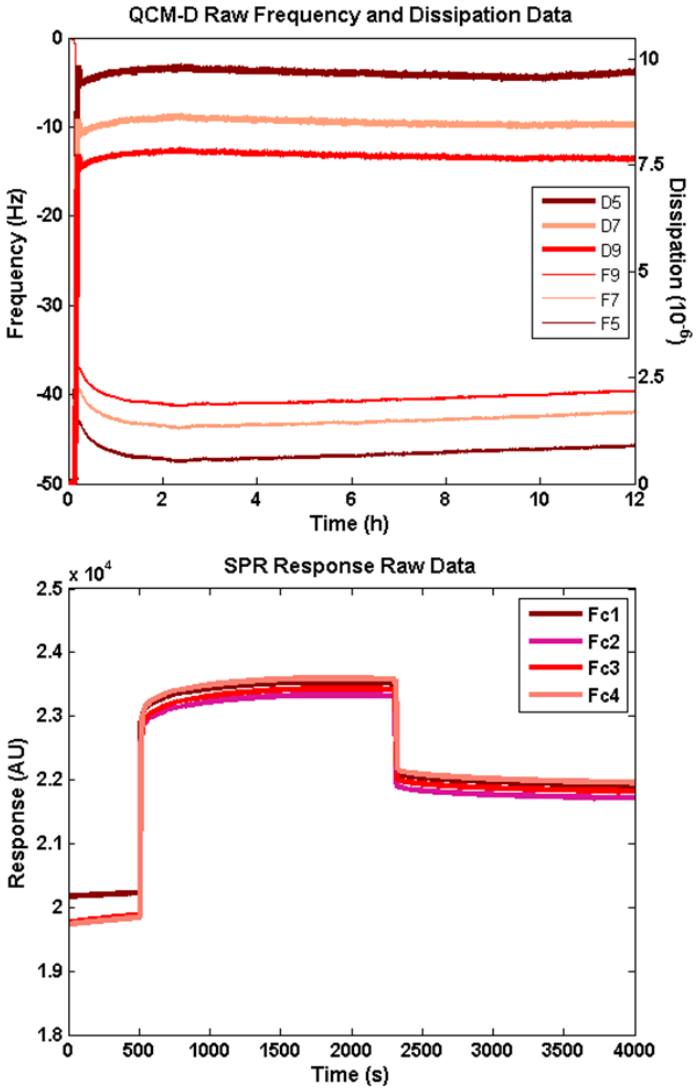

Figure 4.1: Top: Representative curves of QCM-D data. ΔFrequency and ΔDissipation at the 5th, 7th and 9th overtone for albumin adsorption to ELAS 5000 over 12 hours. Bottom: Representative curves of SPR response data from 4 flowcells (Fc) for serum adsorption to ELAS 5000 over 4000 seconds.

4.3.12 ATR-FTIR

Surface water adsorption was measured by attenuated total reflection Fourier transform infrared (ATR-FTIR) analysis. The water stretching (3350 cm^{-1}) and bending (1650 cm^{-1})

peaks were used as indicators. ELAS 2000 and ELAS 5000 were fabricated according to the method described above and incubated in water. At time points of 0, 1, 4, and 24 h, the elastomers were removed from the water, scanned, then returned to the water.

4.3.13 Statistics

Measurements are reported as the average value ± standard deviation of n replicates. Significant differences with respect to attachment and proliferation of the NIH3T3 fibroblasts on the different elastomers was determined using a two way ANOVA with a Bonferroni *post-hoc* test (Prism 6, GraphPad, USA). Significant differences in adsorbed protein mass were determined using a one-way ANOVA with a Bonferroni *post-hoc* test. All other significance differences were determined using a Student's t-test. Populations were considered significantly different at values of $p<0.05$.

4.4 Results and Discussion

Bulk ELAS 2000 and ELAS 5000 and coated QCM-D sensors were prepared and characterized according to the methods described above. Because protein adsorption occurs in an aqueous environment, the elastomers and coated sensors were also characterized in a hydrated state (Table 4.1). As expected, bulk modulus and polymer chain stiffness (as reflected in measured T_g) were higher for the higher crosslink density material (ELAS 2000) and decreased slightly for both elastomers when wet due to the plasticizing effect of water[120] (Table 4.2). No significant differences were observed in surface water contact angle or surface roughness between the bulk elastomers or coated sensors. However, bulk ELAS 2000 absorbed

a slightly higher quantity of water than did the ELAS 5000. This result may be due to the greater quantity of acrylate groups in the bulk ELAS 2000; the acrylate group is relatively more hydrophilic compared to that of the caproyl residues.

Table 4.1: Summary of elastomer sample preparation methods and preconditioning

	Sample Prep Method	Thickness	Preconditioning
Contact angle	Dip coated	1 mm	24 h, DI water
T_g	Bulk slab	1 mm	24 h, DI water
Fibroblast culture	Crosslinked in wells	0.5 mm	24 h, DMEM
Radiolabelling	Bulk slab discs	1 mm	24 h, PBS
SPR	Pipetted onto sensor and crosslinked	15 nm	400 s, DMEM (baseline equilibration)
QCM-D	Spin coated and crosslinked	50 nm	12 h, PBS or DMEM (baseline equilibration)
ATR-FTIR	Bulk slab	1 mm	Various, DI water

Table 4.2: Bulk and surface properties of dry and wet ELAS 2000 and ELAS 5000

	ELAS 2000 (Dry)	ELAS 2000 (Wet)	ELAS 5000 (Dry)	ELAS 5000 (Wet)
ASCP M_n (g/mol)	2000		4300	
ASCP M_w (g/mol)	2200		5200	
Modulus (MPa)	7.6 ± 0.3	7.8 ± 0.5	1.00 ± 0.04	1.2 ± 0.1
Bulk Rq (nm)	1.2 ± 0.2		2.2 ± 0.3	
Sensor Rq (nm)	0.2		0.2	
Tg (^{o}C)	0.4 ± 0.3	0.3 ± 0.1	-6.8 ± 1.1	-8.7 ± 0.9
Water Content (%)		6.6 ± 0.2		4.82 ± 0.01
Bulk Contact Angle (^{o})	86 ± 2	82 ± 3	81 ± 2	85 ± 3
Sensor Contact Angle (^{o})	82 ± 2	80 ± 2	85 ± 2	84 ± 2

4.4.1 Fibroblast Attachment and Proliferation

3T3 murine fibroblasts were cultured on ELAS 2000 and ELAS 5000 surfaces and differences in attachment and proliferation assessed to 14 days (Figure 4.2). Tissue culture polystyrene (TCPS) was used as a control surface. Cell proliferation rate was highest on the TCPS surface and the cells reached confluence by day 7. Cells cultured on the ELAS surfaces showed similar initial attachment (Day 1 and Day 3); however, only cells cultured on ELAS 5000 proliferated until day 14. Cells cultured on ELAS 2000 proliferated until day 7 after which cell number decreased. NIH3T3 cells are anchorage dependent and grow readily in FBS supplemented media on most surfaces to which they can securely attach. In this cell culture result, the lack of cell growth on the ELAS 2000 may have been due to differences in the amount or conformation of adsorbed proteins that provide attachment points to the cells, resulting in poorer attachment and lack of proliferation on the ELAS 2000 surface. These results correspond with what has previously been observed for smooth muscle cells growing on these elastomers. Despite similar cell attachment on ELAS1800 and ELAS4500, smooth muscle cells proliferated more on both the unmodified and base-etched ELAS4500 surface [79]. These results demonstrate that increased cellular proliferation on ELAS 5000 is common to more than one cell type, supporting the hypothesis that the underlying protein layer may be the driving factor for the difference in cell proliferation.

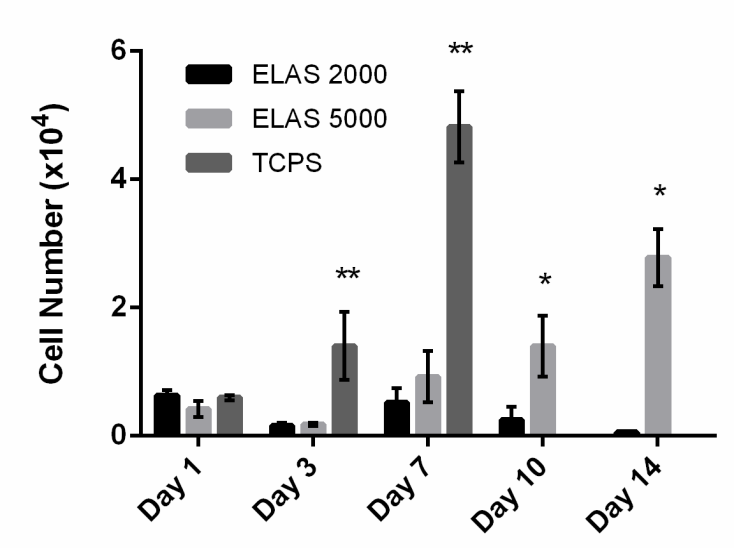

Figure 4.2: Fibroblast attachment and proliferation on ELAS 2000, ELAS 5000, and TCPS surfaces over 14 days. *p<0.05 compared to ELAS 2000 surface. **p<0.05 compared to both elastomer surfaces. Confluence was reached on TCPS surfaces by 7 days (n=6)

4.4.2 Protein Adsorption

Characteristics of adsorbed protein layers were quantified by radiolabelling, SPR, and QCM-D analysis to determine the mass and thickness of the protein layer, and the viscoelastic properties of the adsorbed layers, respectively. The results are present in Figures 4.3A-D. Physical properties of the proteins used in this study are given in Table 4.3. The proteins varied greatly in overall configuration and size, but were all negatively charged at physiological pH.

Table 4.3: Physical properties of the proteins examined

	MW (kg/mol)	Radius (nm)	Configuration	Isoelectric point
Albumin[121]	66	3.5	Globular	4.8
IgG [121,122]	150	5.3	Y-shaped	6.5
Fibronectin[123]	440	120 x 2	Rod-shaped dimer / V-shaped	5.5-6.0
Vitronectin[124]	75	11 x 3	"Peanut"-shaped	5.5

A significantly higher mass of fibronectin (Fn) adsorbed to the ELAS 5000 surface than to the ELAS 2000 surface (Figure 4.3A). Fibronectin is a component of the extracellular matrix and is associated with cell attachment and proliferation[125]. This result suggests that the increased cell proliferation rate on the ELAS 5000 surface is related to the higher mass of fibronectin on the surface. Interestingly, a higher mass of immunoglobulin G (IgG) adsorbed to the ELAS 2000 surface than to the ELAS 5000 surface. While immunoglobulins are not typically associated with cell attachment, IgG is present in serum in the highest concentration after albumin[126]. If IgG adsorbs in a high quantity or different conformation on the ELAS 2000 surface, the adsorbed IgG may have a different likelihood of desorption and replacement by other proteins, and effectively block proteins with integrin binding sites from adsorbing. No other individually adsorbed proteins showed differences in mass adsorbed between the elastomer groups or the PDMS comparison surface.

The adsorbed mass of serum proteins was much lower than the masses adsorbed from solutions of individual proteins. This finding is most likely due to the relative concentration difference between the solutions. Individual proteins were adsorbed from solutions at physiological plasma concentrations whereas serum proteins were adsorbed from supplemented cell culture media (10% serum) in which the proteins were much more dilute. Between the two elastomer surfaces, however, the adsorbed mass of serum was higher on the ELAS 5000 surface. As the adsorption from a serum solution is competitive, the final compositions of the adsorbed protein layers are presently unknown. The adsorbed mass results do indicate, however, that there is likely a difference in the protein adsorption on the two elastomer surfaces in the *in vitro* fibroblast culture. It is also interesting to note that the difference in adsorption measured in the IgG solution (high adsorption on ELAS 2000) is not

reflected in the serum adsorption, suggesting that other proteins are out-competing IgG for the surface in a competitive environment.

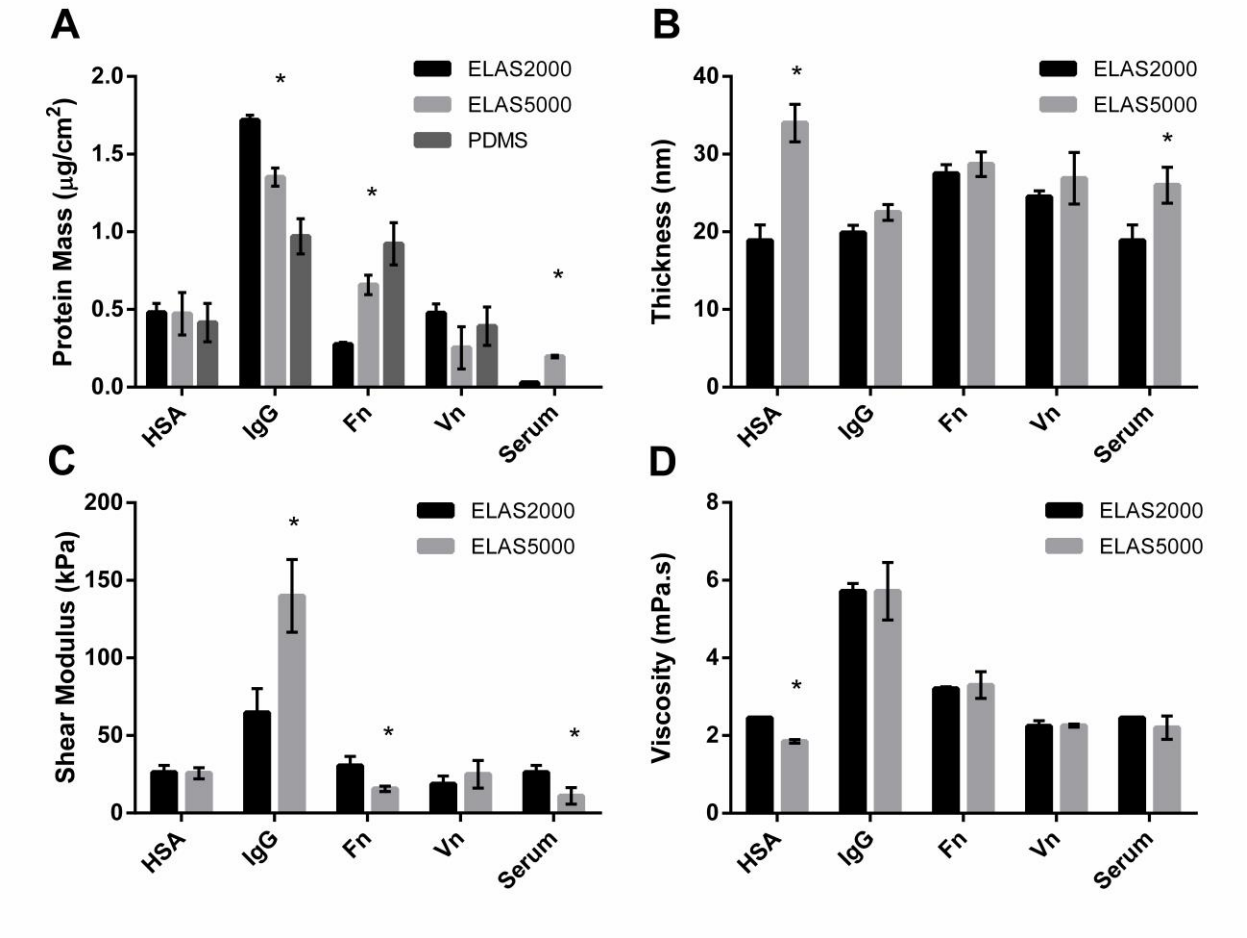

Figure 4.3: A: Mass of protein adsorbed to ELAS 2000 and ELAS 5000 surfaces; B: Thickness of protein layers adsorbed to ELAS 2000 and ELAS 5000 surfaces; C: Shear modulus of protein layers adsorbed to ELAS 2000 and ELAS 5000 surfaces; D: Shear viscosity of protein adsorbed to ELAS 2000 and ELAS 5000 surfaces.*$p<0.05$ compared to ELAS 2000, (n=3).

Quartz crystal microbalance with dissipation (QCM-D) was used to measure the viscoelastic properties of the adsorbed protein layer including thickness (Figure 4.3B), shear

modulus (Figure 4.3C), and shear viscosity (Figure 4.3D). In contrast to radiolabelling, which measures protein mass alone, QCM-D measures the viscoelastic properties of a *hydrated* layer[127]; that is, the measurements include the effects of bound water in the protein layer. Therefore, differences in viscoelastic properties may be related to not only the quantity of protein adsorbed, but also the quantity of bound water in the adsorbed layer and the conformation of the adsorbed protein [128]. Because the proteins were adsorbed statically without a rinse step, it is possible that the thickness measurements included loosely bound (but still acoustically coupled) proteins in the measurement. However, changes in thickness do not significantly impact the other values calculated by the model. In general, shear modulus (i.e. storage modulus) is related to the elastic character of the protein (conformation), and viscosity (i.e. loss modulus) is related to the quantity of water bound in the protein layer.

No differences in protein layer thickness were observed for proteins that are traditionally associated with cellular attachment (fibronectin and vitronectin). The albumin layer adsorbed to the ELAS 5000 was approximately twice as thick as the layer adsorbed on the ELAS 2000. The adsorbed serum layer also was significantly thicker when adsorbed to the ELAS 5000, probably due to the contribution of albumin, as albumin is the most abundant protein in serum[129].

The shear viscosities of all adsorbed protein layers were statistically similar on both elastomer surfaces with the exception of albumin, indicating a similar quantity of water bound in the protein layers adsorbed to the different stiffnesses. The albumin layer adsorbed to the ELAS 2000 had a higher viscosity, possibly due to a difference in albumin conformation, which is also reflected in the albumin layer thickness measurements. This trend was also

observed in the serum layer viscosity, most likely due to the high concentration of albumin in the adsorbed serum.

Significant differences in adsorbed protein layer modulus were observed for IgG, fibronectin and serum. The IgG layer showed the most dramatic difference in stiffness with the protein layer adsorbed to the ELAS 5000 being nearly twice as stiff as the layer adsorbed to the ELAS 2000. Fibronectin displayed significantly higher layer stiffness when adsorbed to the ELAS 2000 surface. Interestingly, this trend is opposite to the trend shown between IgG and fibronectin in the radiolabelling (adsorption mass) data (Figure 4.3A). In general, higher shear moduli are seen on the surfaces that adsorbed lower masses of protein. This result suggests that not only is there a different quantity of protein adsorbed to the surface, but that the protein has adsorbed in a different conformation as well[130]. An illustration of possible differences in the conformation of fibronectin adsorbed to the elastomer surfaces is shown in Figure 4.4.

Fibronectin is a dimer that has a "V-shaped" native configuration (Table 4.3). The stiffer, less massive fibronectin layer on the ELAS 2000 may be a result of fibronectin adsorbing in a flattened conformation, covering more surface area and preventing other protein molecules from adsorbing. The less stifflayer which contained a higher quantity of fibronectin on the ELAS 5000 may be caused by the fibronectin adsorbing in an "on-end" fashion, which also allows more protein to fit on the surface. Such differences in conformation may also affect the presentation and availability of integrin binding sites to attaching cells. Further studies on protein conformation especially regarding the presentation of integrin binding sites may yield information as to the mechanism driving differences in cell behavior. A similar difference in conformation may occur when IgG is adsorbed to the elastomer surface. IgG is a rigid, "Y-

shaped" protein (Table 4.3) which may adsorb in on-end or side-on conformations. As with the fibronectin, a difference in IgG adsorption conformation is likely to result in differences in IgG layer mass and stiffness, both of which were observed in the radiolabelling and QCM-D data. *In vivo,* these differences in immunoglobulin adsorption may affect the immune response to the implanted biomaterial.

The reason for the differences in fibronectin and IgG adsorption and conformation is unclear. ELAS 2000 and ELAS 5000 differ only in their bulk water absorption, bulk modulus and polymer chain flexibility. Protein adsorption is a surface phenomenon and so is unlikely

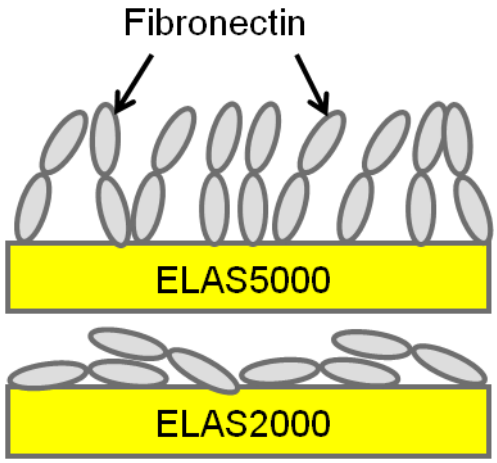

Figure 4.4: Possible configurations of fibronectin (see Table 4.3) adsorbed to the elastomer surfaces. Top: "On end" adsorption of fibronectin on ELAS 5000 allows for more protein as well as a less stiff protein layer. Bottom: Adsorption of fibronectin on ELAS 2000 in a flattened orientation restricts available space and forms a more rigid layer.

to be related to bulk properties. Surface water absorption, however, has been shown to affect protein adsorption in hydrophilic materials[109,126] where the water can act as a steric hindrance to the protein. To assess this possibility, ATR-FTIR scans were used to determine differences in water absorption into the surface regions of ELAS 2000 and ELAS 5000 (Figure 4.5).

The results show a larger quantity of water within the ELAS 5000 surface region at all time points compared to the ELAS 2000 surface. Interestingly, this result contrasts with the bulk water absorption trend. One explanation is that since the polymer chains in ELAS 5000 are more mobile, they are more able to change their orientations to create favorable interactions and a diffuse polymer layer hydrated with the surrounding water.

The differences in water absorption and polymer chain flexibility may be the driving force for differences in protein adsorption and fibroblast behavior. Berglin *et al*. suggested that a stiffer polymer chain may force an adsorbing protein to change its conformation in order to minimize the surface energy [75]. A more flexible polymer chain can adopt its own conformation while preserving the native conformation of the protein. It may also be statistically less probable that a large protein like fibronectin will be able to permanently remain in a denatured conformation bound to several polymer chains if the chains are more mobile.

Increased mobility and hydration of polymer chains may also be associated with a greater entropic gain during protein adsorption and cell adhesion. Guiseppe *et al*. [67] found that hydrogel chain flexibility was proportional to the ratio of water bound to the hydrogel chains to bulk water. Fibroblasts were also found to proliferate more on hydrogels with a higher bound to bulk water ratio. The authors hypothesized that protein adsorption to a hydrogel with more bound water would induce a greater entropic change upon release of the bound water molecules, resulting in more protein adsorption which could provide more cellular binding sites.

While this hypothesis concerns hydrogels, the present data suggests that the hydrophobic ELAS surfaces may behave similarly. The surface of a hydrophobic elastomer will absorb a small amount of water, creating an interfacial region where water is bound to mobile polymer chains. The elastomer with more flexible chains should absorb more water at the surface, which has been confirmed by FTIR analysis. Additionally, the competitive protein

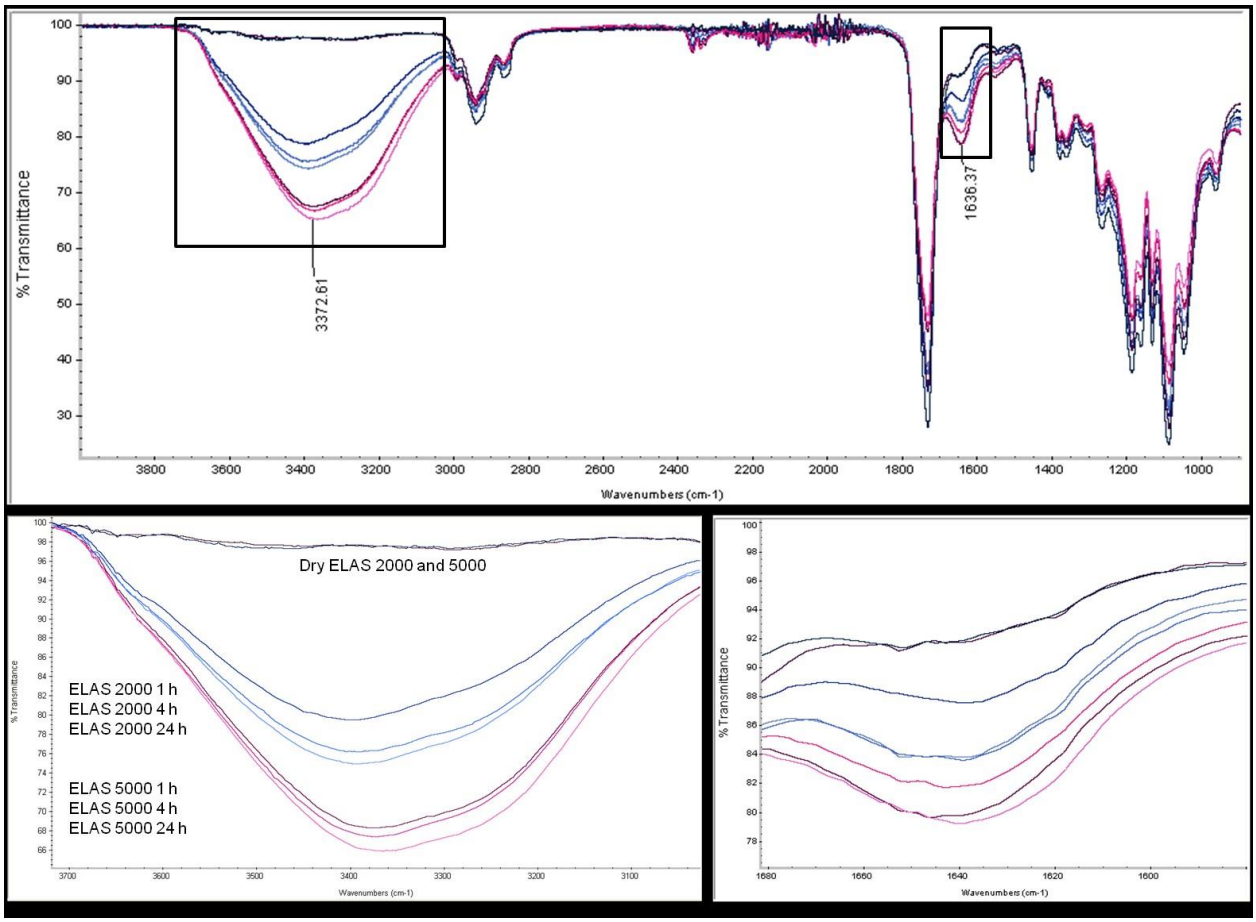

Figure 4.5: ATR-FTIR scans of ELAS 2000 and ELAS 5000 incubated in water for 0, 1, 4, and 24 hours. Top: full spectrum; Lower left: expansion of water peak at 3350 cm-1 (stretching); Lower right: expansion of water peak at 1650 cm-1 (bending).

adsorption data (from serum) showed that more total protein adsorbed to the more flexible elastomer, which further confirms that chain mobility and entropy affect protein adsorption.

Also of interest is how the entropy of the material surface may impact the types of proteins being adsorbed. The individual adsorption data shows that more IgG adsorbed to the less mobile elastomer, whereas more fibronectin adsorbed to the more mobile elastomer. However, the adsorption from serum was also higher on the more mobile elastomer, suggesting that IgG is not a large component of the adsorbed serum layer. This result may also be due to relative entropy gains from the release of water molecules bound to the proteins themselves. Fibronectin is a large flexible protein (450 kDa) whereas IgG is a smaller (150 kDa), rigid protein. Fibronectin most likely experiences a greater entropy gain upon adsorption and so may adsorb in greater quantities in a competitive environment despite its lower abundance in serum.

In addition, IgG and fibronectin also adsorbed to form layers with different shear moduli, suggesting a difference in adsorbed conformation. A more flexible polymer chain may also discourage protein denaturation during adsorption. Denaturation during adsorption frees more water bound to the protein and the surface. A higher entropy polymer chain may offset the need for a protein to denature upon adsorption.

It is worth noting, however, that the result that a greater mass of fibronectin adsorbs to the polymer surface with more flexible polymer chains contrasts with other results reported in the literature. Both Seo *et al*. and Gonzalez-Garcia *et al*. found no influence of polymer chain mobility on mass of fibronectin adsorbed. This discrepancy may be due to differences in material properties, concentration of fibronectin or adsorption time. Gonzalez-Garcia *et al*. measured fibronectin adsorption on polyacrylates with a similar contact angle to the ELAS elastomer (approximately 80 degrees); however, the polyacrylates used were not crosslinked and the range of T_g's reported were different from the ELAS T_g. Additionally, the concentration of fibronectin solution used by Gonzalez-Garcia *et al*. for the adsorption study was 20 μg/mL,

about 10 times lower than the study presented here, which may have altered the adsorption equilibrium or adsorbed protein surface density. Seo *et al*. reported no difference in mass of fibronectin adsorbed to different crosslink densities of PDMS. This is most likely due to differences in surface chemistry between PDMS and ELAS. The PDMS surface at all crosslink densities is more hydrophobic than the ELAS surface. Predictably, the more hydrophobic surface adsorbs more fibronectin due to a more favorable reduction in surface energy. In this study, we measured a similar mass of fibronectin adsorbed to the PDMS control surface (approximately 1 $\mu g/cm^2$).

Despite the differences in fibronectin adsorption quantity between studies, substrates with higher chain mobility are observed to have greater cell adhesion. Entropy has also been hypothesized to be related to cell adhesion [60]. Increasing the length, and thus, mobility, of an RGD graft improved cell spreading and decreased time to form focal adhesions [60]. One possible explanation is that the higher the mobility of the integrin binding sites (either via tethers or proteins adsorbed to polymer chains), the more accessible the integrin binding site is to the integrin and the easier it is to form focal adhesions. On the other hand, Seo *et al*. showed that fibronectin may adsorb to various crosslink densities of PDMS with different conformations; however, the authors found no significant difference in the total number of exposed RGD integrin binding sites [66]. In addition to the number of integrin binding sites alone, cells may also be responding to the viscoelastic properties of the protein layer. Fibronectin adsorbed to ELAS 5000 in higher amounts but formed a less stiff layer than when adsorbed to ELAS 2000. Since cells are known to apply mechanical force to and partially unfold fibronectin when attaching to and moving on biomaterial surfaces [108], stiffness of the

fibronectin layer may also provide a means by which cells can sense information about their surface.

4.5 Conclusion

Smooth muscle cells and fibroblasts proliferated *in vitro* on ELAS 5000, a lower crosslink density elastomer, at a much faster rate compared to ELAS 2000, a higher crosslink density elastomer. Both fibronectin and IgG adsorbed to ELAS 5000 and ELAS 2000 in different amounts and with different layer moduli. As the elastomers differ only in polymer chain mobility between crosslink points, these results suggested that chain mobility at the interface played an important role in determining the nature of protein adsorption. The ELAS 5000 absorbed more water at its surface compared to ELAS 2000, and the increased amount of water may have caused the ELAS 5000 to experience greater entropic gains upon protein adsorption compared to ELAS 2000, which in turn increased total protein adsorption from serum and may have caused the differences in cell behavior. These results demonstrate that it is necessary to consider the adsorbed protein layer when examining the influence of polymer stiffness on cell interactions with polymer surfaces.

Chapter 5

Polymer Chain Flexibility-Induced Differences in In Fetuin A Adsorption and its Implications for Cell Attachment and Proliferation

5.1 Objectives Completed

Chapter 5 describes the fulfillment of objective 2, which was to determine whether polymer chain flexibility can affect the composition of the protein layer that adsorbs in a competitive environment and additionally determine which protein(s) influenced the difference in NIH3T3 fibroblast proliferation observed in chapter 4. NIH3T3 fibroblasts were cultured on elastomers fabricated from 2000 g/mol and 5000 g/mol ASCP (ELAS 2000 and ELAS 5000, respectively, referred to as E2 and E5 in this chapter) in DMEM supplemented with 10% adult bovine plasma as a low growth comparison to fetal bovine serum (FBS) which was used to supplement the previous NIH3T3 fibroblast culture. A relative quantitation proteomics method (reductive methylation followed by tandem liquid chromatography-mass spectrometry (LC-MS/MS)) was used to compare the amount of specific proteins that adsorbed to ELAS surfaces of different stiffness from DMEM supplemented with 10% FBS or 10% adult bovine plasma. A protein, fetuin A, was identified that adsorbed in significantly greater quantities to the ELAS 5000 elastomer, which previously supported higher NIH3T3 proliferation in FBS supplemented media. Fetuin A with and without a growth factor (FGF-2) was used to supplement serum free and plasma supplemented NIH3T3 fibroblast cultures to determine fetuin A's effect on NIH3T3 fibroblast proliferation.

Chapter 5 was submitted to *Acta Biomaterialia* and as of September 30, 2015 has been reviewed as meriting consideration for publication pending revisions. All experiments and data described herein were designed and collected by me with the exception of the reductive methylation and LC-MS/MS which was collected at the University of British Columbia, Center for High Throughput Biology, Proteomics Core Facility as a fee-for-service. SPR measurements were performed by me at the Protein Function Discovery Facility at Queen's University. I am the first author on the manuscript.

5.2 Introduction

Mechanical properties of biomaterials, such as modulus and polymer chain flexibility, are known to affect the attachment [4,10,53] and proliferation [64,79,131] of anchorage dependent cells. However, the mechanism by which the cells sense material stiffness is not yet clearly understood and is the subject of ongoing study. Cell response to a biomaterial is believed to be mediated by the protein layer that adsorbs to the biomaterial surface [14,16], the composition and configuration of which depends on the properties of the material surface [18]. Because cells appear to respond to material stiffness, it has been suggested that substrate stiffness, itself, affects the composition and configuration of the adsorbed protein layer, which subsequently drives cellular response [67,80].

Protein adsorption is primarily an entropically driven phenomenon; the adsorption of a protein to a substrate frees water molecules bound to both the protein and the substrate's polymer chains, increasing the entropy of the system [18,129]. Material stiffness and thus polymer chain flexibility at the interface may influence both the arrangement of the water

molecules bound to the polymer chain and the configurational entropy of the chains themselves, which may, in turn, influence the entropy increase that occurs upon adsorption, and subsequently, the quantities or conformations of the proteins that adsorb [67,80].

Few studies have investigated the means by which material stiffness influences protein adsorption. Previously, we cultured smooth muscle cells [79] and fibroblasts [80] in fetal bovine serum supplemented medium on elastomer substrates of different stiffnesses formed from crosslinking different molecular weights of an acrylated *star*-poly(D,L lactide-*co*-ϵ-caprolactone) (ASCP). For these elastomers, crosslink density impacts the material bulk stiffness and flexibility of the polymer chains without altering surface chemistry. We found that smooth muscle cell and fibroblast proliferation depended on the stiffness of the underlying elastomer and hypothesized that this cell behavior was due to differences in protein adsorption on the surfaces of these elastomers, driven by the difference in polymer chain flexibility at the interface. This hypothesis was supported by initial findings that showed differences in the average mass and viscoelastic properties of adsorbed layers of both individual proteins and fetal bovine serum.

However, it was not possible to conclude if these differences in the properties of adsorbed serum layers were due to differences in which proteins comprised the layers or conformation of the proteins therein. As such, we were unable to determine if material stiffness could affect the composition or conformation of the protein layers that adsorb in a serum supplemented cell culture environment. Furthermore, the proteins examined in the individual protein adsorption experiments (namely fibronectin and vitronectin) were selected due to their well-known contribution to cell attachment and proliferation by way of acting as a source of

integrin binding sites. However, it was unknown whether these proteins were actually affecting fibroblast proliferation in the serum supplemented cell culture environment.

The objective of this study was to determine if polymer chain flexibility at the material interface could affect the composition of protein layers adsorbed from serum as well as determine which protein(s) could be responsible for the observed difference in 3T3 fibroblast proliferation. Since we previously observed differences in the adsorption properties of fibronectin, we hypothesized that fibronectin, or a similar cell adhesive protein, was adsorbing from the serum supplemented media to the elastomer surfaces in different quantities or conformations, affecting the number of integrin binding sites accessible to the cells, and thus cell proliferation. However, due to the multitude of proteins in serum and plasma [132], protein layers that adsorb from these media are comprised of potentially hundreds of different proteins, and measuring the adsorption characteristics of single proteins alone does not capture the complexities of multiple protein adsorption such as protein competition and replacement [133].

In this study, we used relative quantitation proteomics to determine the composition of protein layers adsorbed from serum supplemented media to two different stiffnesses of ASCP elastomer and attempted to identify which adsorbed protein(s) could be driving the previously observed stiffness dependent fibroblast proliferation. Relative quantitation proteomics is a powerful emergent technique for comparing the quantities of individual proteins on multiple surfaces [134]. Upon identifying a protein, alpha-2-HS-glycoprotein (fetuin A), which adsorbed asymmetrically to the elastomer, fetuin A layers on each elastomer were characterized using surface plasmon resonance (SPR) and quartz crystal microbalance with dissipation (QCM-D). Finally, fibroblasts were cultured on the elastomer surfaces in medium

supplemented with fetuin A and with or without basic fibroblast growth factor (FGF-2) to determine the protein's effect on fibroblast proliferation.

5.3 Materials and Methods

Elastomers were prepared from 2000 g/mol and 5000 g/mol acrylated *star*-poly(D,L lactide-*co*-ϵ-caprolactone) (ASCP) according to the procedure described in Amsden *et al.* [110]. Elastomers fabricated from 2000 g/mol and 5000 g/mol pre-polymer are henceforth referred to as E2 and E5, respectively. These molecular weights were chosen because they have been previously shown to induce different degrees of smooth muscle cell [79] and fibroblast proliferation as well as adsorb different amounts of fibronectin, IgG, and serum proteins [80]. To prepare the ASCP, a 1:1 molar ratio of D,L-lactide (Purac, The Netherlands) and ε-caprolactone (Fluka, Switzerland) were added to a flame dried glass ampoule with glycerol (Fisher Scientific, Canada) as the initiator, and tin(II) 2-ethylhexanoate (Sigma, Canada) as a catalyst. The ampoules were sealed under vacuum and reacted for 24 h at 130 °C. For these polymers, the molecular weight is controlled by the ratio of moles of glycerol : moles of monomer added to the polymerization. The resulting polymer was dissolved in dry dichloromethane (Fisher Scientific, Canada) and acrylated at their termini by the drop-wise addition of acryloyl chloride (Sigma, Canada), in the presence of triethylamine (Sigma, Canada) and dimethylaminopyridine (DMAP) (Sigma, Canada) as a catalyst. The resulting ASCP prepolymer was purified by overnight precipitation in cold (-20 °C) isopropanol (Fisher Scientific, Canada). Number average molecular weights (2100 g/mol and 5200 g/mol for E2

and E5, respectively) with degrees of acrylation (above 99% for both pre-polymers) were assessed using ^{1}H-NMR (500 MHz, Bruker).

5.3.1 Microsphere Preparation

To increase the available surface area for protein adsorption, E2 and E5 elastomers were fabricated as microspheres. ASCP pre-polymers were dissolved in toluene in a 1:1 w/v ratio with 2,2 dimethoxy-2-phenyl-acetophenone (DMPA) (Sigma, Canada) as a photoinitiator. 3 mg photoinitiator was added per gram of pre-polymer. 4 mL de-ionized (DI) water and a small stir bar were added to a 5 dram glass vial. 1 mL of pre-polymer was pipetted into the stirred vial (1200 rpm) in a thin stream. A UV light (Lightningcure LC8, Hamamatsu) was then placed over the stirring vial to crosslink the pre-polymer droplets (300-400 nm wavelength, 30 mW/cm^2, 5 min). Crosslinked microspheres were removed from the water by sieving over a 22 μm sieve and were dried in an oven at 120°C for 10 minutes, then overnight at room temperature to remove excess water and solvent before use. Microsphere diameter was measured by image analysis (Image J) of SEM images (Hitachi S-2300 SEM, 15 kV) (Fig. A.6 and Fig. A.7). Average microsphere diameters for the E2 and E5 microspheres were 184 ± 57 μm and 370 ± 132 μm respectively.

5.3.2 Protein Adsorption

To determine which proteins adsorbed to E2 and E5 in a cell culture environment, Dulbecco's modified Eagle's medium (DMEM, D6429, Sigma, Canada) supplemented with 10% fetal bovine serum (FBS, Fisher Scientific, Canada) and DMEM supplemented with 10%

adult bovine plasma (with 10 U/mL sodium heparin, Cedarlane, Canada) were incubated with E2 and E5 microspheres at 37 °C for 24 hours. 2 mL microcentrifuge tubes were filled with either 0.5 g of E2 or 1 g of E5 microspheres, equalizing the available adsorption surface area. The microspheres were incubated in unsupplemented DMEM for 12 hours prior to protein adsorption. The unsupplemented media was then removed and replaced with 1 mL of FBS or plasma supplemented DMEM and the microspheres were stirred with a spatula to ensure complete coverage of the microspheres. The tubes were incubated at 37 °C for 24 h. After 24 h, the DMEM was aspirated and the microspheres were rinsed with 3 washes of 1 mL DI water to remove any excess protein. 0.250 mL of 0.5% sodium dodecyl sulfate (SDS, Fisher Scientific, Canada) was added to each tube, which was then heated to 95 °C for 5 minutes and vortexed for 1 minute. The SDS/protein solutions were removed from the microsphere tubes and the proteins were precipitated from the SDS using an ethanol precipitation. Briefly, a 0.750 mL ethanol, 20 μL of 2.5 M sodium acetate (Fluka, The Netherlands), and 20 μg glycogen (Sigma, Canada) was added to each protein solution. Solutions were incubated at room temperature for 2 hours, followed by centrifuging at 13500 rpm for 10 minutes. The supernatant was aspirated and the protein pellet was lyophilized and stored at -80 °C.

5.3.3 Protein Identification and Quantitation

Proteins adsorbed to E2 and E5 were identified and relatively quantified using reductive methylation followed by LC-MS/MS. All the procedures described herein were performed by the Proteomics Core Facility (PCF) at the Center for High Throughput Biology (CHiBi) at the University of British Columbia (UBC) according to the methods described in

Boersema *et al*. [135]. Lyophilized protein samples described above were reconstituted and digested with porcine trypsin and dried by vacuum centrifugation for 30 minutes. The dried protein digests were reconstituted in triethylammonium bicarbonate. Undeuterated (CH_2O and $NaBH_3CN$) and deuterated (CD_2O and $NaBD_3CN$) formaldehyde and sodium cyanoborohydride were added to the E2 and E5 protein digests, respectively, labeling the digested peptides with either undeuterated or deuterated methyl groups. Labeled peptides were injected into a linear-trapping quadrupole – Orbitrap mass spectrometer (LTQ-Orbitrap Velos, ThermoFisher Scientific) coupled to an Agilent 1290 Series HPLC using a nanospray ionization source (ThermoFisher Scientific) including a 2-cm-long, 100-μm-inner diameter fused silica trap column, 50-μm-inner diameter fused silica fritted analytical column and a 20-μm-inner diameter fused silica gold coated spray tip (6-μm-diameter opening, pulled on a P-2000 laser puller from Sutter Instruments, coated on Leica EM SCD005 Super Cool Sputtering Device). The trap column was packed with 5 μm-diameter Aqua C-18 beads (Phenomenex, www.phenomenex.com) while the analytical column is packed with 3.0 μm-diameter Reprosil-Pur C-18-AQ beads (Dr. Maisch).

The HPLC system included an Agilent 1290 series Pump and Autosampler with Thermostat. The thermostat temperature was set at 6°C. Buffer A consisted of 0.5% aqueous acetic acid, and buffer B consisted of 0.5% acetic acid and 80% acetonitrile in water. Samples were resuspended in buffer A and loaded with the same buffer. Standard 120 min gradients were run from 10% B to 25% B over 60 min, then from 25% B to 60% B in the over 20 min, then increased to 100% B over 7 min period, held at 100% B for 2.5 min, and then dropped to 0% B for another 20 min to recondition the column. Approximately 4 μg of sample was loaded on the trap column at 5 μL/min. The analysis was performed at 0.1 μL/min.

Mass spectrometry was performed using the following source parameters: 500V end plate offset, 4500V Capillary, with the nebulizer at 0.4 Bar, and 180 degree drying gas at 4 L/min. Mass spectra were collected over the 120 run time for the 100-2200 m/z mass range, collecting MS/MS spectra on the top 15 multiply charges precursor ions, using intensity based summing times, and a dynamic exclusion list.

The acquired peak areas were processed by Proteome Discoverer 1.3 (Thermo Scientific) using an untargeted analysis method. The protein identification was performed with the Mascot algorithm (v. 2.4) against a database of bovine protein sequences using the following parameters: peptide mass accuracy 10 parts per million; fragment mass accuracy 0.6 Da; trypsin enzyme specificity, fixed modifications – carbamidomethyl, variable modifications – methionine oxidation, deamidated N, Q and N-acetyl peptides, ESI-TRAP fragment characteristics. Peptides with IonScores exceeding the individually calculated 99% confidence limit or the 1% false discovery rate were considered as accurately identified. The peptide count is the sum of the peptide sequences of each protein identified over all samples and is an approximation of a protein's relative abundance. The results are given as the ratio of protein fragments identified on the E5 surface versus the E2 surface for three independent samples. For protein quantification ratios, values of greater than 1.5 and less than 0.5 are considered significant.

5.3.4 QCM-D Sensor Coating

Fetuin A (Sigma, Canada) was adsorbed individually to E2 and E5 surfaces to determine differences in protein layer mass and viscoelastic properties when adsorbed to

elastomer surfaces of different crosslink densities. Viscoelastic properties (thickness, shear modulus, and viscosity) were quantified using a quartz crystal microbalance with dissipation (QCM-D E1, Q-Sense). QCM-D sensors were coated according to the procedure described in Vyner *et al*. [80]. QCM-D sensors (Au, 4.95 MHz, 14 mm diameter, Q-Sense) were coated with ASCP prepolymer by spincoating (WS-400, Laurell Technologies). 1 mL of a 1% solution of ASCP pre-polymer in ethyl acetate (Fisher Scientific, Canada) with DMPA photoinitiator (3 mg photoinitiator per gram pre-polymer) was pipetted drop-wise onto a spinning sensor (4000 rpm, 5 min). The pre-polymer coated sensors were crosslinked under UV light (30 mW/cm^2, 5 min), dried overnight to remove excess solvent and stored in a desiccator when not in use.

5.3.5 QCM-D Measurements

QCM-D measurements of fetuin A adsorption were performed using the methods described in Vyner *et al.* [80]. To summarize, coated sensors were inserted into the QCM-D chamber and a baseline frequency and dissipation was established using phosphate buffered saline (PBS) (Sigma, Canada) (50 μL/min, 8 hours). Fetuin A solution (2 mg/mL or 20 mg/mL in PBS) was then pumped into the flow cell chamber (50 μL/min) for 10 minutes until the chamber was filled. The fetuin A solution flow rate was stopped and the fetuin A allowed to adsorb statically for 12 hours, approximating the adsorption that takes place on the elastomer surface in an *in vitro* cell culture (n=5). Fetuin A layer thickness, viscosity and shear moduli measurements were calculated using the Kelvin-Voigt viscoelastic model, assuming 1.4 g/mL as the density of a protein [119]. These fetuin A solution concentrations were chosen to

represent the concentration of fetuin A in 10% FBS supplemented culture media and 100% FBS, respectively [136].

5.3.6 Surface Plasmon Resonance

Surface plasmon resonance (SPR) was used to measure the mass of the fetuin A layer adsorbed from solution on E2 and E5. SPR sensor coating and SPR measurements were performed according to the methods in Vyner *et al*. [80]. SPR sensor chips (Au, Biacore) were coated with ASCP pre-polymer (20 μL of 0.1 mg/mL solution in ethyl acetate with 3 mg DMPA photoinitiator per 1 gram pre-polymer). The solvent was evaporated and the coated sensor was cross-linked under UV light (60 seconds, 30 mW/cm^2). The coated SPR sensors were dried overnight before the experiment. To measure the fetuin A adsorption, coated SPR sensors were inserted into SPR flow cell chamber (Biacore 3000, Biacore, Sweden) and a baseline measurement was achieved using PBS flow (10 μL/min, 5 min). After a baseline was established, 330 μL of fetuin A (2 mg/mL or 20 mg/mL) was injected into the flow cell and the coated sensor was exposed to the protein solution for 30 minutes. Following adsorption, the sensor was rinsed with PBS (10 μL/min) to remove loosely bound protein. Adsorbed protein mass was measured as the difference between the post-rinse signal (measured at 4000 s) and the baseline (measured at 500 s). Adsorbed masses were calculated as the average ± standard deviation of 3 sensors with 4 independent flow cells per sensor.

5.3.7 Cell culture

To determine if fetuin A was responsible for the previously observed [80] crosslink density dependent 3T3 proliferation on the E2 and E5 surfaces, cell culture experiments were performed with plasma, fetuin A, and basic fibroblast growth factor (FGF-2) supplemented media (Table 5.1). ASCP pre-polymer was fabricated according to the procedure described above and dissolved in 50 μL ethyl acetate per gram ASCP with 3 mg DMPA as photoinitiator per 1 gram of pre-polymer. 50 μL of the pre-polymer solution were pipetted into the wells of a 96 well TCPS tissue culture plate. The plates were loosely covered in aluminum foil to prevent premature crosslinking and incubated at room temperature overnight to remove residual solvent. The pre-polymer coated wells were then crosslinked under long-wave UV light (300-400 nm, 30 mW/cm^2, 5 minutes), sterilized under shortwave UV light for 30 minutes in a biological safety cabinet, and incubated in unsupplemented DMEM for 24 hours before cell seeding in order to ensure sterility. Frozen NIH-3T3 murine fibroblasts were thawed and expanded in DMEM supplemented with 10% FBS for 1 week

Table 5.1: Media supplementation for cell culture experiments

Figure	Label on graphs	Plasma (10%)	Fetuin A (2 mg/mL)	FGF-2 (37 pg/mL)
Figure 5.1B	E2 and E5 + P	+		
Figure 5.3A	E2 and E5 + Fet + P	+	+	
	E2 and E5 + P	+		
Figure 5.3B	E2 and E5 + Fet		+	
	E2 and E5			
Figure 5.4A	E2 and E5 + Fet + FGF + P	+	+	+
	E2 and E5 + FGF + P	+		+
	E2 and E5 + P	+		
Figure 5.4B	E2 and E5 + Fet + FGF		+	+
	E2 and E5 + FGF			+
	E2 and E5			

before seeding. For all cultures, the cells were passaged with 10X trypsin (Sigma, Canada), centrifuged and rinsed twice in unsupplemented DMEM to remove the FBS before the addition of the experimental culture media (Table 5.1). The cells were counted by hemocytometer, re-suspended in the experimental media and seeded at a density of 10,000 cells per well (n = 6). Cell culture was maintained for 14 days with time points at days 1, 3, 7, and 14 for the fetuin A supplemented culture and days 1, 3, 7, 10, and 14 for all other cultures. The medium in each well was changed every other day.

5.4 Statistics

Measurements are reported as the average value ± standard deviation of n replicates. Significant differences in the cell culture experiments were determined using a two way ANOVA followed by a Bonferroni *post-hoc* test (Prism 6, GraphPad, USA). Significant differences in adsorbed protein mass (SPR data) and protein layer viscoelastic properties (QCM-D data) were determined using a Student's t-test. Populations were considered significantly different at values of $p<0.05$. Differences in relative quantities of proteins from the LC-MS/MS proteomics data were considered significant at ratios of above 1.5 or below 0.5.

5.5 Results

5.5.1 NIH3T3 fibroblast culture with FBS and adult bovine plasma

NIH3T3 immortalized murine fibroblasts were cultured on elastomers prepared from 2000 g/mol (E2) and 5000 g/mol (E5) ASCP pre-polymers in DMEM supplemented 10% fetal bovine serum (FBS) (Fig. 5.1A, reprinted from Vyner, *et al.*, 2013 [80]) and 10% adult bovine plasma as a low growth control (Fig. 5.1B), with tissue culture polystyrene (TCPS) as a comparison surface. The fibroblasts proliferated more on the less stiff elastomer (E5) when cultured in FBS supplemented media over 14 days, whereas, when cultured on the stiffer elastomer (E2), the cells decreased in number after day 7. No proliferation or differences in

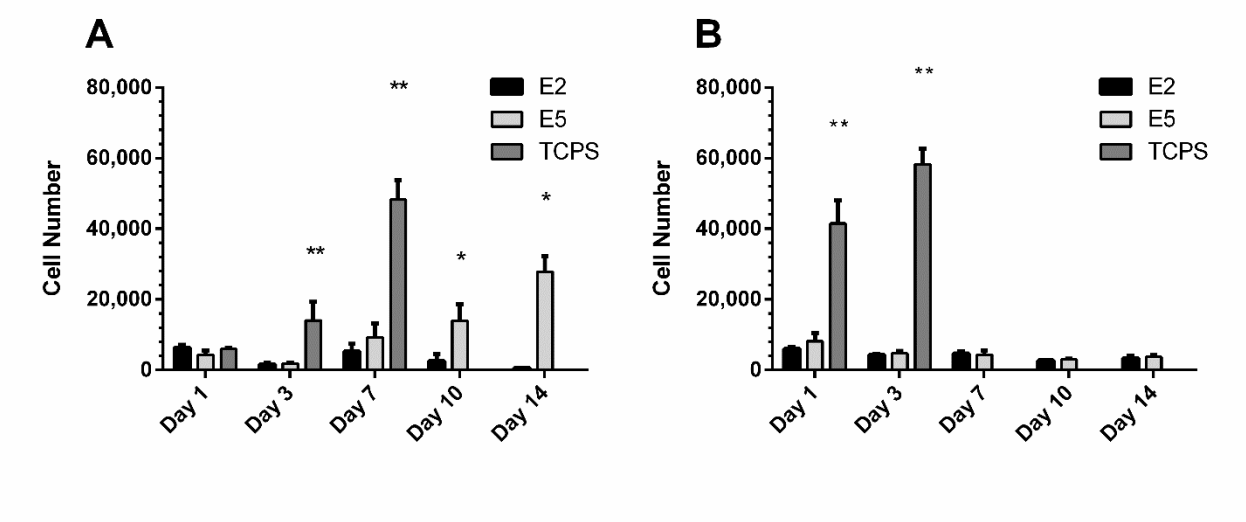

Figure 5.1: NIH3T3 fibroblast number when cultured on E2 and E5 surfaces over 14 days in (A) 10% FBS supplemented DMEM (reprinted with permission from Elsevier from Vyner *et al.*, 2013 [80]) and (B) 10% adult bovine plasma supplemented DMEM. *$p < 0.05$ compared to E2 surface. **$p < 0.05$ compared to both E2 and E5 surfaces (n=6).

proliferation were observed when the fibroblasts were cultured in 10% adult bovine plasma on the elastomer surfaces (Fig. 5.1B). Fibroblasts cultured on TCPS reached confluence when cultured in serum and plasma supplemented media after 7 and 3 days, respectively.

5.5.2 Quantitative Proteomics

Relative quantitation proteomics analysis [137] was used to determine the identities and ratios of proteins that adsorbed to E2 and E5 surfaces from FBS supplemented media in order to ascertain which protein(s), if any, were influencing fibroblast proliferation on the elastomer surfaces (Table 5.2). Because higher NIH3T3 fibroblast proliferation was observed on the E5 elastomer, it was hypothesized that proteins that aid in cell attachment adsorb in significantly greater quantities to the E5 surface. Additionally, because NIH3T3 fibroblasts do not grow on the elastomer surfaces when cultured in adult plasma supplemented media (Fig. 5.1B), a similar proteomics analysis was performed on proteins adsorbed to the elastomers from plasma supplemented media as a control to identify proteins that may influence fibroblast proliferation (Table 5.3).

Table 5.2: Ratios (E5:E2) of proteins that adsorbed from FBS supplemented media

Protein Name	Peptide Count	Sample 1 Ratio	Sample 2 Ratio	Sample 3 Ratio
Serum albumin [ALBU_BOVIN]	105	0.657	0.729	0.901
Alpha-1-antiproteinase [A1AT_BOVIN]	49	0.693	0.926	n.d.
Alpha-2-macroglobulin [A2MG_BOVIN]	27	0.433	**3.489**	1.248
Serotransferrin [TRFE_BOVIN]	24	0.576	**2.321**	**1.682**
Alpha-2-HS-glycoprotein [FETUA_BOVIN]	18	**2.073**	**1.846**	**1.516**
Fetuin-B [FETUB_BOVIN]	9	n.d.	0.829	0.895
Apolipoprotein A-I [APOA1_BOVIN]	8	1.285	1.060	n.d.
Complement C3 [CO3_BOVIN]	8	0.591	n.d.	1.087
Hemoglobin fetal subunit beta [HBBF_BOVIN]	7	**2.749**	n.d.	n.d.
Complement factor H [CFAH_BOVIN]	7	1.004	n.d.	n.d.
Hemoglobin subunit alpha [HBA_TRAST]	3	**3.060**	n.d.	n.d.
Vitamin D-binding protein [VTDB_BOVIN]	2	n.d.	**1.824**	n.d.
Inter-alpha-trypsin inhibitor heavy chain H3	2	n.d.	n.d.	0.865

n.d. = not detected

Table 5.3: Ratios (E5:E2) of proteins that adsorbed from adult bovine plasma suppl. media

Protein Name	Peptide Count	Sample 1 Ratio	Sample 2 Ratio	Sample 3 Ratio
Bovine serum albumin [SWISS-PROT:P02769]	683	0.888	0.828	1.382
FGG protein [Q3SZZ9_BOVIN]	340	0.816	0.650	0.877
Complement C3 [CO3_BOVIN]	197	0.646	0.484	0.721
Fibrinogen alpha chain [A5PJE3_BOVIN]	182	0.760	0.546	0.872
Serotransferrin [G3X6N3_BOVIN]	128	1.000	0.676	1.435
Haptoglobin [G3X6K8_BOVIN]	82	0.614	0.449	0.703
Serpin A3-2 [SPA32_BOVIN]	55	0.892	0.000	1.359
Inter-alpha-trypsin inhibitor chain H4 [F1MMD7_BOVIN]	53	0.842	0.600	1.230
Vitamin D-binding protein [F1N5M2_BOVIN]	37	0.904	0.654	1.259
Plasminogen [E1B726_BOVIN]	35	0.679	0.526	0.831
Complement factor H [F1MC45_BOVIN]	32	0.501	0.401	0.822
Hemopexin [HEMO_BOVIN]	30	0.740	0.534	1.259
Kininogen-1 [F1MNV5_BOVIN]	18	0.972	0.604	1.583
Primary amine oxidase, [AOCX_BOVIN]	15	0.714	0.607	1.192
Complement C5a [F1MY85_BOVIN]	14	0.785	1.087	0.722
Serpin A3-8 [SPA38_BOVIN]	14	0.427	0.000	3.690
Lipopolysaccharide-binding protein [F1MNN7_BOVIN]	12	0.779	0.523	0.500
Complement factor B [TREMBL:Q3KUS7]	12	0.767	0.275	1.145
C-reactive protein [C4T8B4_BOVIN]	12	0.000	0.000	0.703
Cumulus cell-specific fibronectin 1 trans. [B8Y9T0_BOVIN]	10	0.638	0.621	1.195
Gelsolin [F1MJH1_BOVIN]	9	0.673	0.230	0.639
Alpha-1-B glycoprotein [TREMBL:Q2KJF1	8	0.561	0.000	0.747
Complement component C7 [F1N045_BOVIN]	8	1.023	0.525	0.553
Hemoglobin subunit beta [SWISS-PROT:P02070]	8	0.000	0.000	1.004
Antithrombin-III [F1MSZ6_BOVIN]	7	0.986	0.894	1.198
Hemoglobin subunit alpha [SWISS-PROT:P01966]	6	0.643	0.000	0.580
Complement component C6 [F1MM86_BOVIN]	6	0.459	0.000	0.584
Inter-alpha-trypsin inhibitor chain H2 [F1MNW4_BOVIN]	5	0.777	0.462	1.027
Complement C1q subcomponent subunit B [C1QB_BOVIN]	5	0.506	0.000	0.536
Inter-alpha-trypsin inhibitor chain H1 [F1MMP5_BOVIN]	5	0.828	0.000	0.827
Coagulation factor V [F1N0I3_BOVIN]	4	0.376	0.000	0.577
Glutathione peroxidase [G3X8D7_BOVIN]	4	1.698	0.000	3.271

The composition of the protein layers adsorbed from fetal serum and adult plasma reflects the composition of the respective source solutions from which they are adsorbed. Serum albumin is the most abundant protein adsorbed from both solutions, followed by alpha-1-antiproteinase from fetal serum and fibrinogen from adult plasma. Despite our earlier hypothesis, no differences were detected in the adsorption of fibronectin, or any other protein

that supplies integrin binding sites, on the elastomers in the presence of fetal serum. This result suggests that such proteins were not responsible for influencing differences in 3T3 proliferation on these elastomers when cultured in serum supplemented medium.

In the adsorbed serum layer, a few proteins were identified that adsorbed preferentially to the E5 surface, in at least one of the samples, and were considered to have possibly been responsible for the previously observed difference in cell proliferation: alpha-2-HS-glycoprotein (fetuin A), alpha-2-macroglobulin, and serotransferrin. Of these three proteins, fetuin A was considered the most logical candidate for further investigation for three reasons. Firstly, fetuin A has been previously suggested to influence cell attachment and proliferation [138]. While its biological function is still undefined, fetuin A is known to bind large quantities of calcium [138] and is believed to improve cell attachment by promoting annexin binding [139,140]. Secondly, there was a significant difference in the quantity of adsorbed fetuin A between the E2 and E5 surfaces for all three proteomics samples despite FBS batch-to-batch variation, which is consistent with our repeatable cell proliferation results [79,80]. Thirdly, fetuin A is present in high abundance in protein layers adsorbed from fetal serum but is not present in protein layers adsorbed from adult plasma, which is consistent with the result that fibroblast proliferation on the elastomers only occurs in FBS supplemented media.

Finally, it should be noted that there may be proteins differentially adsorbed to the elastomers that are undetectable by LC-MS/MS due to low abundance, such as integrin binding proteins, for which no differences in adsorbed quantity were detected. While it is possible that one or more of these proteins may also influence cell behavior, we do not believe that they would be responsible for the observed differences in cell proliferation, due to their low abundance. Because integrin binding proteins provide physical anchorage to cells, a low

abundance of integrin binding proteins present on a surface would not be able to contribute a significant number of integrin binding sites to attaching cells. Therefore, because these integrin binding proteins did not appear to be present on these elastomers in quantities high enough to detect, they were not considered to be significantly contributing to the previously observed difference in fibroblast proliferation.

5.5.3 Fetuin Adsorption

Surface plasmon resonance (SPR) and quartz crystal microbalance with dissipation (QCM-D) were used to quantify the mass (Fig. 5.2A), thickness (Fig. 5.2B), shear modulus (Fig. 5.2C), and viscosity (Fig. 5.2D) of fetuin A layers adsorbed to E2 and E5 surfaces. SPR measurements quantify the "dry mass" of the protein (*i.e*. the mass of the protein layer excluding bound water), whereas QCM-D measurements are considered "wet measurements" and include the contribution of water molecules bound within the protein layer after adsorption. For both concentrations, significantly more fetuin A adsorbed to the E5 surface, consistent with the FBS proteome results. The fetuin A layers adsorbed to E5 were both thicker and possessed a lower shear modulus. Comparatively, the "dry masses" (SPR measurements) of these layers are more similar than the "wet thicknesses" measured by QCM-D (approximately 7 times thicker on the E5 surface), suggesting that the fetuin A adsorbed to the E5 surface contains much more bound water compared to the E2 surface, which may indicate indicating a difference in adsorbed fetuin A conformation on the elastomer surfaces. Interestingly, these significant differences are less pronounced when the

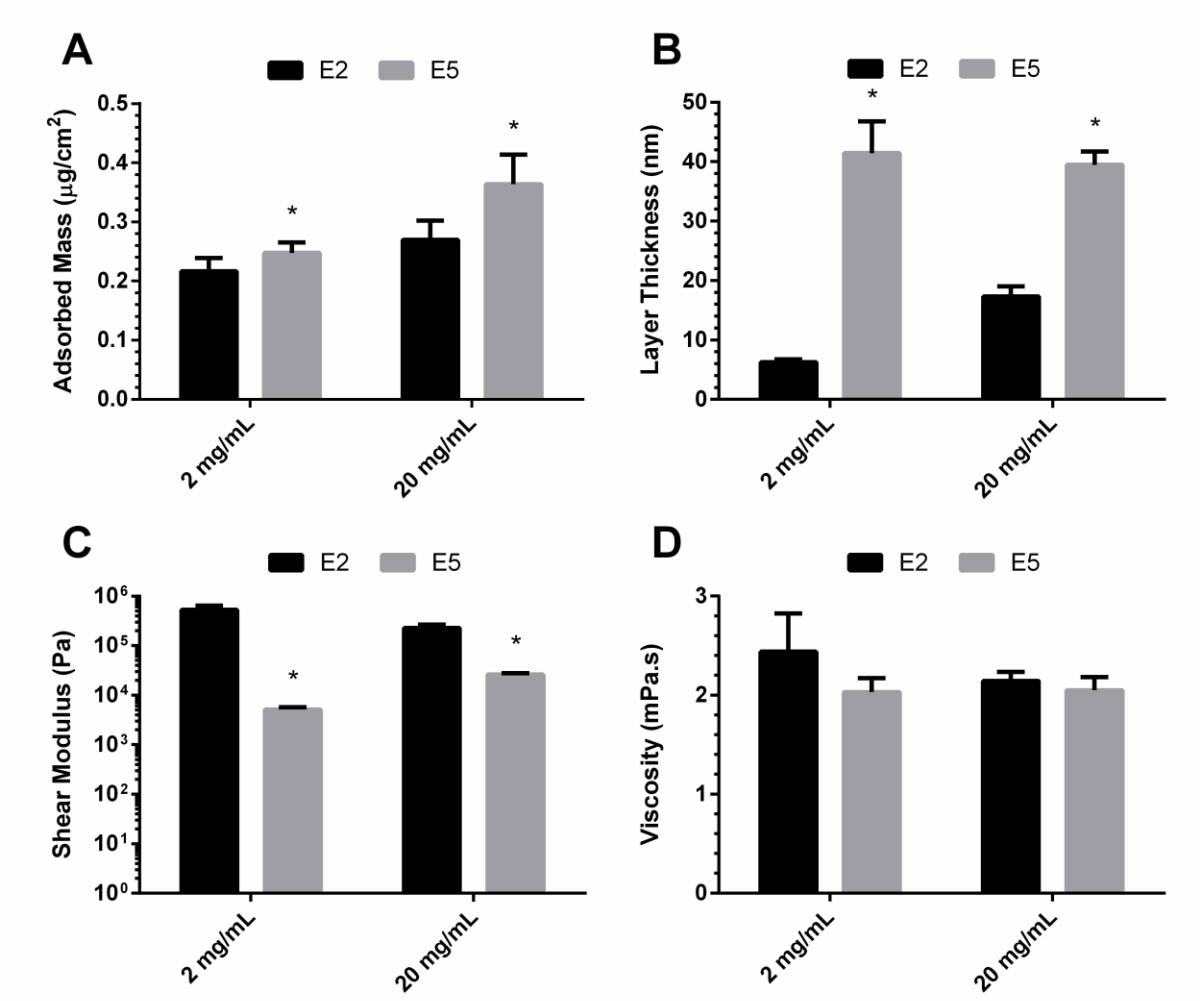

Figure 5.2: Mass and viscoelastic properties of the fetuin A layer adsorbed to the E2 and E5 surfaces from solutions of 2 mg/mL and 20 mg/mL fetuin A in PBS. (A) Fetuin A layer mass, (B) thickness, (C) shear modulus, and (D) viscosity. *$p < 0.05$ compared to E2 surface, (n=5).

fetuin A solution is of higher concentration. It is likely that the elastomer surfaces were saturated with tightly adsorbed protein at both concentrations. However, because the protein was adsorbed in the absence of flow (static adsorption), the protein layers that adsorbed from the higher concentration solution probably included more loosely bound protein, which was incorporated into the thickness measurements.

5.5.4 Fetuin supplemented fibroblast culture

To determine if fetuin A was influencing cell proliferation on the two elastomers, NIH3T3 fibroblasts were cultured on E2 and E5 surfaces in DMEM supplemented with 2 mg/mL fetuin A, with (Fig. 5.3A) and without (Fig. 5.3B) 10% adult bovine plasma. For both the plasma and non-plasma cultures, supplementation with fetuin A significantly improved attachment on both elastomers compared to the cultures without fetuin A supplementation. Furthermore, fetuin A significantly improved the cell attachment on the E5 surface compared to the E2 surface when added to DMEM supplemented with 10% plasma. No differences in cell attachment were observed between the elastomer surfaces when fetuin A was added to DMEM without plasma. It is possible that, when adsorbed in the presence of plasma, the fetuin A that adsorbed to the E2 surface was replaced by other proteins, while the fetuin A

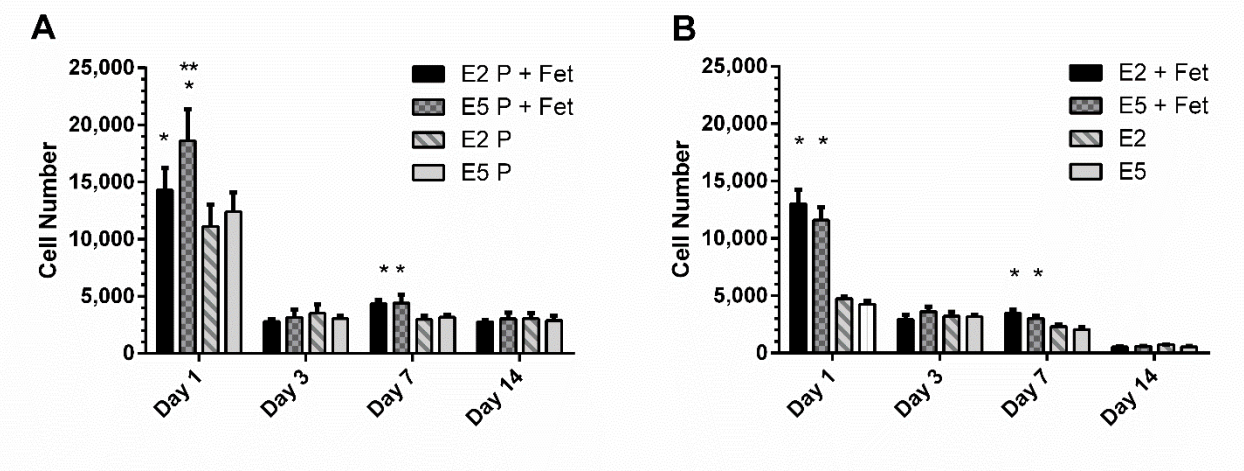

Figure 5.3: NIH3T3 fibroblast number when cultured over 14 days on the E2 and E5 surfaces in DMEM supplemented with (A) 10% plasma, 2 mg/mL fetuin A and (B) 2 mg/mL fetuin A, only. *$p < 0.05$ compared to non-fetuin A group, **$p < 0.05$ compared to E2 surface, (n=6).

that adsorbed to the E5 surface was more tightly bound and resisted replacement. However, when fetuin A was the only protein present in the media, it adsorbed in similar monolayers on both surfaces, which elicited a similar cell response. Finally, in the absence of fetuin A, attachment was significantly improved with the presence of plasma on both the E5 and E2 surface, most likely due to the presence of adsorbed fibrinogen, which can act as a source of integrin binding sites [141].

After day 1, cell number decreased and did not increase again over 14 days, suggesting that fetuin A alone is not responsible for the observed difference in fibroblast proliferation. Because the original fibroblast proliferation result was observed in a fetal serum supplemented environment and not in an adult plasma supplemented environment, it was hypothesized that fetuin A acts in conjunction with a growth factor present in serum to promote fibroblast proliferation. To determine the effect of fetuin A in the presence of a growth factor on fetuin supplemented culture, 3T3 fibroblasts were cultured in DMEM supplemented with 10% plasma, fetuin A (2 mg/mL), and basic fibroblast growth factor (FGF-2, 37 pg/mL) (Fig. 5.4A) or fetuin A and FGF-2 alone (Fig. 5.4B). FGF-2 was chosen because it is a relatively abundant growth factor in FBS, but is present in very low concentrations in adult bovine plasma [132].

Cells grown in media supplemented with plasma, fetuin A and FGF-2 proliferated after day 10 on the E5 surface, but no proliferation occurred on the E2 surface. This result resembles the previously observed NIH3T3 fibroblast proliferation result (Fig. 5.1A), however the onset of proliferation was delayed (after day 10 *vs.* after day 3) compared to the previous result. In the absence of fetuin A, despite the addition of growth factor, no proliferation occurred on either elastomer surface.

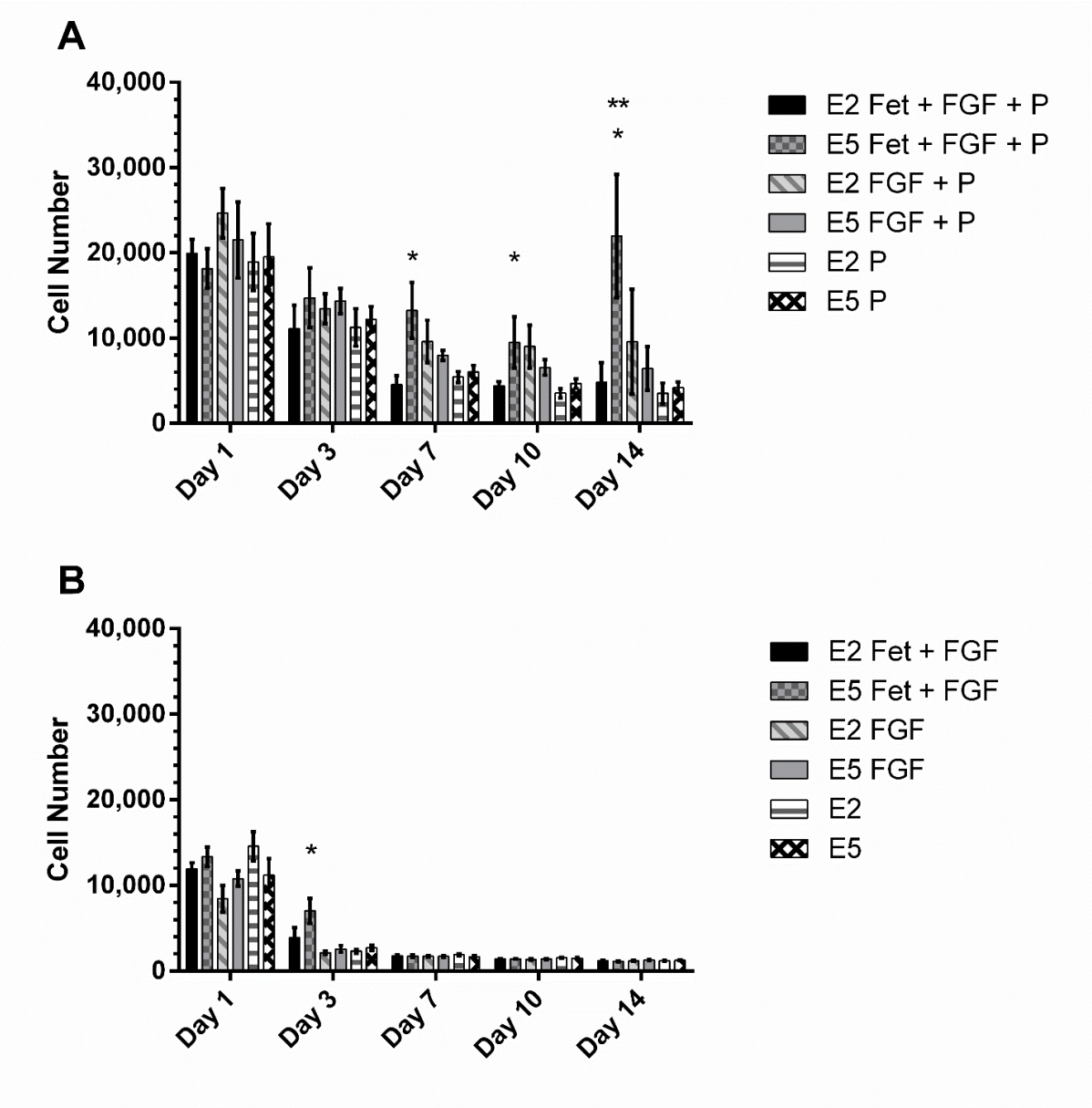

Figure 5.4: NIH3T3 cell number when cultured over 14 days on the E2 and E5 surfaces in DMEM supplemented with (A) fetuin A (2 mg/mL), FGF-2 (37 pg/mL) and 10% plasma or (B) fetuin A (2 mg/mL) and FGF-2 (37 pg/mL), only. *$p < 0.05$ compared to E2 surface, **$p < 0.05$ compared to E5 + FGF + P and E5 + P, (n=6).

Fibroblasts grown without plasma supplementation did not proliferate over 14 days. Cells grown in fetuin A and FGF-2 supplemented media without plasma maintained their number longer than the FGF-2 and unsupplemented groups, but decreased in number after day

3, suggesting that other plasma/serum proteins in addition to fetuin A are necessary for cells to attach and proliferate beyond the initial days of culture.

5.6 Discussion

Previously, NIH3T3 fibroblasts were found to proliferate more on a less stiff elastomer when cultured in FBS supplemented media. It was hypothesized that the observed difference in cell proliferation on the different elastomer surfaces was due to a difference in the proteins that adsorbed to the surfaces from the serum-supplemented culture media. Polymer stiffness is dependent on chain mobility, and bulk elasticity is reflected in surface elasticity [84]. The purpose of this study was two-fold: to determine if polymer chain mobility at the interface could affect the protein layers that adsorb from competitive protein environments (e.g. FBS or plasma supplemented media) and to identify which adsorbed protein(s), if any, could be responsible for the observed difference in fibroblast proliferation.

NIH3T3 fibroblasts cultured in 10% FBS proliferated on the E5 surfaces much more than the E2 surface, however fibroblasts cultured in 10% plasma supplemented media did not proliferate at all. Compared to FBS, adult plasma is comprised of greater amounts of fibrinogen and immunoglobulins, and lower concentrations of fetal proteins and growth factors [132,142,143]. That the fibroblasts did not proliferate on either elastomer in adult plasma supplemented environments, suggested that the protein(s) responsible for the difference in fibroblast growth on the elastomer surfaces was(were) likely to be of much lower abundance in adult plasma. Interestingly, 3T3 cells attached in higher numbers and reached confluence on TCPS surfaces faster when cultured on TCPS surfaces in adult plasma supplemented media.

This is likely due to a higher concentration of fibrinogen (not found in FBS) adsorbed to the TCPS surfaces in plasma supplemented environments. Additionally, the fibrinogen adsorbed to relatively hydrophilic TCPS may be adsorbed in a conformation that exposes more of its integrin binding sites than on the hydrophobic elastomer surfaces. A higher concentration of integrin binding sites would promote both attachment and proliferation of 3T3 cells.

The composition of the protein layers adsorbed to the elastomers from fetal serum and adult plasma reflect their relative abundance in the source solution [132,144], and elastomer stiffness affected the composition of protein layers adsorbed in a competitive adsorption environment. Previously, we proposed that polymer chain mobility influenced the configurational entropy and arrangement of the water bound to the polymer chains at the polymer aqueous interface, which affected the adsorption of proteins from single protein solutions. In our previous study, ATR-FTIR measurements showed that despite no difference in surface chemistry, the elastomer with more flexible polymer chains (E5) absorbed more water into its surface compared to E2 [80]. Additionally, other studies have emphasized the influence of absorbed and bound water in the adsorption of individual proteins and cell response [67,77].

Similar principles would apply to a competitive adsorption environment, such as serum or plasma supplemented cell culture media. In solutions of multiple proteins, small, abundant proteins adsorb first, and may be replaced later by larger proteins of lower abundance, which frees more bound water and generates an increase in the entropy of the system. A difference in system entropy prior to adsorption via differences in polymer chain flexibility may alter the likelihood that a particular protein will adsorb or, in a competitive environment, whether an

adsorbed protein will be replaced, leading to a difference in the final composition of the equilibrium protein layer.

The adsorbed serum proteomics analysis also identified a protein that adsorbed preferentially to the E5 surface: alpha-2-HS-glycoprotein (fetuin A), which we considered to be a likely candidate as a protein responsible for influencing fibroblast proliferation. Approximately twice as much fetuin A adsorbed to the E5 surface compared to the E2 surface and the fibroblast proliferation on the E5 surface was more than two-fold greater. When fetuin A was adsorbed individually to the elastomers, differences were measured in adsorbed protein mass, layer thickness and shear modulus, indicating differences in adsorbed protein conformation [75] or compositional differences such as more water bound in the protein layer. Because fetuin A is a calcium binding protein, it is possible that the protein conformation and amount of water bound in the protein layer are also related to the calcium binding capabilities of the protein. A thinner, stiffer protein layer suggests that fetuin A is adsorbed in a more unfolded conformation on the E2 surface, which has reduced its ability to support cell proliferation.

Fibroblasts cultured in serum free media with adult plasma, fetuin A, and FGF-2 (Fig. 5.4A) increased in cell number on the E5 surface only, resembling the fibroblast number trends observed in the earlier culture (Fig. 5.1A), and suggesting that the presence of surface adsorbed fetuin A combined with at least one growth factor influenced fibroblast proliferation. In the absence of fetuin A and/or plasma, however, no proliferation occurred on either surface, implying that the presence of fetuin A, alone, is not sufficient to support proliferation and other proteins and growth factors present in plasma may also contribute to the fibroblast response. Additionally, the onset of proliferation was delayed (after day 10 *vs*. after day 3) compared to

the previous result (Fig. 5.1A), suggesting that there are most likely other growth factors and/or proteins present in FBS that interact with fetuin A to improve proliferation. Possible candidates for other growth factors are IGF and TGF-β1, both of which are highly abundant in FBS [132].

Previously, fetuin A has been investigated as a supplement added to serum free media where it improved attachment and proliferation for a variety of cell types [145–147]. However, this study is the first to associate cell proliferation to quantities of fetuin A adsorbed to a biomaterial surface. Given its ability to bind calcium, a fetuin A influenced increase in cell proliferation could be due to a local increase in calcium concentration at the material surface. An increase in calcium may improve cell attachment via cadherin and annexin binding, both of which are calcium dependent. Though no differences in integrin binding proteins were detected on the elastomer surfaces, they may have been present below the limit of detection of the proteomics method. Integrin binding is known to mediate cellular behavior via intracellular calcium concentration [148]. Though the amount of integrin binding proteins on the surfaces may have been low, a high local concentration of calcium may have improved the efficacy of integrin binding. An increase in the local calcium concentration may also improve the efficacy of growth factors and the activity of growth factor receptors. High affinity fibroblast growth factor receptors are able to bind calcium, which alters the receptor conformation and is hypothesized to stabilize interactions between the receptor and cell adhesion molecules or other growth factors [149]. Further calcium depletion studies must be performed to determine whether the Fetuin A improves cell attachment and/or proliferation via calcium binding mechanisms. Fetuin A, therefore, may be useful as a biomaterial co-coating or co-surface modifier, as an inexpensive method to improve cell attachment and proliferation when used in conjunction with integrin binding proteins/peptides or added growth factors.

Given this discussion of calcium binding mechanisms, it is important to note the sources of calcium present in *in vitro* cell culture systems. DMEM comes in many formulations which may vary in calcium concentration. Additionally, many proteins (e.g. albumin, fetuin A) found in FBS and adult plasma bind calcium and may increase the calcium concentration in the culture media when used as supplements. 3T3 fibroblasts, specifically, have been shown to reach a proliferative maximum at calcium concentrations above 0.5 mM [150], far below the calcium concentration in the basal DMEM used here (1.8 mM), before the addition of FBS/adult plasma. Fetuin A is hypothesized here to promote growth by affecting the local calcium concentration at the material surface, however further studies which both deplete calcium and increase calcium concentration would be useful in determining the extent to which fetuin A may function to influence 3T3 proliferation.

Finally, this research emphasizes the importance of investigating competitive protein adsorption instead of the adsorption of individual proteins, as well as the use of quantitative proteomics to investigate protein adsorption to biomaterials and improve biomaterial compatibility. There is a prominent focus in biomaterials literature on the adsorption of proteins that provide integrin binding sites as a way to improve cell attachment and proliferation on tissue scaffolds. The proteome data presented here shows that integrin binding proteins were not present in different quantities on these surfaces and, therefore, suggests that such proteins are unlikely to be responsible for the differences in fibroblast attachment and proliferation observed. Instead, cell attachment and proliferation appear to be mediated via calcium dependent attachment mechanisms. Emphasis on adsorption of, and cellular response to, individual protein layers gives an incomplete understanding of protein adsorption *in vivo* or *in vitro*. As proteomics technology improves, more focus should be directed to investigating

biomaterial interactions with complete serum in contrast to plasma environments, and the subsequent effects on cell behavior.

5.7 Conclusions

The objective of this work was to determine the effect of polymer chain flexibility on protein adsorption in a competitive protein adsorption environment. We also wanted to determine if a previously observed polymer chain flexibility dependent fibroblast proliferation was due to the adsorption of a particular protein(s). The proteomics results showed that polymer chain flexibility affected protein adsorption in competitive adsorption environments such as FBS and adult bovine plasma supplemented culture media. Identification and relative quantitation of protein adsorbed to the elastomers from FBS supplemented media suggested that the adsorption of fetuin A on the elastomer surfaces may be influencing cell proliferation. Further cell culture experiments showed that fetuin A improved cell proliferation over 14 days when plasma and FGF-2 were also present in the media, suggesting that fetuin A acts in conjunction with other proteins and growth factors to mediate cell proliferation. Because fetuin A appears to be acting at the material surface, possibly by increasing the local calcium concentration, it may be useful as a biomaterial co-coating or co-surface modifier along with cell adhesion molecules to improve cell attachment or the efficacy of growth factors.

Chapter 6

The Effect of Poly(trimethylene carbonate) Molecular Weight on Macrophage Behavior and Enzyme Adsorption and Conformation

6.1 Objectives Completed

Chapter 6 describes fulfillment of objective 3 which was to determine whether the molecular weight dependent macrophage mediated degradation of poly(trimethylene carbonate) (PTMC) was due to a difference in macrophage attachment, macrophage activity or enzymatic activity on the 60 kg/mol and 100 kg/mol PTMC surfaces (60PTMC and 100PTMC, respectively). It was hypothesized that 100PTMC degrades faster than 60PTMC because the macrophages either adhere in greater numbers or secrete more degradative species on the 100PTMC surface. 60PTMC and 100PTMC surface hydrophilicity, bulk modulus, surface modulus, glass transition temperature, surface roughness and surface water absorption were determined by water contact angle, double indentation test, nano-indentation, DSC, AFM, and ATR-FTIR, respectively. RAW 264.7 macrophages were cultured on 60 kg/mol and 100 kg/mol PTMC surfaces and macrophage attachment and proliferation, reactive oxygen species secretion and esterase secretion were measured. To compare the susceptibility of 60PTMC and 100PTMC to enzymatic degradation, 60PTMC and 100PTMC were incubated in solutions of cholesterol esterase and lipase, two enzymes which are thought to be responsible for the degradation of PTMC. Enzymatic adsorption quantity, thickness, shear modulus and viscosity were measured by SPR and QCM-D.

Chapter 6 was published in *Biomaterials* on August 7, 2014. All experiments and data described herein were performed and collected by me with the exception of the experiment measuring the enzymatic degradation of PTMC (Figure 6.3), which was performed by Anne Li, an undergraduate thesis student under my supervision and the nano-indentation experiments performed by Tong Liu at the Department of Mechanical and Mechatronics Engineering, University of Waterloo as a fee-for-service. SPR experiments were performed by me in the Protein Function Discovery Facility at Queen's University. I am the first author of the paper and Anne Li is listed as second author.

6.2 Introduction

High molecular weight poly(trimethylene carbonate) (PTMC) is increasingly being investigated as a biomaterial for soft tissue regeneration [1,151,152], surgical devices [81,153,154], and drug delivery applications [155–157]. This interest is, in part, due to its degradation mechanism. PTMC degrades *in vivo* but, unlike the commonly used poly(hydroxy acids) such as poly(lactide-*co*-glycolide), does not do so via hydrolysis and does not yield acidic degradation products [82,158]. Rather, PTMC degrades *in vivo* via macrophage mediated enzymatic and/or oxidative degradation as a result of frustrated phagocytosis [65,103]. Upon failure to engulf the material, macrophages attach to the surface and secrete hydrolytic enzymes and reactive oxygen species to attempt to degrade the surface [159].

Interestingly, the *in vivo* degradation behavior of PTMC is molecular weight dependent. PTMC with molecular weight greater than 100 kg/mol has been reported to degrade faster *in vivo* than lower molecular weight (<70 kg/mol) PTMC [82]. Similar degradation

behavior has been reported for other poly(alkylene carbonates) such as poly(ethylene carbonate) (PEC) [160].

The reason for the molecular weight dependent degradation rate of PTMC is, as yet, unclear and there is evidence for different mechanisms. PTMC is known to be susceptible to enzymatic degradation by cholesterol esterase [161] and lipase [82]. Zhang et al. observed that *in vitro* incubation in lipase alone resulted in faster degradation of 291 kg/mol PTMC compared with 69 kg/mol PTMC. This result was proposed to be caused by the greater hydrophilicity of the lower molecular weight surface after aqueous conditioning, which could alter the conformation of the enzyme when adsorbed at the PTMC interface, thereby reducing its activity [162].

It has also been suggested that the primary degradation mechanism of both PTMC and PEC is oxidation [103,163,164]. Oxidative degradation occurs *in vivo* as part of frustrated phagocytosis when macrophages attach to the material surface and secrete reactive oxygen species such as nitrates/nitrites, hydroxyl radicals and superoxide anions [165]. Of these, the superoxide anion is believed to be responsible for the *in vivo* oxidative degradation of PTMC [65,103,163,166].

A third explanation for the difference in degradation rate may be that the macrophages preferentially attach to, or are more active on, PTMC with molecular weights greater than 100 kg/mol PTMC as compared to PTMC with molecular weights lower than 70 kg/mol [74]. For example, the molecular weight of PTMC may influence the polymer surface properties, such as chain mobility or orientation of hydrophilic regions of the polymer chain, which, in turn, may influence the adsorption of adhesive or antibody proteins such as fibronectin and immunoglobulins [60,75,66,80]. A difference in quantity or conformation of proteins may then

affect macrophage attachment, secretion of reactive oxygen species, or production of degradative enzymes [74].

In this study, we attempted to determine the reason for the molecular weight dependence of degradation rate observed with PTMC. Macrophage number and the secretion of both reactive oxygen species and esterase were measured when cultured on the surfaces of 60 kg/mol PTMC and 100 kg/mol PTMC *in vitro*. To determine whether there were differences in enzyme conformation following adsorption to the 60PTMC and 100PTMC surfaces, we also examined the quantity and viscoelastic properties of adsorbed cholesterol esterase and lipase, two enzymes implicated in the macrophage mediated degradation of poly(alkylene carbonates) [65,82,167].

6.3 Materials and Methods

6.3.1 PTMC Synthesis

Poly(trimethylene carbonate) was synthesized from trimethylene carbonate (TMC) monomer by ring-opening melt polymerization. TMC monomer (Biomatrik, China), initiator and stannous 2-ethylhexanoate (Fisher Scientific, Canada) catalyst were placed in a flame-dried glass ampoule and flame-sealed under vacuum. Molecular weights were targeted at 60 kg/mol (60PTMC) and 100 kg/mol (100PTMC). 1-pentanol (Sigma Aldrich, Canada) was used as an initiator for the preparation of 60PTMC. For 100PTMC, no initiator was added and residual water served as the acting initiator. The polymerization proceeded for 15 h at 130 ºC. After polymerization was completed, the PTMC was dissolved in dichloromethane (DCM, Fisher Scientific, Canada), filtered through a 20 μm filter (P8, Fisherbrand) to remove glass

particles, and purified by precipitation in methanol at -20 ºC. Molecular weight was measured using gel permeation chromatography (GPC, Viscotek GPCmax VE 2001) at 25 ºC using tetrahydrofuran (THF, Fisher Scientific, Canada) as the eluent (1 mL/min). Molecular weight was determined by a universal calibration using a polystyrene standard.

6.3.2 Contact Angle Measurements

Sessile drop water contact angles were measured on films of 60PTMC and 100PTMC. To form the films, a 0.3 g/mL PTMC in DCM solution was pipetted onto glass coverslips (22 mm x 22 mm), covered with aluminum foil to prevent the formation of bubbles, and dried overnight. Even layers were confirmed by caliper measurement of the edge thickness of the coated coverslips. Coating thickness was approximately 0.7 mm. Contact angles were measured for both dry samples and samples that had been conditioned for 24 h and 7 days in distilled water. For these measurements, 1 μL of distilled water was deposited on the surface of the flat, coated coverslip. (VCA Optima XE, AST Products Inc.). Measurements were taken after 30 seconds of equilibration. Contact angles are reported as the average ± standard deviation of 3 samples with 5 drops measured at random locations per sample.

6.3.3 Glass Transition Temperature Measurements

Glass transition temperatures (T_g) of 60PTMC and 100PTMC were measured using differential scanning calorimetry (DSC 1, Mettler Toledo). The samples were cooled to -45 °C and run using a heating-cooling-heating cycle from -45 to 25 °C. Glass transition temperatures

were determined for both dry samples and samples that had been conditioned in distilled water for 24 h (n=2) and 7 days (n=2). Glass transition temperatures were measured from the second heating cycle.

6.3.4 Water Uptake Measurement

Water uptake was determined by gravimetric analysis. Dry samples (n=2) of 60PTMC and 100PTMC were weighed and conditioned in distilled water for 24 h and 7 days. Surface water was removed by blotting with Kimwipes™ before weighing the samples a second time. Water content is reported as average percent mass gained after conditioning in water.

6.3.5 Enzymatic Degradation of pTMC

Discs (6 mm diameter, 0.3 mm thick) were punched from films of 60PTMC and 100PTMC and incubated in solutions of porcine pancreas cholesterol esterase [168] (1 U/mL, phosphate buffered saline (PBS), Worthington) and lipase [169] (Thermomyces languinosus, >100,000 U/mL, Sigma, used as received). The discs were dried and weighed prior to incubation. Enzyme solutions were replaced every other day. Samples were removed from the solutions at 1, 5, 7 and 9 weeks. At each time point, the PTMC samples were removed from the enzyme solution, rinsed in distilled water, lyophilized for 48 h and weighed. Degradation is reported as percent of original mass lost (n=3).

6.3.6 Macrophage Culture

Macrophages were cultured on 60PTMC and 100PTMC surfaces to determine differences in cell number, esterase production and ROS/superoxide anion production. 60PTMC and 100PTMC were dissolved in DCM (0.3 g/mL). The PTMC solutions were pipetted into the wells of 96-well TCPS plates (50 μL/well). Coated well plates were dried for 16 h, sterilized under UV irradiation in a laminar flow hood for 30 min and conditioned in media for 12 h prior to seeding. RAW 264.7 immortalized murine monocyte derived macrophages were seeded in the coated wells, as well as into uncoated TCPS wells to act as a comparison surface, at a density of 30,000 cells/cm^2. The cells were cultured in DMEM supplemented with 10% fetal bovine serum (FBS) and 1% antibiotic/antimycotic. The medium was replaced every other day.

6.3.7 Macrophage Culture Analysis

Adherent macrophages were removed from the wells prior to analysis. 200 μL of non-enzymatic cell dissociation media (Sigma) was added to the wells. Macrophages were then removed from the wells by scraping followed by sonication for 30 seconds.Macrophage number was determined by a fluorescent DNA binding assay (Quantifluor, Promega, n=6) and ROS/superoxide production was measured using a ROS/superoxide fluorescent detection kit (Enzo, n=6). Macrophage esterase production was determined by measuring the change in absorbance of p-nitrophenol (pNP) which is generated when active esterases hydrolyze p-nitrophenyl acetate (pNPA) [170] (n=6). Briefly, 50 μL of sample cell suspension and 50 μL of phosphate buffer (50 mM, pH 7.4) were pipetted into the wells of a black 96-well assay

plate. 20 μL of pNPA (10 mM, DMSO) were added to the wells with a multichannel pipette. Absorbance of pNP (410 nm) was immediately measured for 90 seconds with one measurement per second. Activity of esterase was measured as change in absorbance of pNP (410 nm) per second.

6.3.8 Scanning Electron Microscopy

To acquire images of PTMC degradation by macrophages, the bottoms of cell culture inserts (PET, Falcon, 12 well format) were coated with 60PTMC and 100PTMC (0.3 g/mL in DCM), covered in aluminum foil and allowed to dry overnight. Coated cell culture inserts were sterilized by UV irradiation in a laminar flow hood and conditioned in media for 12 h prior to cell seeding. Cells were seeded at 30,000 cells/cm^2. At days 1 and 14, the cells were removed from the PTMC surfaces by incubation in non-enzymatic cell dissociation solution (Sigma) for 5 min. The surfaces were dehydrated in a graduated ethanol series and chemically dried overnight using hexamethyldisilazane. After drying, the cell culture insert membranes were cut out of the inserts using a scalpel, affixed to SEM stubs, sputter coated with gold (10 mA, 4 min), and imaged using a Hitachi S-2300 scanning electron microscope at an accelerating voltage of 15 kV.

6.3.9 QCM-D Sensor Coating

Thickness, modulus and viscosity of enzyme layers adsorbed to 60PTMC and 100PTMC were quantified using a quartz crystal microbalance with dissipation (QCM-D E1,

Q-Sense). Gold QCM-D sensors (4.95 MHz, 14 mm diameter, Q-Sense) were spin-coated (WS-400, Laurell Technologies) with a 1% solution of PTMC in chloroform. 50 μL of the solution was pipetted onto the stationary sensor before spinning (1400 rpm, 5 min). The coated sensors were dried overnight at room temperature and stored in a desiccator until used. The thickness and surface roughness of the polymer coating were determined using QCM-D measurements and atomic force microscopy, described below, respectively.

6.3.10 QCM-D Protein Adsorption

Dry PTMC coated sensors were inserted into the QCM-D chamber. Phosphate buffered saline (pH 7.4, Sigma) was flowed over the sensor (50 μL/min) for 8 h until stable frequency and dissipation baselines were measured. Enzyme solution (1 mg/mL cholesterol esterase in PBS or 1 mg/mL lipase (porcine pancreas, Sigma in PBS) was then flowed into the sensor chamber (50 μL/min) for 10 min until the chamber was filled. The flow of the enzyme solution was then halted and the enzyme allowed to adsorb statically for 24 h, approximating the adsorption that takes place in a static degradation study (n=3).

6.3.11 Surface Plasmon Resonance

Surface plasmon resonance was used to quantify mass of enzyme adsorbed from a solution of cholesterol esterase (1 U/mL) or lipase (1 mg/mL). Unmodified gold SPR sensor chips (Au, Biacore) were coated with 60PTMC and 100PTMC. Briefly, 20 μL of a 0.1 mg/mL solution of PTMC in chloroform was pipetted onto the surface of a SPR sensor. The coated

SPR sensors were dried for 8 h before the experiment. The sensors were inserted into the SPR (Biacore 3000, Biacore, Sweden) and PBS was flowed over the sensor until a baseline measurement was achieved (400 seconds). 330 μL of enzyme solution was then injected into the flowcell (10 μL /min). The coated sensor was exposed to the enzyme solution for 1800 seconds. Following adsorption, PBS was injected into the flow cell as a rinse step. Adsorbed protein mass was measured as the difference in signal between the stabilized post-rinse data and the baseline.

6.3.12 ATR-FTIR

Surface water adsorption was measured by attenuated total reflection Fourier transform infrared (ATR-FTIR) spectroscopy [171]. The water stretching (3350 cm^{-1}) and bending (1650 cm^{-1}) peaks were used as indicators. 60PTMC and 100PTMC were fabricated according to the method described above and incubated in water for up to 7 days. Samples were removed from the water and scanned at 0 min, 15 min, 30 min, 1 h, 2.5 h, 6 h, 24 h, 5 d and 7 d.

6.3.13 Atomic Force Microscopy

Surface roughness of PTMC slabs (n=3) and spin-coated sensors (n=1) was determined by atomic force microscopy. 60PTMC and 100PTMC was prepared in slabs or spin coated onto gold QCM-D sensors as described above. A Veeco Multimode Microscope equipped with a Nanoscope IIIa Controller with a Veeco Probes TESP AFM tip was operated in tapping mode

to scan the surfaces. Root-mean-squared roughness (R_q) was quantified using the NanoScope V6.13 Software (Veeco).

6.3.14 Dual Indentation Testing

PTMC bulk modulus and Poisson's ratio was measured by a dual indentation test. 0.3 g/mL solutions of 60PTMC and 100PTMC in DCM were cast onto glass coverslips in 1.5 cm x 1.5 cm squares and dried overnight, covered to prevent the formation of bubbles. The PTMC polymer slabs were removed from the coverslips and sample height was measured on all sides using calipers. Sample height was approximately 1 mm. The indentation test was performed using two circular indenters with 1 mm and 2 mm diameters on dry PTMC samples (n=2) and samples that had been soaked in water for 24 h (n=2). The deformation rate was 0.03 mm/sec (TA.XT plus Texture Analyzer, Stable Micro Systems). Poisson ratio and Young's modulus was calculated by Hayes' method [172] using the slope of the linear regression of the applied stress versus applied strain between 5% and 20% strain.

6.3.15 Nanoindentation Testing

Surface modulus 60PTMC and 100PTMC were measured by nanoindentation. Samples were prepared by the same method as the samples for dual indentation described above. Nanoindentation was performed using an atomic force microscope (AFM, Park Systems, XE-100) on both dry PTMC and PTMC which had been soaked in water for 24 h. Indentation depth

was approximately 1.5 μm and the deformation rate was 50 nm/sec. Young's modulus was calculated from force-displacement data using the Hertzian model [173] (n=3).

6.3.16 Statistics

Measurements are reported as the average value ± standard deviation of n replicates. Statistical significance of the cell culture data was determined using a two way ANOVA followed by the Bonferroni *post-hoc* test (Prism6, GraphPad, USA). All other significances were determined using a Student's t-test. For glass transition temperature, dual indentation and nanoindentation testing measurements, standard deviations were pooled between samples of the same molecular weight. Data was considered statistically significantly different at $p<0.05$.

6.4 Results and Discussion

6.4.1 Polymer Characterization

60PTMC and 100PTMC were measured for surface roughness (R_q), polymer chain mobility (T_g), surface hydrophilicity (water contact angle), bulk water content and bulk and surface modulus (Table 6.1). Coated QCM-D sensors were also measured for roughness and surface hydrophilicity to ensure that the spin coating procedure had not changed any surface properties of PTMC. No significant differences were measured in roughness, bulk modulus or hydrophilicity. The values obtained for bulk water contact angles agree with previous measurements reported by Zhang et al. for the dry polymer and the 24 h conditioned polymer [82]. However, after 7 days of conditioning in aqueous media, Zhang et al. reports a dramatic decrease in contact angle for the lower molecular weight PTMC (to about 55 degrees), while

our results show no significant differences. The significant decrease in PTMC contact angle after 7 days of conditioning in aqueous media may have been due to delamination of the spin coated PTMC layers from the glass coverslips, exposing the underlying glass and lowering the contact angles. The contact angles in the present study were measured on slabs 0.7 mm thick, ensuring complete coverage of the underlying glass. Significant differences were measured between glass transition temperatures (T_g) for 60PTMC and 100PTMC that had been conditioned in water. As expected, soaking decreased the glass transition temperature for both molecular weights of PTMC due to plasticization by absorbed water [174].

Table 6.1: Bulk and surface properties of dry and wet 60PTMC and 100PTMC

	60PTMC (Dry)	60PTMC (Wet) 24h	60PTMC (Wet) 7d	100PTMC (Dry) 1d	100PTMC (Wet) 24h	100PTMC (Wet) 7d
M_n (g/mol)	61,000			102,000		
Bulk R_q (nm)	4.6 ± 0.3			4.5 ± 0.5		
Sensor R_q (nm)	1.2			2.4		
T_g (^{o}C)	-16.3 ± 0.3	-19.5 ± 0.2	-19.1 ± 0.8	-15.4 ± 0.6	-16.0 ± 0.4	-16.3 ± 0.1
Water Content (%)		3 ± 1	3 ± 1		2 ± 1	4 ± 1
Bulk Contact Angle (^{o})	75 ± 2	77 ± 2	76 ± 1	80 ± 1	75 ± 1	74 ± 1
Sensor Contact Angle (^{o})	79 ± 2	80 ± 1		81 ± 1	81 ± 1	
Bulk Modulus (MPa)	1.1 ± 0.4	1.1 ± 0.2		1.3 ± 0.2	1.4 ± 0.1	
Surface Modulus (MPa)	1.17 ± 0.04	0.82 ± 0.02		1.34 ± 0.05	1.09 ± 0.06	

No significant differences were measured in bulk modulus between the 60PTMC and 100PTMC. However, the surface moduli measured by nanoindentation were significantly different between both dry and wet 60PTMC and 100PTMC. Furthermore, upon soaking in water for 24 h, the surface modulus of 100PTMC decreased 19% while that of the 60PTMC decreased 30%. Both glass transition temperature and surface modulus are associated with

polymer chain flexibility. The surface modulus results suggest that the polymer chains at the surface of 60PTMC become much more mobile in aqueous conditions.

6.4.2 Macrophage Behavior

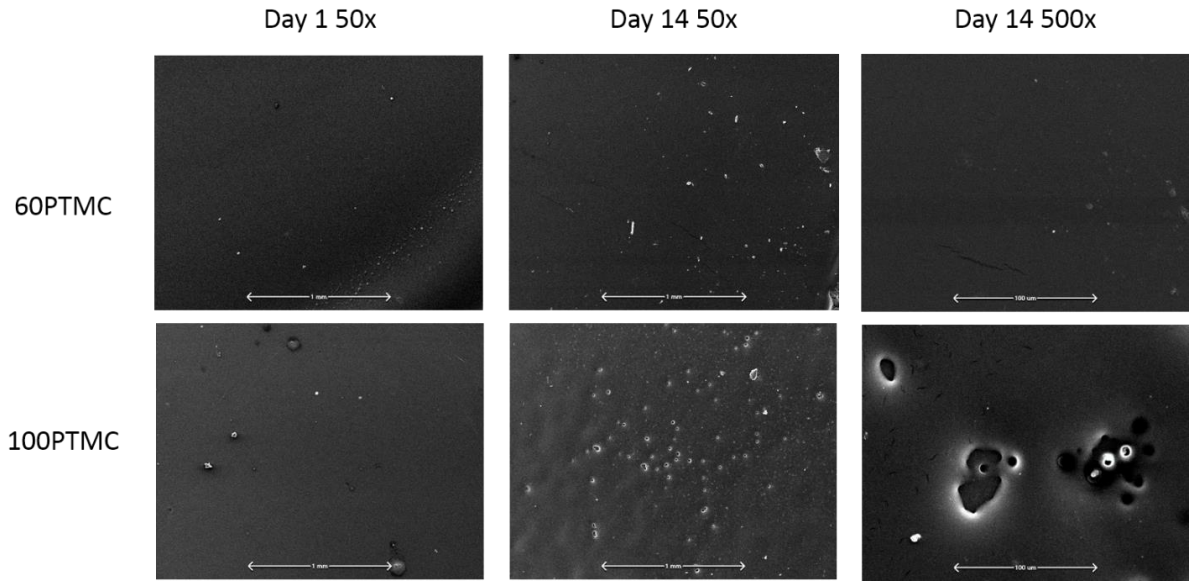

Figure 6.1: SEM images of 60PTMC and 100PTMC at days 1 and 14 with macrophages removed. No degradation is observed on the 60PTMC surface at day 14, while significant degradation is observed on the 100PTMC surface, evidenced by the presence of cavities on the surface.

RAW 264.7 murine macrophages were cultured on the surfaces of 60PTMC and 100PTMC. At days 1 and 14 the macrophages were removed and the surfaces were imaged for signs of degradation. Neither the 60PTMC nor 100PTMC surface showed any sign of degradation at day 1. By day 14 there was significant pitting on the surface of 100PTMC, while no pitting was observed on the 60PTMC surface (Figure 6.1).

Cell number, superoxide anion (O_2^-), reactive oxygen species ($ONOO^-$, NO^-, H_2O_2, OH^-), and esterase production per cell were measured over 14 days (Figure 6.2). The initial

number of macrophages attached at 24 h (Figure 6.2A) was similar for all three surfaces. By 10 days, macrophage number was maintained on the TCPS surface but had decreased significantly on both the 60PTMC and 100PTMC surfaces. Throughout the time period, there was no difference in macrophage number between the PTMC surfaces.

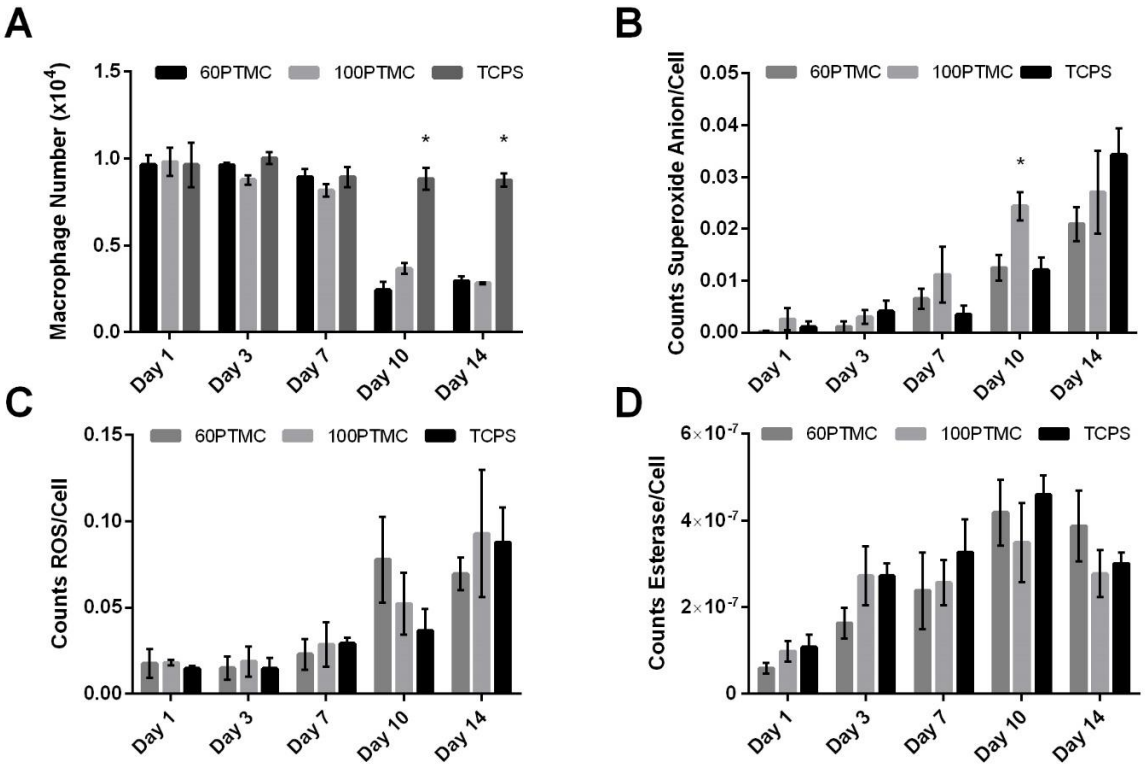

Figure 6.2: Macrophage attachment and proliferation (A), superoxide anion secretion per cell (B), Reactive oxygen species secretion per cell (C), and esterase secretion per cell (D) over 14 days on 60PTMC, 100PTMC and TCPS. *p<0.05, (n=6).

No significant differences were observed in superoxide anion production per cell with the exception of day 10, which did not continue through day 14 (Figure 6.2B). No significant differences were observed in the production of other ROS/cell between any of the surfaces at any time point, though overall ROS production increased over 14 days (Figure 6.2C). Between

the PTMC surfaces, the macrophages on the 100PTMC surface secreted more superoxide anion than those on the 60PTMC on day 7 and significantly so on day 10. Previous literature findings suggested that the superoxide anion is the reactive oxygen species primarily responsible for the degradation of PTMC [103,161]. However, the difference in ROS/superoxide secretion on the two PTMC surfaces by day 14 is minimal and not large enough to explain the reported difference in PTMC degradation rates with respect to molecular weight.

6.4.3 Enzymatic Degradation

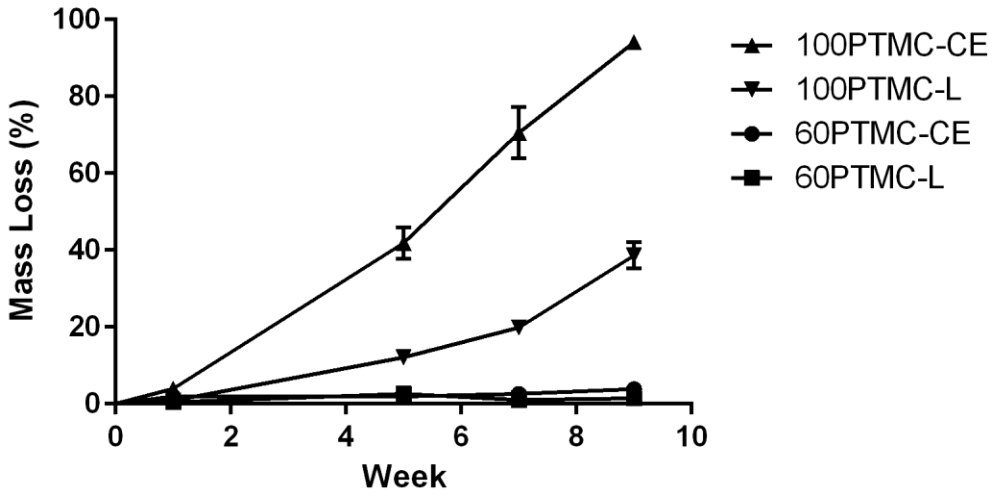

Figure 6.3: Degradation of 60PTMC and 100PTMC by cholesterol esterase (CE) and lipase (L), (n=3).

To determine differences in rates of enzymatic degradation in the absence of macrophages, 60PTMC and 100PTMC were incubated in solutions of cholesterol esterase and lipase and the mass loss was measured over 9 weeks. By 9 weeks, the 100PTMC incubated in the cholesterol esterase and lipase solution had lost 98% and 39% of its mass, respectively.

The 60PTMC experienced less than 4% and 2% mass loss, respectively. Cholesterol esterase was more active than lipase on the surface of 100PTMC. These results show that both enzymes have different activities on the 60PTMC and 100PTMC surfaces in the absence of macrophages and suggest that enzymatic activity is responsible for the reported molecular weight dependence of degradation rates of the PTMC surfaces.

6.4.4 Enzyme Adsorption

A quartz crystal microbalance with dissipation (QCM-D) was used to monitor the adsorption of cholesterol esterase and lipase on the PTMC surfaces over 96 and 25 h, respectively. The QCM-D frequency and dissipation data shows differences in adsorption pattern on the 60PTMC and 100PTMC surfaces, which could be indicative of a difference in adsorption conformation of the enzyme. The cholesterol esterase adsorption to the 100PTMC is accompanied by a frequency (F5) decrease and dissipation (D5) increase (Figures 6.4A and C), indicating mass increase and a greater amount of bound water up to 36 h when the cholesterol esterase begins to degrade the surface. The cholesterol esterase adsorption to the 60PTMC is accompanied by a frequency increase and dissipation decrease indicating overall mass decrease as a result of loss of bound water. The mass loss can be attributed to loss of bound water, as the 60PTMC surface is not degraded by the cholesterol esterase within 96 h (Figure 6.3).

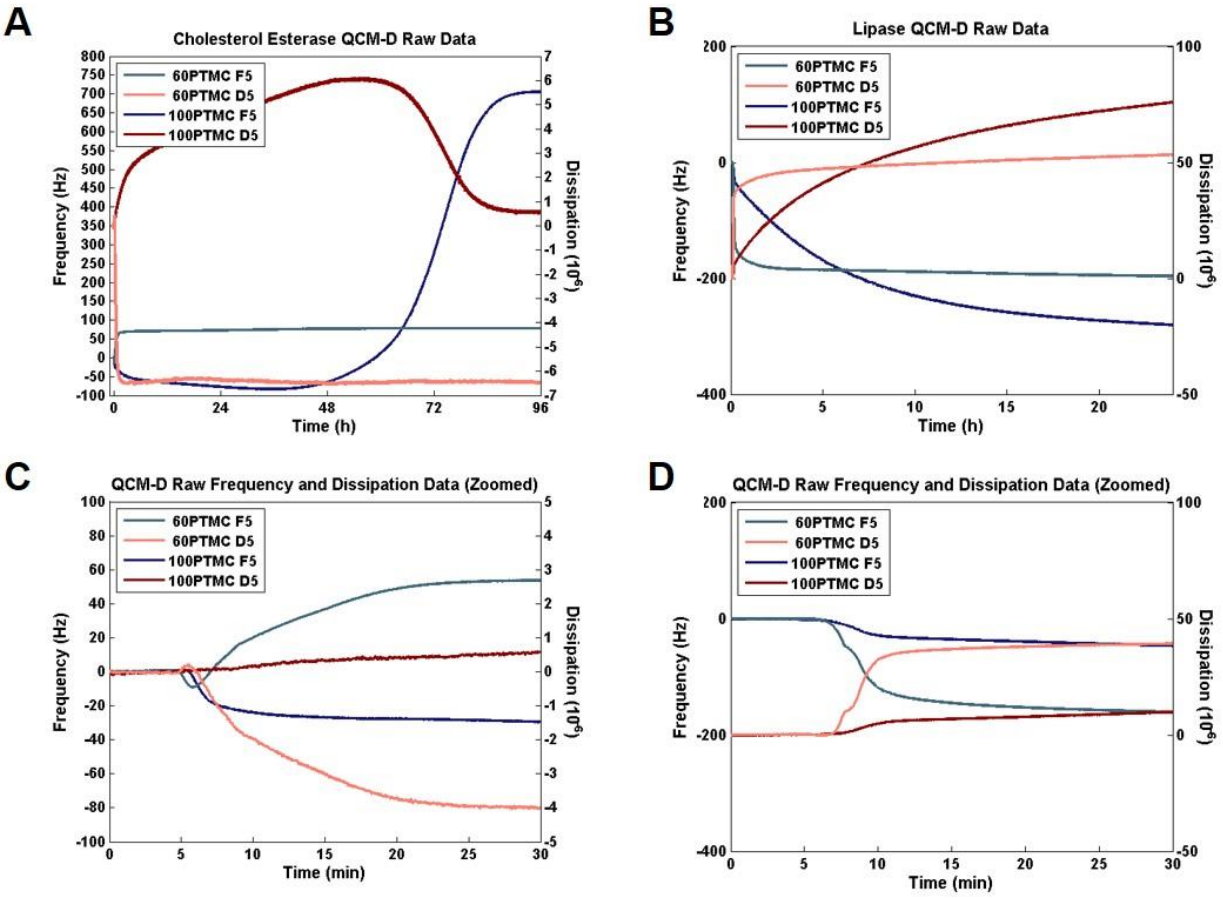

Figure 6.4: QCM-D frequency (F5) and dissipation (D5) data (5th overtone) for the adsorption of cholesterol esterase over 96 h (A) and 30 min (C) and lipase over 24 h (B) and 30 min (D) on 60PTMC and 100PTMC.

Lipase also shows differences in adsorption pattern on the two surfaces. While lipase adsorption on both 60PTMC and 100PTMC is associated with decreases in frequency and increases in dissipation, adsorption on the 60PTMC reaches equilibrium at 10 min while lipase adsorbing to the 100PTMC surface requires more than 25 h to reach equilibrium. These differences in adsorption pattern suggest that the adsorption mechanism of cholesterol esterase and lipase changes when adsorbing on the 60PTMC and 100PTMC surfaces. In particular, the data suggests differences in enzyme interactions with polymer-surface bound water and overall enzymatic conformation following adsorption.

Surface plasmon resonance (SPR) was used to measure the adsorbed layer mass, and viscoelastic modeling of QCM-D data was used to measure the shear thickness, modulus and viscosity of the adsorbed enzyme layers. Significantly more cholesterol esterase mass adsorbed to the surface of 100PTMC compared to 60PTMC (Figure 6.5A). There was no significant difference in the thickness of the cholesterol esterase layer on the two PTMC surfaces (Figure 6.5B), which, at 25 nm is several times larger than the size of a cholesterol esterase molecule (5.2 nm [175]). This is likely due to loosely bound protein that associates with the adsorbed protein layer in a static adsorption environment [176,177]. Significant differences were found in both cholesterol esterase layer modulus (Figure 6.5C) and viscosity (Figure 6.5D) on the two PTMC surfaces.

About twice as much cholesterol esterase adsorbed to the 100PTMC, however this difference, alone, does not explain the slower *in vivo* degradation of 60PTMC, since the enzyme is clearly present on the 60PTMC surface as well. However, the shear modulus and viscosity differences between the two adsorbed enzyme layers suggest that this enzyme is adsorbing in different conformations on the PTMC surfaces [178,179]. The cholesterol esterase may be adsorbing to the 60PTMC surface in a denatured conformation or a conformation in which its active site is less capable of accessing the PTMC carbonate group.

No significant differences were measured for the adsorbed lipase layer in any of the properties with the exception of layer thickness (Figure 6.5B). Lipase is a globular protein with a hydrodynamic radius of approximately 3.2 nm [180]. The measured enzyme layer thickness is about 30 times the hydrodynamic diameter, suggesting that, as was the case for the cholesterol esterase, in a static adsorption environment, lipase may be loosely associating or aggregating on top of the lipase adsorbed to the PTMC. What the difference in thickness suggests, however,

is that the lipase is associating or aggregating differently on the two PTMC surfaces which may also be due to differences in lipase conformation that result when adsorbed to the 60PTMC surface versus the 100PTMC surface.

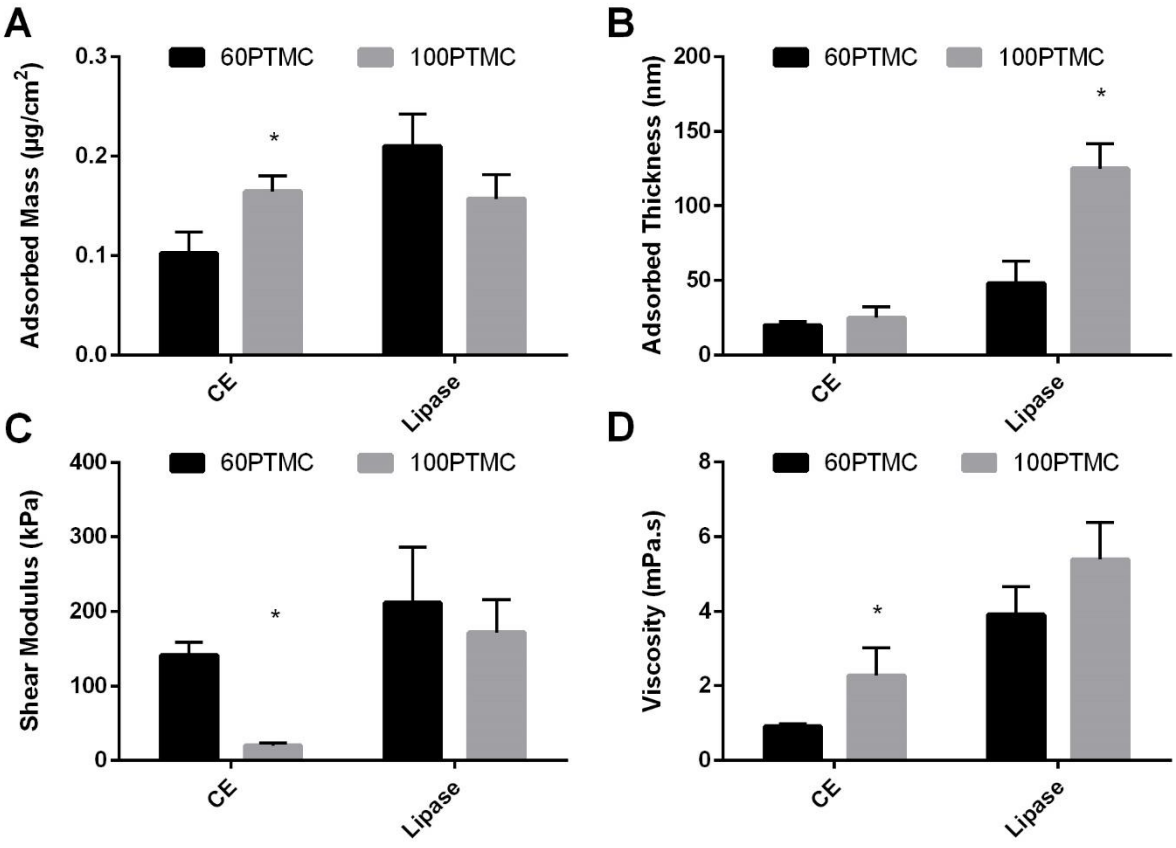

Figure 6.5: Mass (A), thickness (B), shear modulus (C) and viscosity (D) of cholesterol esterase and lipase adsorbed to 60PTMC and 100PTMC surfaces. *$p<0.05$, (n=3).

6.4.5 Surface Water Absorption

The extent of hydration of a polymer can affect the quantity and conformation of adsorbed proteins [174]. To determine differences in water absorption at the PTMC surfaces, PTMC slabs were soaked in water for 0, 15 min, 30 min, 1 h, 2.5 h, 6 h, 24 h, and 7 days and analyzed by ATR-FTIR (Figure 6.6). The water stretching (3350 cm^{-1}) peak was used as an indicator for absorbed water. The 60PTMC surface absorbed water faster; however, by 7 days, there was no difference in the amount of water absorbed by the two PTMC surfaces.

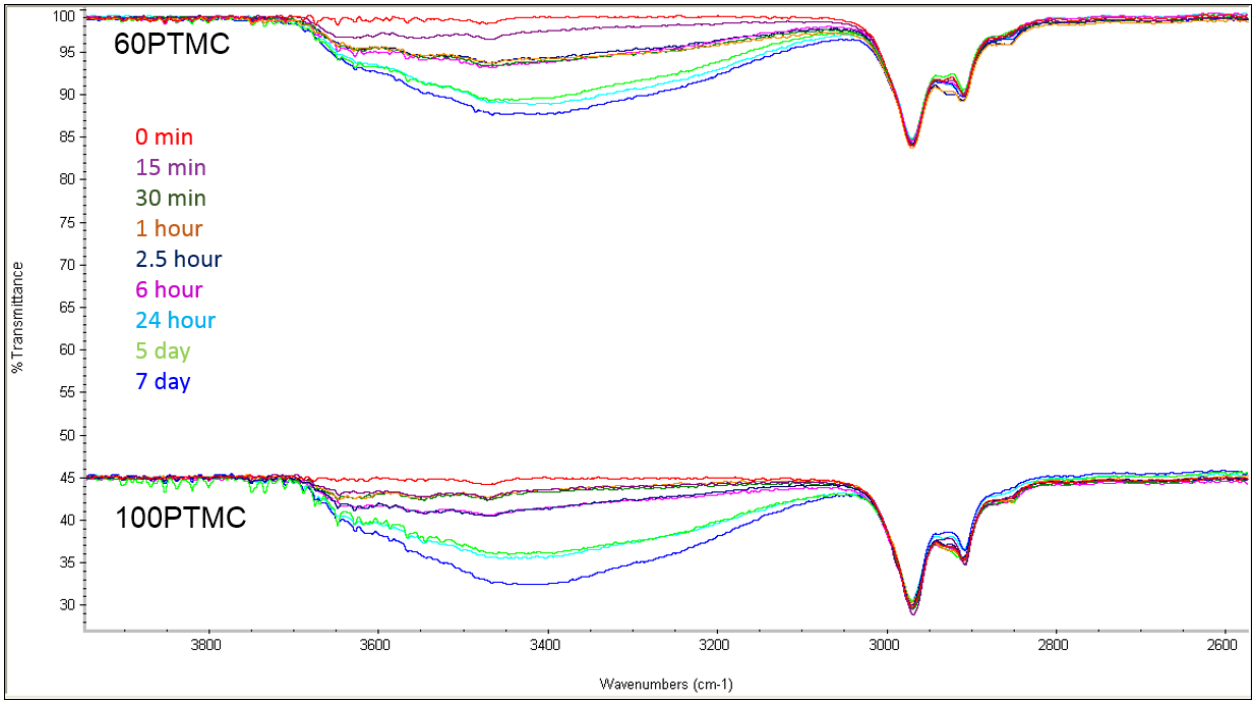

Figure 6.6: ATR-FTIR scans of 60PTMC (top group) and 100PTMC (bottom group) incubated in water for 0 min, 15 min, 30 min, 1 h, 2.5 h, 6 h, 24 h, 5 days and 7 days (lines top to bottom).

It is possible that despite similar amounts of surface water adsorption there may be differences in local hydrophilicities between the PTMC surfaces. The 60PTMC may be able to adopt a more hydrophilic interface in response to the aqueous environment, compared to the 100PTMC, exposing its hydroxyl groups and reducing the interfacial energy at the surface.

Zhang et al. suggested that the difference in lipase activity on PTMC surfaces of differing molecular weights was due to an increase in hydrophilicity of the 60PTMC after 7 days which interfered with the conformation of the enzyme [82]. However, in this study, no significant difference in contact angle was observed on the PTMC surfaces at any time point, yet the enzymes still degraded 100PTMC significantly faster than 60PTMC.

Glass transition temperature and surface moduli data showed a significant difference in polymer chain mobility between 60PTMC and 100PTMC when the polymers were conditioned in water for 24 h. Polymer chain mobility has previously been proposed as an explanation as to why some polyesters were degradable by lipases while others were resistant to degradation [181,182]. It was hypothesized that long chain polymers were required to be mobile enough to form a protruding "loop" in the enzyme solution in order to make their target site accessible to the enzyme. This conclusion does not seem to apply to the present study, however, where the less mobile 100PTMC chains were more susceptible to degradation compared to the more mobile 60PTMC chains. It may be that for these PTMC surfaces the increased flexibility of 60PTMC interferes with enzymatic attachment.

Polymer chain mobility has also been hypothesized to affect protein adsorption and conformation [75,66,80]. Protein adsorption is primarily driven by the increase in entropy caused by “freeing” water bound to the polymer chains [67,129,183]. Though there were no differences measured in the quantity of water absorbed to the PTMC surfaces, there may be differences in the interaction of the water molecules with the polymer chains. Both differences in water arrangement and differences in polymer chain mobility (and thus, mobility of the water bound to the chains) could affect the total entropy gained during protein/enzyme

adsorption. An increase or decrease in entropy could affect the amount or conformation of the adsorbed enzyme, and thus activity of the enzyme between the two surfaces [67].

The QCM-D frequency and dissipation data showed that cholesterol esterase freed more water when adsorbing to the 60PTMC surface, as well as adsorbing in a lower quantity and different conformation compared to the 100PTMC surface. It is proposed that the difference in entropy caused by differences in polymer chain mobility and water interaction causes the cholesterol esterase to adopt a conformation upon adsorption to 60PTMC that is less active, resulting in a much slower degradation rate for 60PTMC compared to 100PTMC.

6.5 Conclusion

PTMC with molecular weights above 100 kg/mol has been reported to degrade faster *in vivo* than PTMC with molecular weights below 70 kg/mol, which may be due to differences in macrophage behavior, or enzymatic adsorption or activity on the surface[82]. Macrophages attached in equal amounts and secreted mostly equivalent amounts of ROS, superoxide anion, and cholesterol esterase when cultured on the 60PTMC and 100PTMC surfaces. Thus, the difference in the degradation rate of the PTMC with respect to molecular weight could not be due to differences in macrophage response to the polymer surfaces. Enzymatic degradation and adsorption experiments using cholesterol esterase and lipase demonstrated that the 100 kg/mol PTMC was degraded more rapidly than the 60 kg/mol PTMC, and that the difference in PTMC degradation rates with respect to polymer molecular weight was due to the nature of the enzyme interaction with the surfaces. Cholesterol esterase adsorbed in greater quantities to the 100PTMC surface, and also in a significantly less stiff and more viscous protein layer. The time dependent adsorption data showed that both cholesterol esterase and lipase appear to

interact differently with surface bound water when adsorbing to the 60PTMC or 100PTMC surface. Since the two molecular weights of PTMC differ only in polymer chain mobility, this result suggests that the polymer chain mobility at the interface affects the conformation of the enzyme adsorbed to the polymer chains. It is proposed that polymer chain mobility affects the arrangement or entropy of the water molecules bound to the polymer chains, which then affects the entropy gained when the enzyme adsorbs and the surface is dehydrated. The difference in water arrangement and entropy may affect the amount or conformation, and thus activity, of the enzyme adsorbed on the PTMC surfaces.

Chapter 7

The Effect of Protein Adsorption and Subsequent Macrophage Activity on Acryl *star*-Poly(D,L lactide-co-ϵ-caprolactone) Elastomer and Poly(trimethylene carbonate) Degradation

7.1 Completed Objectives

Chapter 7 describes the fulfillment of Objective 4, which was to determine whether the faster macrophage mediated degradation rate of 100PTMC compared to ELAS 5000, despite similar susceptibility to enzymatic degradation, was due to a difference in macrophage attachment or activity at the surfaces driven by a difference in protein adsorption. 100PTMC and ELAS 5000 differ in polymer chain flexibility and surface chemistry, and thus may adsorb different quantities of proteins from plasma-supplemented culture. It was hypothesized that the higher degradation rate of 100PTMC is due to either higher levels of macrophage attachment or that the macrophages secrete more degradative enzymes on the 100PTMC surface due to higher levels of adsorbed opsonins, such as immunoglobulins or complement. 100PTMC and ELAS 5000 were incubated in solutions of cholesterol esterase and lipase so as to confirm similar susceptibility to enzymatic degradation. RAW 264.7 monocyte derived macrophages were cultured on 100PTMC and ELAS 5000 surfaces in an adult bovine plasma supplemented environment and cell attachment and proliferation, and esterase, reactive oxygen species, and superoxide anion secretion were measured. Relative quantitation proteomics was used to compare the proteins that adsorbed to the 100PTMC and ELAS 5000 surfaces from adult bovine plasma.

All experiments described herein were designed and completed by me with the exception of the reductive methylation and LC-MS/MS which was completed at the Proteomics Core Facility at the Center for High Throughput Biology, University of British Columbia as a fee-for-service, and the nano-indentation of ELAS 5000 performed by Tong Liu at the Department of Mechanical and Mechatronics Engineering, University of Waterloo as a fee-for-service. I performed the SPR measurements in the Protein Function Discovery Facility, Queen's University.

7.2 Introduction

Polymers and elastomers fabricated from lactide, caprolactone and trimethylene carbonate monomers are currently under investigation as biomaterials for a variety of soft tissue applications due to their tailorable mechanical and degradation properties [83,184,185]. Of these polymers, polycarbonates have generated particular interest due to their uncommon degradation behavior. Unlike polyesters such as poly(lactide), poly(caprolactone), poly(glycolide) and co-polymers thereof, polycarbonates are not susceptible to hydrolytic degradation due to the stability of the carbonate functionality to nucleophilic attack. *In vivo*, polycarbonates are degraded by macrophages which attach to and erode the polycarbonate surface [82,84]. Polyesters, interestingly, resist macrophage mediated degradation and still degrade *in vivo* primarily via bulk hydrolysis [186,187].

The reason for this difference in macrophage degradation behavior is not well understood. Monocyte adhesion and response to biomaterials is believed to be mediated by the proteins that adsorb to the biomaterial surface [27,74], which, in turn, is believed to be

influenced by the surface properties of the biomaterial. Adsorption of opsonins such as complement C3 (and its activated form C3b) and immunoglobulin G have been associated with extended monocyte/macrophage attachment and phagocytosis [33,74,188,189]. Additionally, monocytes are able bind to surfaces via the RGD and other integrin binding motifs found in proteins such as fibrinogen, fibronectin, and vitronectin [35,190], though whether these proteins affect the activation of macrophage activation is still unclear. Surfaces pre-coated with fibrinogen and fibronectin reduced foreign body giant cell formation in LPS activated monocytes [190] but increased endocytosis and matrix metalloproteinases (MMPs) including MMP2 and MMP9 production by unactivated monocytes [191]. Adsorbed vitronectin increased macrophage fusion into foreign body giant cells in IL-4 activated monocytes [192] while no effects were shown other studies [74].

For both pre-coated surfaces [190] and uncoated surfaces [193] used in serum supplemented monocyte/macrophage cultures, the surface properties of the underlying substrate influence cell behavior. Material properties, including surface chemistry [193] and stiffness [8] affect monocyte/macrophage behavior [194,195], possibly due to the type or conformation of serum/plasma proteins that preferentially adsorb to the surfaces. It is, therefore, likely that the observed differences in macrophage mediated degradation between polyesters and polycarbonates were also driven by a difference in the type or conformation of plasma proteins adsorbed to the polymers.

However, the ability of surface adsorbed proteins to activate otherwise unactivated monocytes is not well understood. The vast majority of studies investigating monocyte/macrophage-biomaterial response have used monocytes pre-activated by LPS, interleukin-4 (IL-4) and so on. This is partly due to physiological relevance; monocytes *in vivo*

are activated by microbial antigens and inflammatory cytokines secreted by cells at the site of inflammation. It is also partly due to necessity in order to induce non-adherent monocytes to adhere to the material in order to measure cell response. However, activating monocytes with a single molecule may affect macrophage polarization into either the M1 (proinflammatory) phenotype activated by LPS) or the M2 (anti-inflammatory) phenotype activated by IL-4 or interleukin-13 (IL-13) [100]. This pre-activation step, therefore, results in an incomplete understanding of monocyte/macrophage response to biomaterials and the proteins adsorbed to their surfaces.

In this study, poly(trimethylene carbonate) was used to investigate the effect of protein adsorption on the degradation of polycarbonates by adherent monocyte/macrophages. Previously, we determined that 100 kg/mol PTMC (100PTMC) degraded primarily via enzymatic erosion from esterases secreted by adherent macrophages [84]. A polyester elastomer fabricated from acrylated *star* poly(D,L lactide-*co*-ϵ-caprolactone) (ELAS 5000), which does not degrade *in vivo* via macrophage mediated degradation [186,196] but has a similar susceptibility to enzymatic degradation, was used as a control surface. RAW 264.7 murine monocyte/macrophages were cultured on the surfaces of 100 kg/mol PTMC and ELAS 5000, and analyzed for differences in cell number and secretion of enzymatic and oxidative degradative species. Subsequently, relative quantitation proteomics (reductive methylation followed by liquid chromatography-tandem mass spectrometry (LC-MS/MS) was used to measure the relative quantities of specific proteins that adsorbed to the 100PTMC and ELAS 5000 surfaces from adult bovine plasma, in order to determine if differences in macrophage attachment or activity were driven by differences in the composition of the protein layers adsorbed to the polymers.

7.3 Materials and Methods

7.3.1 Polymer Fabrication

Elastomer formed from 5000 g/mol acrylated *star* poly(D,L lactide-*co*-ϵ-caprolactone) (ELAS 5000) and polymers formed from 100 kg/mol poly(trimethylene carbonate) (100PTMC) were fabricated according to the methods described in Amsden *et al.* 2004 [110] and Vyner *et al*. 2014 [84], respectively. For the elastomer, D,L-lactide (Purac, the Netherlands) and ϵ-caprolactone (Fluka, Switzerland) monomers were added to a flame dried glass ampoule with glycerol as an initiator (Fisher, Canada) and stannous 2-ethylhexanoate (Sigma, Canada) as a catalyst and reacted under vacuum (-10 psig) at 130°C for 24 h. The resulting polymer was dissolved in dichloromethane (DCM) (Fisher, Canada) dried over 3 Å molecular sieves (Acros, USA) and the terminal hydroxyl groups converted to acrylates by the dropwise addition of acryloyl chloride (Sigma, Canada) in the presence of triethylamine (TEA) (Sigma, Canada) as an H^+ ion scavenger and dimethylaminopyridine (Fisher, Canada) as a catalyst. The acrylated polymer was purified by the addition of ethyl acetate (Fisher, Canada) to precipitate TEA•HCl salt, filtered, and precipitated in isopropanol (Fisher, Canada) at -20°C to remove unreacted monomer. The purified ASCP pre-polymer was determined by ^{1}H-NMR to have a number average molecular weight of 5200 g/mol and a degree of acrylation of 98%. To form the elastomer, the acrylated pre-polymer (ASCP) was dissolved in a minimal amount of ethyl acetate containing 2,2 dimethoxy-2-phenyl-acetophenone (DMPA) (Sigma, Canada) as a photoinitiator at a ratio of 3 mg per gram pre-polymer, poured into a glass mould, then irradiated with UV light (365 nm, 30 mW/cm^2, Lightningcure LC8, Hamamatsu) for 5 min. To

prepare the 100PTMC, trimethylene carbonate monomer (Biomatrik, China) was added to a flame-dried ampoule with stannous 2-ethylhexanoate as a catalyst, vacuum sealed (-10 psig), and reacted at 130 °C for 24 h. No additional material was added to initiate the polymerization, instead residual water served as the initiator. The resulting polymer was dissolved in DCM and purified by precipitation in -20 °C methanol (Fisher, Canada). Molecular weight was confirmed by gel permeation chromatography (GPC, Viscotek GPCmax VE 2001) equipped with two PAS-106M columns (from the PolyAnalytik SupeRes Series) at 25 ºC using tetrahydrofuran (THF, Fisher Scientific, Canada) as the eluent (1 mL/min). The number average molecular weight (M_n) was determined to be 110, 000 g/mol with a dispersity of 1.6 by a relative calibration using polystyrene standards.

7.3.2 Nanoindentation of ELAS 5000

Nanoindentation measurements of dry and hydrated ELAS 5000 were performed by Tong Liu of the Mechanical and Mechatronics Engineering Department at the University of Waterloo, Ontario, Canada. Slabs of ELAS 5000 approximately 20 x 10 mm and 1 mm thick were prepared according to the method described above (n=2). All samples were rinsed briefly with methanol to remove surface contaminants. Hydrated samples were incubated in de-ionized water for 24 h prior to testing. Force-displacement curves were generated by probing the ELAS 5000 surfaces in contact mode using a cantilever with a four sided pyramid tip (spring constant 0.2 N/m) at a rate of 50 nm/sec to a depth of 1.5 μm (AFM, Park Systems, XE-100). Young's modulus was calculated from the measured force-displacement curves using the Hertzian model [197] and assuming a Poisson's ratio of 0.5.

7.3.3 Scanning Electron Microscopy

ASCP pre-polymer and 100PTMC were fabricated according to the method above and used to coat 15 mm diameter circular glass cover slips. For the ELAS 5000 coated coverslips, 1 mL of a 1% w/v solution of ASCP pre-polymer in ethyl acetate with 3 mg per gram pre-polymer DMPA photoinitator was pipetted dropwise onto a glass coverslip spinning at 1400 rpm. The ASCP coated coverslips were crosslinked under UV irradiation as described above. For the PTMC coated coverslips, 50 μL of a 1% solution of 100PTMC in chloroform was pipetted onto the surface of a glass coverslip which spinning at 4000 rpm (WS-400, Laurell Technologies). Coated coverslips were dried overnight, sterilized under UV light for 30 min, placed in the wells of sterile 12 well tissue culture polystyrene (TCPS) cell culture plates and incubated in unsupplemented Dulbecco's Modified Eagle Medium (DMEM) prior to cell seeding. RAW 264.7 immortalized murine monocyte-macrophages were thawed and expanded in T-175 flasks in DMEM supplemented with 10% fetal bovine serum (FBS). The cells were rinsed with unsupplemented DMEM to remove the FBS, removed from the flasks with non-enzymatic cell dissociation media (Sigma, Canada), and re-suspended in DMEM supplemented with 10% bovine plasma (Cedarlane), 1% antibiotic/anti-mycotic (ABAM) (Sigma, Canada). Cells were seeded on the coated coverslips at a density of 30,000 cells/cm^2 and cultured for 14 days. At each time point (days 1 and 14), the cells were removed from the cover slips with non-enzymatic cell dissociation media (Sigma, Canada) and the coverslips were dried overnight and chemically dried with hexamethyldisilazane (Sigma, Canada). The

dried coverslips were affixed to scanning electron microscopy (SEM) mounting stubs, sputter coated with gold (10 mA, 4 min), and imaged using a Hitachi S-2300 scanning electron microscope at an accelerating voltage of 15 kV.

7.3.4 Macrophage Adhesion and Activity on 100PTMC and ELAS 5000

To determine differences in macrophage adhesion and secretion of degradative species, RAW 264.7 monocyte-macrophages were cultured on 100PTMC and ELAS 5000 surfaces for 14 days. 70 μL of a 1:1 w:v solution of ASCP in ethyl acetate with 3 mg per gram pre-polymer photoinitiator or a 1:5 w:v solution of PTMC in DCM was pipetted into the wells of TCPS tissue culture plates. The plates were dried overnight to remove residual solvent and the ASCP was crosslinked by UV irradiation as described above. The plates were sterilized under UV irradiation in a laminar flow biological safety cabinet for 30 min and incubated in unsupplemented DMEM for 12 h prior to cell seeding. No methods were undertaken to remove endotoxin from the polymer surfaces, however given the similar preparation procedures, differences in endotoxin level are not suspected to be factors in the macrophage mediated degradation of one polymer over another. Frozen RAW 264.7 murine monocyte-macrophages were thawed and expanded in DMEM supplemented with 10% FBS, 1% ABAM. The expanded cells were washed with unsupplemented media to remove the FBS and re-suspended in DMEM supplemented with 10% bovine plasma, 1% ABAM. The re-suspended cells were seeded in the coated TCPS plates at a density of 30,000 cells/cm^2. The cells were cultured for 14 days and analyzed on days 1, 3, 7, 10, and 14. At each time point, the media in each well was aspirated and the cells were removed from the surface with Non-enzymatic Cell

Dissociation Buffer (Sigma, Canada). Cell number was quantified by the Quantifluor ds DNA assay (Promega) (n = 6). Secretion of reactive oxygen species and superoxide anion by the cells was measured by the Total ROS/Superoxide Detection Kit (Enzo, Canada) (n = 6) which measures the secretion of reactive oxygen species (NO, $ONOO^-$, H_2O_2, HO^-) and superoxide anion (O_2^-). Secretion of esterases was measured by the colorimetric quantification of p-nitrophenol (abs = 410 nm), which is produced when active esterases cleave p-nitrophenyl acetate (n=6) [170].

7.3.5 Enzymatic and Oxidative Degradation

To determine the susceptibility of ELAS 5000 and 100PTMC to enzymatic and oxidative degradation, discs of ELAS 5000 and 100PTMC were incubated in solutions of cholesterol esterase (1 U/mL in phosphate buffered saline (PBS, Sigma, Canada)), lipase (Sigma, used as received) (9 weeks), and superoxide anion (O_2^-) which was generated by a solution of 0.01M KO_2, 0.002 M 18-crown-6 ether in THF (Fisher, Canada) [198] (8 days). Degradation was reported as the percent mass loss between the day 0 sample and the sample at each time point (n=3).

7.3.6 Proteomics

In order to determine whether differences in macrophage behavior could be influenced by differences in protein adsorption, relative quantitation proteomics was used to determine the relative quantities of specific proteins that adsorb to ELAS 5000 and 100PTMC surfaces.

7.3.6.1 Microsphere fabrication

To increase the adsorption surface area of the polymer surfaces, ELAS 5000 and 100PTMC were fabricated into microspheres. Briefly, ASCP pre-polymer was dissolved in a 1:1 w:v ratio of ASCP to toluene with 3 mg per gram pre-polymer photoinitiator. 1 mL of dissolved pre-polymer was pipetted in a thin stream into 4 mL of de-ionized water in a 5 dram vial stirring at 1400 rpm under UV irradiation (30 mW/cm^2) for 5 min. The crosslinked microspheres were sieved to remove particles < 20 μm using X sieve, heated to 130 °C for 10 min under vacuum and dried overnight to remove residual water and toluene prior to protein adsorption. 100PTMC microspheres were fabricated by the dropwise addition of a 10% solution of 100PTMC in DCM to a liquid nitrogen:methanol (700:300 mL) bath. The 100PTMC microspheres were incubated in the liquid nitrogen:methanol bath overnight, sieved to remove particles < 20 μm, and dried overnight to remove excess methanol and DCM. ELAS 5000 and 100PTMC microspheres had average diameters of approximately 500 μm and 1 mm, respectively.

7.3.6.2 Plasma Adsorption to Microspheres

Samples of 500 mg of ELAS 5000 microspheres and 1035 mg of 100PTMC microspheres were incubated in unsupplemented DMEM for 12 h prior to adsorption. The unsupplemented DMEM was removed and replaced with DMEM supplemented with 10% adult bovine plasma. The microspheres were incubated in the plasma supplemented media for 12 h at 37 °C. After adsorption, the supplemented media was removed and the microspheres with rinsed with 3 washes of de-ionized water to remove unadsorbed protein. The microspheres

were incubated in 500 μL of 0.5% SDS at 95 °C for 5 min and vortexed to elute the adsorbed protein from the microspheres. The resulting protein solutions were flash frozen in liquid nitrogen, lyophilized, and stored at -20°C until further processing.

7.3.6.3 Proteomics Analysis

The relative quantities of proteins adsorbed to the ELAS 5000 and 100PTMC surfaces were quantified by reductive methylation followed by LC-MS/MS. The method described herein was performed by the Proteomics Core Facility at the Center for High Throughput Biology at the University of British Columbia according to the methods described in Boersema *et al*. [135]. Briefly, the lyophilized protein samples described above were reconstituted, digested with porcine trypsin and dried by vacuum centrifugation for 30 min. The dried protein digests were reconstituted in triethylammonium bicarbonate. The digested peptides were labelled with either undeuterated (light) or deuterated (heavy) methyl groups by the addition of undeuterated (CH_2O and $NaBH_3CN$) and deuterated (CD_2O and $NaBD_3CN$) formaldehyde and sodium cyanoborohydride, respectively. The labeled peptides were injected into a linear-trapping quadrupole – Orbitrap mass spectrometer (LTQ-Orbitrap Velos, ThermoFisher Scientific) coupled to an Agilent 1290 Series HPLC using a nanospray ionization source (ThermoFisher Scientific) running at a flow rate of 0.1 μL/min at 6 °C. The acquired peak areas were processed by Proteome Discoverer 1.3 (Thermo Scientific) for identification and quantitative comparison. The protein identification was performed with the Mascot algorithm (v. 2.4) against a database comprised of the bovine protein sequences using the following parameters: peptide mass accuracy 10 parts per million; fragment mass accuracy 0.6 Da;

trypsin enzyme specificity, fixed modifications – carbamidomethyl, variable modifications – methionine oxidation, deamidated N, Q and N-acetyl peptides, ESI-TRAP fragment characteristics. The results are given as the ratio of identified protein fragments adsorbed to the ELAS 5000 surface versus the protein fragments adsorbed to the 100PTMC surface for three independent samples.

7.3.7 Statistics

Measurements are reported as the average value ± standard deviation of n replicates. Statistical significance of the cell culture data was determined using a two way ANOVA followed by the Bonferroni *post-hoc* test (Prism6, GraphPad, USA). Data was considered statistically significantly different at $p<0.05$. Significance for the relative quantitation proteomics was determined at ratios of greater than 1.5 or less that 0.5 as determined by the Proteome Discoverer 1.3 software.

7.4 Results

7.4.1 Surface Characterization

To determine differences in the surface properties of the 100PTMC and ELAS 5000 that may affect the protein adsorption and drive differences in macrophage degradation behavior, previously measured [80,84] glass transition temperatures, water content, contact angles, and bulk moduli for both 100PTMC and ELAS 5000 and surface moduli for 100PTMC are restated here (Table 7.1). The dry and hydrated surface modulus of ELAS 5000 and 100PTMC were measured using nano-indentation. The polymers had similar surface

hydrophobicity and dry bulk moduli as measured by both indentation and nano-indentation testing. The glass transition temperature of 100PTMC was significantly lower than that of ELAS 5000, though both were below 37 °C. Therefore the polymer chains of both ELAS 5000 and 100PTMC were flexible and mobile at physiological temperature. When the materials were hydrated, the surface moduli of both polymers decreased by approximately 0.2 MPa, despite no difference in bulk modulus.

Table 7.1: Surface and bulk material properties of 100PTMC and ELAS 5000

	ELAS 5000 (Dry)	ELAS 5000 (Wet)	100PTMC (Dry) 1d	100PTMC (Wet)
M_n (g/mol)	5200		110,000	
T_g (^{o}C)	-6.8 ± 1.1	-8.7 ± 0.9	-15.4 ± 0.6	-16.0 ± 0.4
Water Content (%)		4.82 ± 0.01		2 ± 1
Contact Angle (^{o})	81 ± 2	85 ± 3	80 ± 1	75 ± 1
Bulk Modulus (MPa)	1.00 ± 0.04	1.22 ± 0.09	1.3 ± 0.2	1.4 ± 0.1
Surface Modulus (MPa)	1.03 ± 0.01	0.81 ± 0.04	1.34 ± 0.05	1.09 ± 0.06

7.4.2 Scanning Electron Microscopy

To confirm differences in macrophage mediated degradation of PTMC and ELAS 5000, RAW 264.7 monocyte-macrophages were cultured on 100PTMC and ELAS 5000 surfaces in DMEM supplemented with 10% bovine plasma for 14 days (Figure 7.1). After 14 days, macrophage mediated erosion was prevalent on the 100PTMC surface, however no signs of degradation were observed on the ELAS 5000 surfaces.

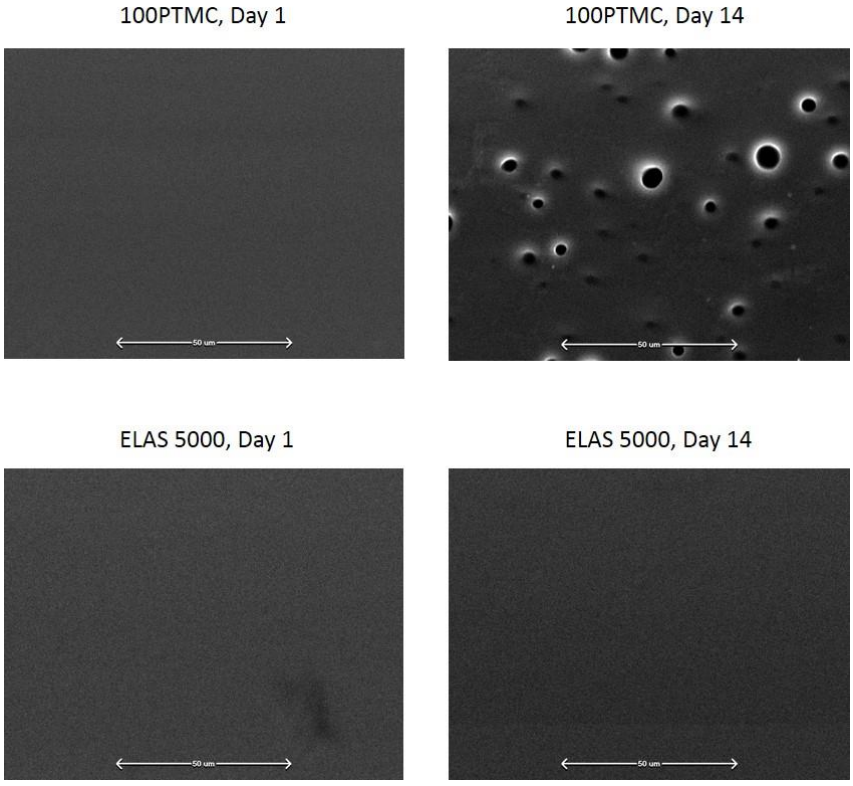

Figure 7.1: RAW 264.7 monocyte-macrophage degradation of 100PTMC and ELAS 5000 over 14 days of plasma supplemented culture (scalebar = 50 μm).

7.4.3 Oxidative and Enzymatic Degradation of 100PTMC and ELAS 5000

To confirm the susceptibility of 100PTMC to oxidative and enzymatic degradation, discs of 100PTMC were incubated in solutions of superoxide anion (Figure 7.2A), cholesterol esterase and lipase (Figure 7.2B) with ELAS 5000 as a comparison material. Superoxide anion

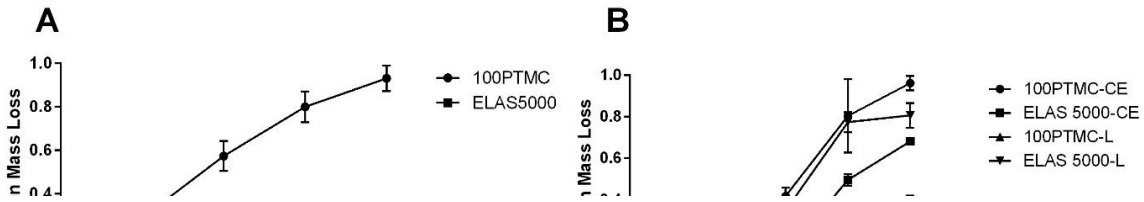

Figure 7.2: A: Oxidative degradation of 100PTMC and ELAS 5000. B: Enzymatic degradation of 100PTMC and ELAS 5000 by cholesterol esterase and lipase, (n=3).

[103], cholesterol esterase [167] and lipase [162] have been suggested to be responsible for the degradation of 100PTMC *in vivo*. Both 100PTMC and ELAS 5000 were degraded by cholesterol esterase and lipase, although the ELAS 5000 degraded at a slower rate, likely because the presence of crosslinks reduced the accessibility of the ester bond to the enzyme. Only 100PTMC was susceptible to oxidative degradation by the superoxide anion and degraded completely by 8 days. ELAS 5000 did not degrade oxidatively and did not experience any mass loss between days 2 and 8. The initial mass loss of ELAS 5000 between days 0 and 2 was likely due to the extraction of the uncrosslinked soluble fraction of the elastomer by THF in the degradation media.

7.4.4 Macrophage Adhesion and Activity on 100PTMC and ELAS 5000

Differences in macrophage degradation behavior on the polymers were determined by culturing RAW 264.7 monocyte-macrophages for 14 days on 100PTMC and ELAS 5000 surfaces with tissue culture polystyrene (TCPS) as a comparison surface. Macrophage number (Figure 7.3A) and secretion of degradative species including ROS (Figure 7.3B), superoxide anion (Figure 7.3C) and esterase (Figure 7.3D) were analyzed at days 1, 3, 7, 10 and 14. Significantly more cells were present on the 100PTMC surface compared to the ELAS 5000 and TCPS surfaces over 14 days despite only a small difference in cell attachment after 24 h. Cells grown on the 100PTMC surface secreted significantly more esterase and significantly less ROS, while the cells grown on ELAS 5000 secreted the opposite: significantly more ROS but significantly less esterase. No differences were measured in superoxide anion secretion by the macrophages on any of the surfaces over 14 days.

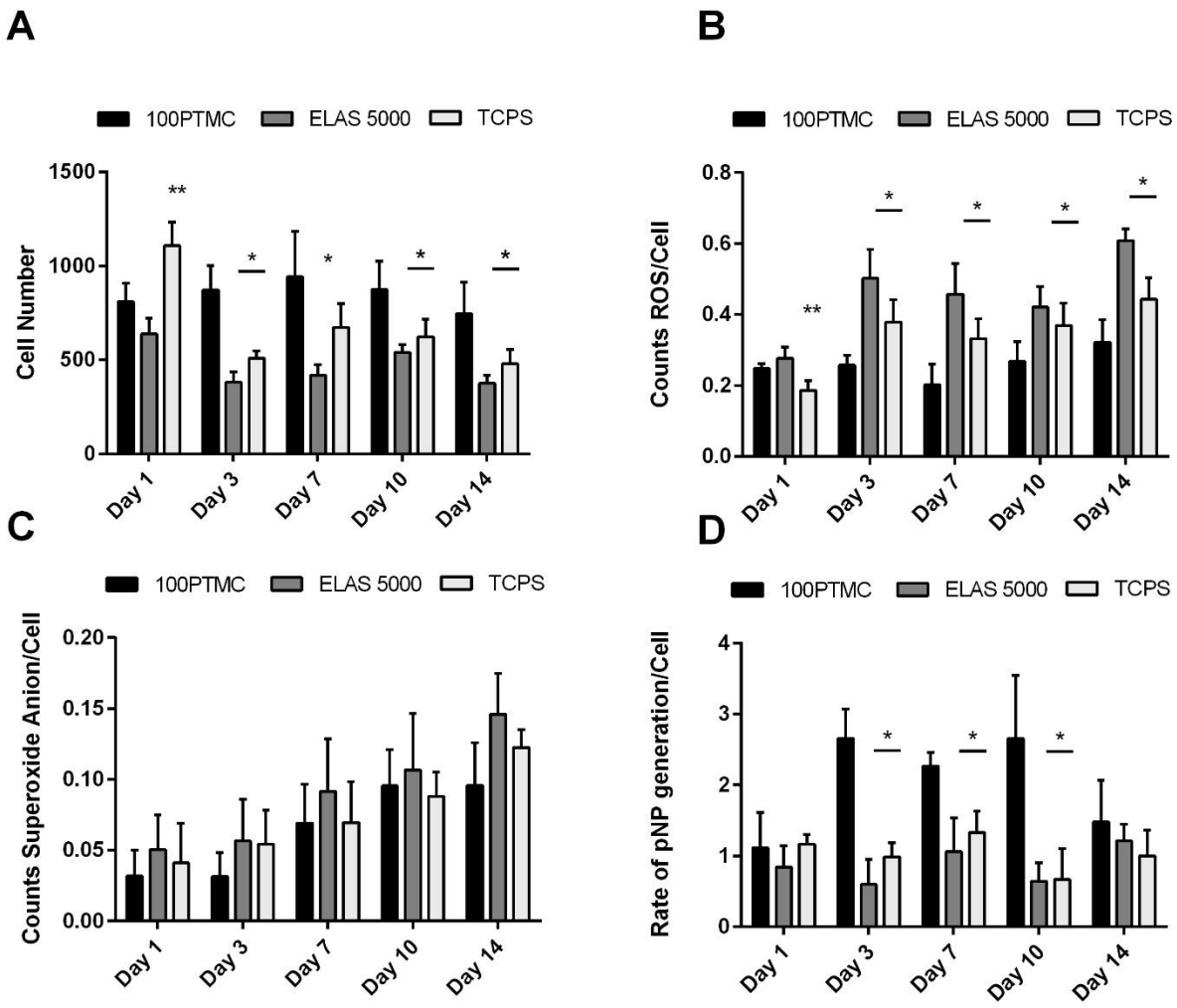

Figure 7.3: Number and degradative species secretion of RAW 264.7 cells cultured on 100PTMC, ELAS 5000 and tissue culture polystyrene (TCPS) surfaces. A: Cell number. B: Reactive oxygen species (excluding superoxide anion) secretion per cell. C: Superoxide anion secretion per cell. D: Esterase secretion per cell. *$p<0.05$ compared to 100PTMC, **$p<0.05$ compared to 100PTMC and ELAS 5000, (n=6).

7.4.5 Protein Adsorption to 100PTMC and ELAS 5000

Relative quantitation proteomics was used to determine ratios of the quantities of specific proteins that adsorbed from plasma to the 100PTMC and ELAS 5000 surfaces. 35 proteins or protein fragments were detected consistently across all 3 independent samples.

Table 7.2 reports the ratio of the number of peptides detected on the ELAS 5000 surface *vs.* 100PTMC surface of the 15 most abundant unique, identified proteins and those proteins (i.e. vitronectin) whose relative abundance was deemed significant (ratios greater than 1.5 or less than 0.5). Similar levels of total protein adsorption on the 100PTMC and ELAS 5000 surfaces (0.31 ± 0.04 and 0.2400 ± 0.05 $\mu g/cm^2$, respectively, $p < 0.15$) were confirmed by surface plasmon resonance. Albumin, fibrinogen and complement C3 were amongst the most abundant proteins in the protein layer adsorbed to the polymer surfaces, reflecting their relatively high abundance in plasma; however, no significant differences in the adsorption of these proteins were detected on the cell surfaces. Vitronectin, an extracellular matrix protein previously shown to influence foreign body giant (FBGC) formation [192] in IL-4 activated monocytes, adsorbed in significantly higher quantities to the ELAS 5000 surface in all three samples.

Table 7.2: Ratio of protein adsorbed from plasma suppl. media to ELAS 5000 : 100PTMC

Proteins adsorbed from Plasma	Peptide Count	Sample 1	Sample 2	Sample 3
Bovine serum albumin	43	0.88436	0.81248	0.68833
Serotransferrin	28	0.95449	0.77047	0.70508
Fibrinogen	26	1.1394	1.0145	1.347
Alpha-2-macroglobulin	23	1.0447	0.96416	1.0844
Complement C3	22	1.1596	1.1557	1.2007
Haptoglobin	14	1.0203	0.86863	0.70608
Inter-alpha-trypsin inhibitor	10	1.0569	0.88551	1.216
Serpin A3-1	9	0.94489	0.98697	0.92804
IGHM protein	9	1.0807	1.0037	1.0945
Serpin A3-5	9	0.82922	0.80093	0.7633
Hemopexin	7	0.9388	0.78575	0.61116
Apolipoprotein A-I	6	1.4001	1.3722	1.2029
C4b-binding protein alpha chain	6	0.75218	1.1841	0.5816
Alpha-1-antiproteinase OS	6	0.91507	1.0448	0.71688
Plasminogen	5	1.1577	0.97053	1.2271
Vitronectin	3	**1.9887**	**2.1107**	**2.286**

7.5 Discussion

7.5.1 Degradation of 100PTMC and ELAS 5000

In vivo, 100PTMC degrades by macrophage mediated oxidative/enzymatic surface erosion, but polyesters such as ELAS 5000 resist macrophage degradation despite similar susceptibility to enzymatic degradation (Figure 7.2B). This difference in the degradation mechanism was hypothesized to be due to a difference in macrophage activity on the polymer surfaces driven by differences in the adsorbed protein layers.

Macrophages were found to adhere and respond differently to the ELAS 5000 and 100PTMC surfaces. Despite similar levels of initial attachment (Figure 7.3A, day 1), significantly more macrophages remained on the 100PTMC surface between days 3 and 14. Furthermore, the type of degradative species secreted by the macrophages was dependent on the polymer surface to which they were attached; cells on the 100PTMC surface preferentially secreted degradative enzymes, and cells on the ELAS 5000 surface preferentially secreted oxidative degradation species.

This difference in macrophage response is considered to be responsible for the difference in macrophage mediated degradation rate of the polymers *in vivo*. Firstly, fewer macrophages remain attached to the ELAS 5000 surface, possibly due to oxidative stress resulting from the increased generation and secretion of ROS [98,199], decreasing the number of macrophages that are able to degrade the surface. Secondly, because ELAS 5000 is only susceptible to macrophage mediated degradation via enzymatic hydrolysis, lower generation of esterase in favor of higher generation of ROS results in limited degradation of the ELAS 5000 surface.

7.5.2 Protein Adsorption to 100PTMC and ELAS 5000

Macrophage response to biomaterials is believed to be influenced by proteins, especially immunoglobulins and complement, that adsorb to the biomaterial surface from the surrounding environment [27]. Despite differences in macrophage adherence and degradative species secretion on the 100PTMC and ELAS 5000 surfaces, no significant differences were found in the ratio of complement or immunoglobulin proteins adsorbed to the polymer surfaces. Interestingly, vitronectin, an integrin binding protein also associated with macrophage adhesion and FBGC formation [74], adsorbed in significantly higher quantities to the ELAS 5000 surface, which resists macrophage adhesion and undergoes no macrophage mediated degradation. It is possible that more complement and integrin binding proteins are present on the polymer surfaces other than those listed here; however, their concentrations in the adsorbed protein layers may be below the detection limits of this method.

Despite the generally accepted hypothesis that adsorbed proteins mediate cell response to biomaterials, few studies have directly examined the effect of adsorbed protein on monocyte/macrophage response to and activation on biomaterial surfaces in the absence of an additional activation factor (LPS, etc.). Previous studies using unactivated human primary monocytes have identified adsorbed IgG and α-2-macroglobulin as a potential mediators of monocyte activity [189,200], however the proteome results in this study did not show any differences in α-2-macroglobulin adsorption and did not identify IgG on these surfaces.

Higher amounts of vitronectin adsorption have been previously shown to increase attachment of unactivated monocytes [200] which is not consistent with the macrophage attachment data shown here. Additionally, adsorbed vitronectin was found to induce FBGC formation in macrophages activated by IL-4 [27,192]. For the monocyte derived macrophages

used in this study, no activation molecules were present in the culture beyond what was present in the adult bovine plasma and material surface itself, and it is unclear whether surface adsorbed vitronectin alone is sufficient to induce macrophage fusion or influence the secretion of degradative species. Interestingly, in this study, the presence of adsorbed vitronectin reduced the amount of ROS secretion in favor of enzyme production. The vitronectin receptor (an $\alpha_v\beta_3$ integrin) is used by certain populations of monocytes/macrophages to phagocytose apoptotic cells [201]. Adsorbed Vitronectin is also known to increase rates of phagocytosis for particles previously opsonized by IgG and complement C3b for phagocytosis [202]. Adsorbed vitronectin may be similarly capable of mediating macrophage activation during frustrated phagocytosis and altering levels of ROS and enzyme secretion

It is important to note that, relative quantitation proteomics only measures relative quantity of proteins/peptides adsorbed to the surface. It is possible that some of the proteins which appear to be adsorbed in similar quantities, including complement C3, may be adsorbed in different conformations on the polymer surfaces. These differences in conformation may induce a difference in macrophage adhesion or activation. Further studies investigating monocyte activation by these materials should focus on determining differences in adsorbed opsonin conformation. Additionally, there may be other complement factors or proteins capable of promoting monocyte adhesion (e.g. fibronectin [203]) that are present on the surfaces in quantities below the limits of detection, but assist or otherwise influence macrophage activation. Furthermore, activated macrophages are able to attract and activate other macrophages via secretion of chemotactic factors [27]. It is possible that the effect of small differences in protein conformation or adsorption quantity may become amplified as macrophages stimulate surrounding cells.

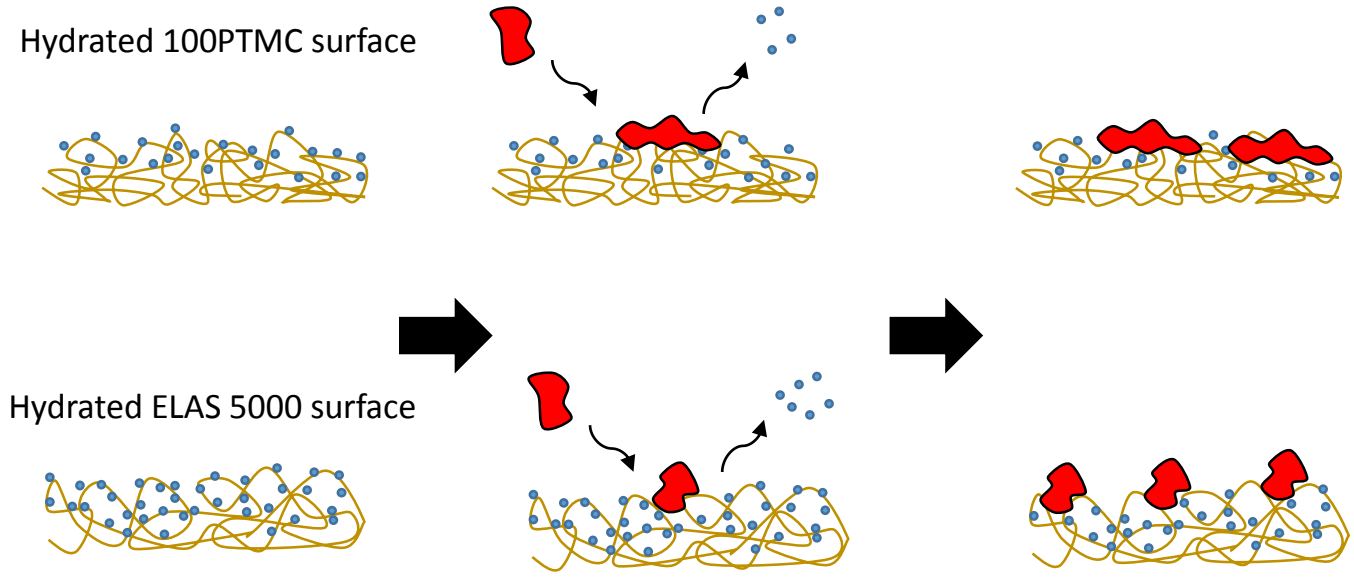

Figure 7.4: Proposed schematic for the influence of polymer chain flexibility and surface hydration on protein adsorption. Polymer chain flexibility influences the organization of water molecules bound to and around the polymer chains. This difference in organization affects the amount of bound water freed from the surface upon protein adsorption, affecting the preferred adsorbed conformation of the adsorbed protein.

Finally, protein adsorption is believed to mediate cell response to the biomaterial; however biomaterial properties that affect protein adsorption and especially competitive protein adsorption (e.g. from plasma and serum) are still unclear. Protein adsorption to PTMC and ELAS 5000 is influenced by the arrangement of bound water at the polymer aqueous interfaces [67,77]. ELAS 5000 and PTMC are hydrophobic polymers with similar bulk moduli, yet differences were present in the quantities and possibly conformations of adsorbed proteins. When hydrated, the surface moduli of both polymers were significantly different despite there being no difference in bulk modulus. The contact angle and nanoindentation results imply that these hydrophobic polymers, when conditioned in water, developed hydrated aqueous-polymer "interphase" regions [16], with a higher water content and different mechanical properties from the bulk polymer (Figure 7.4). Despite being similarly hydrophobic in the dry state, these polymers possess different functional groups (carbonates vs. esters) and different polymer

chain flexibilities, therefore, it is likely that the polymer chains in this surface interphase region possess a different arrangement of water molecules on and around the chains and therefore induce differences in subsequent protein adsorption.

7.6 Conclusion

100PTMC degrades *in vivo* via macrophage mediated oxidative/enzymatic degradation mechanisms. However ELAS 5000, despite a similar surface hydrophobicity, is resistant to macrophage mediated degradation. We hypothesized that this difference in degradation mechanisms was due to a differences macrophage response to the polymers driven by differences in the composition of the protein layer that adsorbs from plasma. Macrophages adhered to PTMC in higher numbers compared to ELAS 5000 and furthermore, macrophages adhering to the ELAS 5000 surface secreted higher amounts of oxidative degradative species and lower amounts of enzymatic degradative species. Relative quantitation proteomics showed that abundant plasma opsonin proteins (e.g. C3, and IgM) adsorbed in similar quantities to both surfaces, however, vitronectin adsorbed in significantly greater quantities to the ELAS 5000 surface. It is possible that surface adsorbed vitronectin affected the activation of the macrophages resulting in a preferential secretion of ROS over degradative enzymes.

Chapter 8

Conclusions and Recommendations for Future Work

8.1 Conclusions

8.1.1 The Effect of Polymer Chain Flexibility on Protein Adsorption

Polymer chain flexibility was hypothesized to influence both protein conformation and adsorbed protein layer composition by affecting the arrangement of water molecules bound to the polymer chains. In both individual and competitive adsorption environments, polymer chain flexibility was shown to affect the quantities of proteins that adsorb from solution. Polymer chain flexibility also altered the conformation of adsorbed proteins to the extent of changing the viscoelastic properties (thickness, shear modulus, and viscosity) of adsorbed proteins and inactivating adsorbed enzymes.

These results were explained in terms of the thermodynamics governing protein adsorption, which is primarily an entropically driven phenomenon. The organization of water molecules around the mobile polymer chains at the interface affects the quantity of water molecules released and the associated system entropy gain as proteins adsorb. The conformation in which a protein adsorbs also influences the amount of water released from both the protein molecule and the surface. Altering the entropy of the system prior to adsorption, may impact the probability that a protein will adsorb in a specific conformation.

Differences in preferred adsorbed protein conformation are able to affect the final equilibrium composition of the adsorbed protein layer. Firstly, adsorbed conformation affects the amount of physical space occupied by the adsorbed protein. Secondly, the conformation of

an adsorbed protein affects both the interfacial energy and entropy barrier to desorption, influencing the likelihood that the adsorbed protein will desorb or be displaced by another protein [14,18].

8.1.2 The Effect of Polymer Chain Flexibility on Water Adsorption/Absorption

Upon hydration, both ELAS and PTMC developed an "interphase" region at their surfaces formed by water molecules penetrating into the polymer surface, which was different from their bulk, as previously described by Vogler [16]. This surface interphase region possessed both different mechanical properties and water content than the bulk polymer as shown by nano-indentation measurements (Table A.1) and ATR-FTIR data, respectively. The polymers studied here (ELAS and PTMC) are generally hydrophobic, but include hydrophilic functional groups (i.e. carbonate or ester functionalities) in their polymer backbones. Water molecules are able coordinate with the hydrophilic functionalities and penetrate into the surface of the polymer around the flexible and mobile polymer chains. The polymer chains at the surface of the elastomer are less confined and more mobile than the chains in the polymer bulk and so may reorient themselves into conformations more favorable to water-polymer interactions. Therefore, the aqueous-polymer interface becomes a super-hydrated region compared to the bulk which contains less water.

Polymer chain mobility influenced the depth and water content of this super-hydrated, interphase region. Between polymers with nearly identical surface chemistry, the polymer with more flexible polymer chains experienced a larger decrease in surface modulus upon hydration (Table A.1), suggesting that the polymer-aqueous interphase region for polymers with more

chain flexibility possessed a higher water content and a less dense arrangement of polymer chains than their stiffer counterparts. ATR-FTIR scans (penetration depth up to 2 μm) showed differences in surface absorbed water content of ELAS but not for PTMC, suggesting that the interphase region for ELAS (avg T_g = -3 °C), may be less than 2 μm deep, but extends beyond depths of 2 μm for PTMC which has more flexible polymer chains (T_g = -15 °C).

8.1.3 Polymer Chain Flexibility, Fetuin A Adsorption and Subsequent Cell Behavior

The influence of ELAS polymer chain mobility on the composition of the adsorbed protein layer affected subsequent cell response to the material. Surface adsorbed alpha-2-HS-glycoprotein (fetuin A) increased NIH3T3 fibroblast proliferation when basic fibroblast growth factor (FGF-2) was also present in the medium. Fetuin A, a calcium binding protein, was hypothesized to improve cell proliferation by increasing the local concentration of calcium, affecting calcium mediated mechanisms such as annexin or possibly integrin binding or divalent cation mediated growth factor receptors.

Polymer chain mobility influenced the mass and viscoelastic properties of fetuin A when adsorbed individually, suggesting differences in adsorbed conformation. Due to these differences in adsorbed conformation, the fetuin A adsorbed to the ELAS 5000 surface may have resisted replacement by other proteins, leading to a higher quantity of fetuin A in the protein layers adsorbed from serum. Differences in fetuin A adsorbed conformation may also influence its calcium binding properties, which, in turn, would influence its ability to promote calcium mediated cell behaviors.

8.1.4 Individual and Competitive Protein Adsorption and the Non-Physiologic Nature of FBS

Polymer chain mobility was found to impact the mass and conformation of both fibronectin and immunoglobulin G adsorbed from solutions of individual proteins, and therefore it was hypothesized that fibronectin, specifically, was affecting fibroblast proliferation (Chapter 4). However, no differences in the amount of these proteins were detected on the ELAS or PTMC surfaces in the protein layers that adsorbed from serum and plasma, possibility due to a low abundance of these proteins on the material surfaces.

These results reinforce the importance of investigating competitive protein adsorption from serum and plasma to gain a more complete picture of protein adsorption both *in vivo* and *in vitro* in supplemented cell culture. The biomaterials literature has focused primarily on proteins that include integrin binding motifs within their sequences (e.g. fibronectin and vitronectin) which promote integrin driven cell attachment or immunoglobulins/complement proteins that influence the immunogenic response to a material. However, these proteins are present in relatively low abundance (compared to albumin, fetuin A, etc.) in serum and plasma supplemented culture environments. Therefore, in competitive adsorption environments, these proteins may comprise a much lower percentage of the adsorbed protein layer and subsequently induce a lessened or negligible effect on cell response compared to more abundant, less well-known proteins. It is important therefore to study protein adsorption and cell response in serum and plasma supplemented systems, to identify other proteins that are not well understood, but which may be relevant to biomaterial cell response due to their high concentration in serum/plasma.

Finally, fetuin A, the protein that was found to contribute to the difference in fibroblast proliferation, is present in high concentrations in FBS but only in low concentration in newborn

or adult plasma/serum. Fetal bovine serum is an extremely common growth supplement due to its relatively low cost and its effectiveness in promoting *in vitro* cell attachment and proliferation compared to adult serum/plasma. The observed influence of surface adsorbed fetuin A, specifically, on cell response, emphasizes the non-physiological nature of FBS. It is therefore important to confirm protein adsorption and cellular response results *in vivo* or in an adult plasma supplemented environment.

8.1.5 Conflicts in RAW 264.7 Macrophage Results

RAW 264.7 murine monocyte derived macrophages were cultured on 60PTMC and 100PTMC (Chapter 6) in FBS supplemented media and again on 100PTMC and ELAS 5000 in adult bovine plasma supplemented media. Because RAW 264.7 cells have been reported to grow very well on TCPS [204], TCPS was used as a comparison surface and a high growth control. However, there were some discrepancies between the literature reported proliferation of these cells and the cell proliferation results in chapters 6 and 7.

In chapter 6, RAW 264.7 macrophages attached but did not proliferate on TCPS in FBS supplemented media. Because the cells expanded well in the T-175 flasks prior to seeding (in FBS supplemented media), the lack of proliferation suggests that the environment (and thus, the cell response) in the 96 well plate was different from the flasks. During preparation, the 96 well plates were removed from a sterile environment in order to coat the experimental wells with PTMC, and were re-sterilized under UV light. It is possible that endotoxin was present in the TCPS wells, which activated the monocyte/macrophages towards a more macrophage like phenotype, increasing ROS/enzyme production (as the results indicate) which may reduce

proliferation by inducing NO mediated apoptosis [205]. If endotoxin was present on the re-sterilized TCPS, it was likely also present on the PTMC coated experimental wells in similar quantities, and did not result in "extra activation" of the macrophages on the TCPS comparison surface.

In chapter 7, macrophages were cultured on TCPS in adult bovine plasma supplemented media. The previous results (Chapter 6) showed that approximately 10,000 cells attached per well and cell number was maintained over 14 days. In Chapter 7, only 1,000 cells attached and decreased in number over 14 days. The most likely explanation for this lower cell attachment and proliferation is the absence of fetal serum. Fetal serum, with its abundant growth factors and lower immunoglobulin concentration, is used as a common growth culture supplement and is the recommended culture supplement for RAW 264.7 macrophages (ATCC culture methods). Additionally, it has been reported that the removal of fetal serum from media can induce apoptosis [206] in these cells, suggesting that some of the nutrients FBS provides must be essential for proliferation. A second possible reason for low growth may be related to activation. Adult plasma contains higher levels of immunoglobulins and complement compared to fetal serum. It is possible that the cells were comparatively more activated in adult plasma supplemented culture at earlier time points, as evidenced by the similar levels of surface erosion of 100PTMC in Chapter 6 and Chapter 7 despite the differences in cell number. Monocyte/macrophages that are highly activated may attach in higher numbers but may be subject to less proliferation and greater amounts of NO mediated apoptosis. As the first time point was at 24 hours (*i.e*. survival instead of initial attachment), low cell numbers may not be due to lower levels of attachment, but because fewer cells survived until the first time point.

A final possibility is that the batches of RAW 264.7 cells used in the chapter 6 and chapter 7 studies were different in some way. The cell studies in chapter 6 and chapter 7 were performed approximately 3 years apart, and the cells used in the studies were likely at different passages and perhaps different growth phases during seeding. However, RAW 264.7 cells are an immortalized cell line which are typically used at up to 20 passages [207] and so this is not expected to be a factor in the discrepancy between the Chapter 6 and Chapter 7 results.

8.2 Recommendations for Future Work

8.2.1 Improvements on Relative Quantitation Proteomics

The limiting factor in the use of proteomics methods to analyze serum/plasma adsorption to biomaterial surfaces is the quantity of the protein sample required for the method to detect proteins of lower abundance. Adsorbed protein sample size is, in turn, limited by the material surface area available for adsorption. The proteomics analysis presented herein only identified and relatively quantified the most abundant proteins present in the adsorbed protein layer. Proteins of lower abundance were either undetectable, or their calculated adsorption ratios were prone to inconsistency due to the low number of peptides detected. It is possible that there were other proteins adsorbed in quantities below this detection limit that affected cell response. A method to increase adsorption surface area by further decreasing microsphere size or creating textured polymer surfaces would allow for the detection of more proteins and thereby improve the accuracy of this technique.

8.2.2 Other Uses of Relative Quantitation Proteomics for Analysis of Cell Response

8.2.2.1 Cellular Modification of Biomaterial Surfaces

In this thesis, relative quantitation proteomics was used to compare protein layers adsorbed to surfaces after 12 h of adsorption, prior to cell attachment. However, as cells survive and grow on a substrate, they may alter the surfaces on which they are attached by secreting extracellular matrix proteins (*e.g*. fibroblasts) or changing the surface chemistry of the substrate via degradation (*e.g*. macrophages), which may subsequently alter the proteins that are adsorbed to the material. Relative quantitation proteomics has the potential to be used to compare protein adsorbed/deposited on the ELAS surface after several days of cell culture to determine possible differences in longer-term protein adsorption and/or extracellular matrix deposition.

8.2.2.2 Relative Quantitation Proteomics for Analysis of Cell Response

The proteomics method described in this thesis is limited to the analysis of proteins adsorbed to biomaterial surfaces. Proteomics methods have also previously been used to analyze cell lysates [208,209] and cell culture supernatants [194,210] to determine differences in protein and cytokine expression in response to biomaterials. Similarly, relative quantitation proteomics could be used to detect differences in cell response which may help identify differences in surface adsorbed proteins to which the cells may be responding, including possible adhesion/integrin recruitment on surfaces with high numbers of integrin binding sites [211] and differences in monocyte/macrophage activation [194]. Experiments of this nature would be particularly useful to complement the proteomics results of chapters 5 and 7, where

no differences in integrin binding proteins or complement and immunoglobulin, respectively, were detected, despite observed differences in fibroblast proliferation and macrophage secretion of degradative species. Differences in integrin recruitment or macrophage activation markers may give additional evidence to differences in adsorbed integrin binding proteins or opsonins which may have been present on the material surfaces in quantities below the limits of detection.

8.2.3 Additional Adsorbed Protein Conformation Studies

The individual and competitive protein adsorption studies detailed in this thesis are primarily focused on the mass of the protein adsorbed with only a qualitative examination of adsorbed protein conformation. Most cellular response to adsorbed protein, however, is not mediated by protein quantity, alone, but rather the exposure of various functionalities in the proteins to receptors on the attaching cells (*e.g.* integrin binding motifs, immunoglobulin epitopes, *etc*.). While measuring protein mass is a logical first step to determine which proteins are influencing cell response, the continuation of this research should focus on a more specific determination of adsorbed protein conformation in terms of exposure of this cell-reactive sites. This is especially relevant to Chapter 7, in which IgM and complement C3 adsorbed to the polymer surfaces in equal amounts but could have adsorbed in different conformations, resulting in differences in monocyte/macrophage activity. ELISA or molecular force microscopy studies that measure the binding of antibody molecules to specific regions of protein that include active cell-reactive motifs would be useful to quantitatively measure

differences in conformation and give information as to the mechanism by which cells respond to adsorbed proteins.

8.2.4 Macrophage Activation by Biomaterial Surfaces

Current biomaterials literature pertaining to monocyte/macrophage activation on biomaterial surfaces is focused on monocyte/macrophage response to biomaterials after activation by LPS, IL-4, and so on. Very few studies have examined monocyte/macrophage activation by surface adsorbed proteins alone [189,200,212]. The results from chapter 7 indicated that RAW 264.7 monocyte derived macrophages attach in high quantities and preferentially secrete degradative enzymes instead of reactive oxygen species when grown on 100PTMC compared to ELAS 5000. The results of the proteomics analysis showed that vitronectin adsorbed in significantly higher quantities to the ELAS surface, where the RAW cells secreted more reactive oxygen species. While surface adsorbed vitronectin has been associated previously with higher foreign body giant cell formation in IL-4 activated macrophages, it is unclear as to whether adsorbed vitronectin alone directly affects macrophage activation. Further analysis of the macrophages, including staining for foreign body giant cell formation or expression of activation markers, could be used to determine if differences in surface adsorbed plasma or individually adsorbed vitronectin induces differences in macrophage activation without the addition of IL-4.

8.2.5 Macrophage Cell Lines vs. Primary Cells

The macrophage cultures performed in chapters 6 and 7 use RAW 264.7 cells, an immortalized monocyte derived macrophage cell line derived from murine blood. The goal of this thesis was to determine the effect of protein adsorption on cell behavior. Therefore, the RAW 264.7 cell line was chosen because it is a naturally adherent cell line which did not require activation by the addition of LPS to adhere to and degrade the 100PTMC surface. It is also well characterized in the literature, and, as an immortalized cell line, generally yields consistent and repeatable results, which was an important factor given the variability of competitive protein environments such as FBS or adult plasma. However, there are some variable characteristics of RAW 264.7 monocyte/macrophages phenotype that emphasize the need to develop a more physiologically relevant model environment for biomaterial-macrophage activation.

RAW 264.7 cells are referred to as a monocyte/macrophage cell line, having qualities of both undifferentiated monocytes and differentiated macrophages [30]. Unactivated RAW cells possess a monocyte-like phenotype. When activated by the addition of a stimulatory molecule (LPS, IFN-γ, etc.), RAW cells transform into a macrophage-like phenotype [30]. However, RAW cells have been shown to have variations in their macrophage-like behavior depending on the activation molecule used [213], including expression of iNOS [214,215], the enzyme that synthesizes ROS, and the secretion of other activation and signaling molecules such as TNF-α [216,217]. Because the goal of this thesis was to examine biomaterial (and adsorbed protein) mediated activation, the RAW cells used in these studies were not activated by the addition of an activation molecule. However, a similar study in which *activated* RAW cells are cultured on PTMC and ELAS surfaces could yield different results, including

degradation of 60PTMC or ELAS by the RAW cells, depending on the activation molecule used. Furthermore, the monocytes that respond to implanted biomaterials *in vivo* are not immortalized monocyte/macrophage hybrids but rather exist as monocytes in the blood or tissue, which then extravasate and differentiate into macrophages when activated at the site of the biomaterial implantation. For this reason, neither unactivated nor activated RAW 264.7 monocyte/macrophages are an ideal cell type to examine biomaterial/protein mediated activation of monocytes.

The eventual purpose of most biomaterials is to be implanted into a living body, so perhaps the most obvious physiologically relevant model for macrophage response is an *in vivo* animal model. This model would allow the examination of the effects of tissue inflammation and macrophage mediated degradation on the biomaterial and activated macrophages. However, it would prove difficult to measure protein adsorption and protein mediated activation of monocytes using this model due to the adherence of tissue and other cells to the implanted material. So for the purpose of studying protein adsorption and monocyte activation via adsorbed proteins, an *in vivo* system is too complex. An *in vitro* cell culture model would yield more consistency in the results.

Upon implantation, a biomaterial will come into contact with the tissue and fluid at the site into which it is implanted, and thus one model *in vitro* culture system could focus on the adsorption of proteins from the interstitial fluid and the activation of monocytes found in the surrounding tissue. The composition of interstitial fluid depends on the tissue but typically contains less albumin and other proteins responsible for maintaining oncotic pressure in the circulatory system [218]. Thus, the ideal model system would utilize the interstitial fluid and

resident monocytes of the intended location of the implant, though collection of interstitial fluid and isolation of the monocytes to use in culture may prove inconvenient.

Alternatively, even though a biomaterial may be eventually implanted into tissue, at the time of surgery, the first fluid to make contact with the biomaterial is whole blood at the incision site. Thus, plasma proteins are the first proteins to adsorb to the biomaterial (though they may later be replaced by proteins from interstitial fluid) and the first monocytes to respond to the biomaterial are monocytes present in the blood. A second *in vitro* protein-cell response model could examine the adsorption of blood plasma and the response of primary monocytes derived from blood. The collection of blood plasma and isolation of monocytes in this system is much more convenient, and is a logical next step to improve the physiological relevance of the biomaterial-protein-cell response model.

References

[1] Shi R, Chen D, Liu Q, Wu Y, Xu X, Zhang L, et al. Recent advances in synthetic bioelastomers. Int J Mol Sci 2009;10:4223–56.

[2] Chen Q, Liang S, Thouas GA. Elastomeric biomaterials for tissue engineering. Prog Polym Sci 2013;38:584–671.

[3] Dhandayuthapani B, Yoshida Y, Maekawa T, Kumar DS. Polymeric scaffolds in tissue engineering application: A review. Int J Polym Sci 2011;2011:1–19.

[4] Engler A, Richert L, Wong J, Picart C, Discher D. Surface probe measurements of the elasticity of sectioned tissue, thin gels and polyelectrolyte multilayer films: Correlations between substrate stiffness and cell adhesion. Surf Sci 2004;570:142–54.

[5] Beningo KA, Wang Y. Fc-receptor-mediated phagocytosis is regulated by mechanical properties of the target. J Cell Sci 2002;115:849–56.

[6] Féréol S, Fodil R, Labat B, Galiacy S, Laurent VM, Louis B, et al. Sensitivity of alveolar macrophages to substrate mechanical and adhesive properties. Cell Motil Cytoskeleton 2006;63:321–40.

[7] Irwin EF, Saha K, Rosenbluth M, Gamble LJ, Castner DG, Healy KE. Modulus-dependent macrophage adhesion and behavior. J Biomater Sci Polym Ed 2008;19:1363–82.

[8] Blakney AK, Swartzlander MD, Bryant SJ. The effects of substrate stiffness on the in vitro activation of macrophages and in vivo host response to poly(ethylene glycol)-based hydrogels. J Biomed Mater Res - Part A 2012;100 A:1375–86.

[9] Engler AJ, Sen S, Sweeney HL, Discher DE. Matrix elasticity directs stem cell lineage specification. Cell 2006;126:677–89.

[10] Discher DE, Janmey P, Wang Y-L. Tissue cells feel and respond to the stiffness of their substrate. Science 2005;310:1139–43.

[11] Wells RG. The role of matrix stiffness in regulating cell behavior. Hepatology 2008;47:1394–400.

[12] Kowalczyńska HM, Nowak-Wyrzykowska M. Modulation of adhesion, spreading and cytoskeleton organization of 3T3 fibroblasts by sulfonic groups present on polymer surfaces. Cell Biol Int 2003;27:101–14.

[13] Lo CM, Wang HB, Dembo M, Wang YL. Cell movement is guided by the rigidity of the substrate. Biophys J 2000;79:144–52.

[14] Wilson CJ, Clegg RE, Leavesley DI, Pearcy MJ. Mediation of biomaterial-cell interactions by adsorbed proteins: a review. Tissue Eng 2005;11:1–18.

[15] Xia Z, Triffitt JT. A review on macrophage responses to biomaterials. Biomed Mater 2006;1:R1–9.

[16] Vogler EA. Protein adsorption in three dimensions. Biomaterials 2012;33:1201–37.

[17] Roach P, Eglin D, Rohde K, Perry CC. Modern biomaterials: a review - bulk properties and implications of surface modifications. J Mater Sci Mater Med 2007;18:1263–77.

[18] Rabe M, Verdes D, Seeger S. Understanding protein adsorption phenomena at solid surfaces. Adv Colloid Interface Sci 2011;162:87–106.

[19] Ruoslahti E, Pierschbacher M. New perspectives in cell adhesion: RGD and integrins. Science (80-) 1987;238:491–7.

[20] Morgan MR, Humphries MJ, Bass MD. Synergistic control of cell adhesion by integrins and syndecans. Nat Rev Mol Cell Biol 2007;8:957–69.

[21] Pelham RJ, Wang YL. Cell locomotion and focal adhesions are regulated by substrate flexibility. Proc Natl Acad Sci U S A 1997;94:13661–5.

[22] Wang N, Butler JP, Ingber DE. Mechanotransduction across the cell surface and through the cytoskeleton. Science 1993;260:1124–7.

[23] Xu H, Bihan D, Chang F, Huang PH, Farndale RW, Leitinger B. Discoidin domain receptors promote α1β1- and α2β1-integrin mediated cell adhesion to collagen by enhancing integrin activation. PLoS One 2012;7.

[24] Elbert DL, Hubbell JA. Surface treatments of polymers for biocompatibility. Annu Rev Mater Sci 1996;26:365–294.

[25] Siever DA, Erickson HP. Extracellular annexin II. Int J Biochem Cell Biol 1997;29:1219–23.

[26] Ballet T, Boulange L, Brechet Y, Bruckert F, Weidenhaupt M. Protein conformational changes induced by adsorption onto material surfaces: an important issue for biomedical applications of material science. Bull Polish Acad Sci Tech Sci 2010;58.

[27] Anderson JM, Rodriguez A, Chang DT. Foreign body reaction to biomaterials. Semin Immunol 2008;20:86–100.

[28] Hashimoto D, Chow A, Noizat C, Teo P, Beasley MB, Leboeuf M, et al. Tissue-resident macrophages self-maintain locally throughout adult life with minimal contribution from circulating monocytes. Immunity 2013;38:792–804.

[29] Brown BN, Valentin JE, Stewart-Akers AM, McCabe GP, Badylak SF. Macrophage phenotype and remodeling outcomes in response to biologic scaffolds with and without a cellular component. Biomaterials 2009;30:1482–91.

[30] Chamberlain LM, Godek ML, Gonzalez-Juarrero M, Grainger DW. Phenotypic non-equivalence of murine (monocyte-) macrophage cells in biomaterial and inflammatory models. J Biomed Mater Res - Part A 2009;88:858–71.

[31] Van Lookeren Campagne M, Wiesmann C, Brown EJ. Macrophage complement receptors and pathogen clearance. Cell Microbiol 2007;9:2095–102.

[32] Henson PM. The immunologic release of constituents from neutrophil leukocytes. II. Mechanisms of release during phagocytosis, and adherence to nonphagocytosable surfaces. J Immunol 1971;107:1547–57.

[33] Collier T, Anderson JM. Protein and surface effects on monocyte and macrophage adhesion, maturation, and survival. J Biomed Mater Res 2002;60:487–96.

[34] McNally AK, Anderson JM. Beta1 and beta2 integrins mediate adhesion during macrophage fusion and multinucleated foreign body giant cell formation. Am J Pathol 2002;160:621–30.

[35] Shen M, Pan Y V, Wagner MS, Hauch KD, Castner DG, Ratner BD, et al. Inhibition of monocyte adhesion and fibrinogen adsorption on glow discharge plasma deposited tetraethylene glycol dimethyl ether. J Biomater Sci Polym Ed 2001;12:961–78.

[36] Anderson JM, Defife K, McNally A, Collier T, Jenney C. Monocyte, macrophage and foreign body giant cell interactions with molecularly engineered surfaces. J Mater Sci Mater Med n.d.;10:579–88.

[37] Brevig T, Holst B, Ademovic Z, Rozlosnik N, Røhrmann JH, Larsen NB, et al. The recognition of adsorbed and denatured proteins of different topographies by β 2 integrins and effects on leukocyte adhesion and activation. Biomaterials 2005;26:3039–53.

[38] Vogler EA. Structure and reactivity of water at biomaterial surfaces. Adv Colloid Interface Sci 1998;74:69–117.

[39] Chuang W. Swelling behavior of hydrophobic polymers in water/ethanol mixtures. Polymer (Guildf) 2000;41:8339–47.

[40] Randall GC, Doyle PS. Permeation-driven flow in poly(dimethylsiloxane) microfluidic devices. Proc Natl Acad Sci U S A 2005;102:10813–8.

[41] Collier TO, Jenney CR, DeFife KM, Anderson JM. Protein adsorption on chemically modified surfaces. Biomed. Sci. Instrum., vol. 33, 1997, p. 178–83.

[42] Vroman L. Effect of adsorbed proteins on the wettability of hydrophilic and hydrophobic solids. Nature 1962;196:476–7.

[43] Van Tam JK, Uto K, Ebara M, Pagliari S, Forte G, Aoyagi T. Mesenchymal stem cell adhesion but not plasticity is affected by high substrate stiffness. Sci Technol Adv Mater 2012;13:064205.

[44] Brown XQ, Ookawa K, Wong JY. Evaluation of polydimethylsiloxane scaffolds with physiologically-relevant elastic moduli: interplay of substrate mechanics and surface chemistry effects on vascular smooth muscle cell response. Biomaterials 2005;26:3123–9.

[45] Califano JP, Reinhart-King CA. Substrate stiffness and cell area predict cellular traction stresses in single cells and cells in contact. Cell Mol Bioeng 2010;3:68–75.

[46] Choquet D, Felsenfeld DP, Sheetz MP. Extracellular matrix rigidity causes strengthening of integrin-cytoskeleton linkages. Cell 1997;88:39–48.

[47] Zhu C, Bao G, Wang N. Cell mechanics: mechanical response, cell adhesion, and molecular deformation. Annu Rev Biomed Eng 2000;2:189–226.

[48] Rowlands AS, George PA, Cooper-White JJ. Directing osteogenic and myogenic differentiation of MSCs: interplay of stiffness and adhesive ligand presentation. Am J Physiol Cell Physiol 2008;295:C1037–44.

[49] García JR, García AJ. Cellular mechanotransduction: sensing rigidity. Nat Mater 2014;13:539–40.

[50] Yip AK, Iwasaki K, Ursekar C, MacHiyama H, Saxena M, Chen H, et al. Cellular response to substrate rigidity is governed by either stress or strain. Biophys J 2013;104:19–29.

[51] Paszek MJ, Zahir N, Johnson KR, Lakins JN, Rozenberg GI, Gefen A, et al. Tensional homeostasis and the malignant phenotype. Cancer Cell 2005;8:241–54.

[52] Brown XQ, Bartolak-Suki E, Williams C, Walker ML, Weaver VM, Wong JY. Effect of substrate stiffness and PDGF on the behavior of vascular smooth muscle cells: Implications for atherosclerosis. J Cell Physiol 2010;225:115–22.

[53] Yeung T, Georges PC, Flanagan LA, Marg B, Ortiz M, Funaki M, et al. Effects of substrate stiffness on cell morphology, cytoskeletal structure, and adhesion. Cell Motil Cytoskeleton 2005;60:24–34.

[54] Shi X, Qin L, Zhang X, He K, Xiong C, Fang J, et al. Elasticity of cardiac cells on the polymer substrates with different stiffness: an atomic force microscopy study. Phys Chem Chem Phys 2011;13:7540–5.

[55] Solon J, Levental I, Sengupta K, Georges PC, Janmey P a. Fibroblast adaptation and stiffness matching to soft elastic substrates. Biophys J 2007;93:4453–61.

[56] Buxboim A, Ivanovska IL, Discher DE. Matrix elasticity, cytoskeletal forces and physics of the nucleus: how deeply do cells “feel” outside and in? J Cell Sci 2010;123:297–308.

[57] Balcioglu HE, van Hoorn H, Donato DM, Schmidt T, Danen EH. Integrin expression profile modulates orientation and dynamics of force transmission at cell matrix adhesions. J Cell Sci 2015:1316–26.

[58] Levental I, Georges PC, Janmey PA. Soft biological materials and their impact on cell function. Soft Matter 2007;3:299.

[59] Park JS, Chu JS, Tsou AD, Diop R, Tang Z, Wang A, et al. The effect of matrix stiffness on the differentiation of mesenchymal stem cells in response to TGF-β. Biomaterials 2011;32:3921–30.

[60] González-García C, Moratal D, Oreffo ROC, Dalby MJ, Salmerón-Sánchez M. Surface mobility regulates skeletal stem cell differentiation. Integr Biol 2012;4:531–9.

[61] Hern DL, Hubbell J a. Incorporation of adhesion peptides into nonadhesive hydrogels useful for tissue resurfacing. J Biomed Mater Res 1998;39:266–76.

[62] Tokuda EY, Leight JL, Anseth KS. Modulation of matrix elasticity with PEG hydrogels to study melanoma drug responsiveness. Biomaterials 2014;35:4310–8.

[63] Sukarto A, Yu C, Flynn LE, Amsden BG. Co-delivery of adipose-derived stem cells and growth factor-loaded microspheres in RGD-grafted N-methacrylate glycol chitosan gels for focal chondral repair. Biomacromolecules 2012;13:2490–502.

[64] Tan P, Teoh S. Effect of stiffness of polycaprolactone (PCL) membrane on cell proliferation. Mater Sci Eng C 2007;27:304–8.

[65] Bat E, van Kooten TG, Feijen J, Grijpma DW. Macrophage-mediated erosion of gamma irradiated poly(trimethylene carbonate) films. Biomaterials 2009;30:3652–61.

[66] Seo JH, Sakai K, Yui N. Adsorption state of fibronectin on poly(dimethylsiloxane) surfaces with varied stiffness can dominate adhesion density of fibroblasts. Acta Biomater 2013;9:5493–501.

[67] Guiseppi-Elie A, Dong C, Dinu CZ. Crosslink density of a biomimetic poly(HEMA)-based hydrogel influences growth and proliferation of attachment dependent RMS 13 cells. J Mater Chem 2012;22:19529.

[68] Baneyx G, Baugh L, Vogel V. Fibronectin extension and unfolding within cell matrix fibrils controlled by cytoskeletal tension. Proc Natl Acad Sci U S A 2002;99:5139–43.

[69] Ricart BG, Yang MT, Hunter C a., Chen CS, Hammer DA. Measuring traction forces of motile dendritic cells on micropost arrays. Biophys J 2011;101:2620–8.

[70] Mitrossilis D, Fouchard J, Guiroy A, Desprat N, Rodriguez N, Fabry B, et al. Single-cell response to stiffness exhibits muscle-like behavior. Proc Natl Acad Sci U S A 2009;106:18243–8.

[71] Tang X, Yakut Ali M, Saif MTA. A novel technique for micro-patterning proteins and cells on polyacrylamide gels. Soft Matter 2012;8:7197.

[72] Sagvolden G, Giaever I, Pettersen EO, Feder J. Cell adhesion force microscopy. Proc Natl Acad Sci U S A 1999;96:471–6.

[73] Engler A, Bacakova L, Newman C, Hategan A, Griffin M, Discher D. Substrate compliance versus ligand density in cell on gel responses. Biophys J 2004;86:617–28.

[74] Jenney CR, Anderson JM. Adsorbed serum proteins responsible for surface dependent human macrophage behavior. J Biomed Mater Res 2000;49:435–47.

[75] Berglin M, Pinori E, Sellborn A, Andersson M, Hulander M, Elwing H. Fibrinogen adsorption and conformational change on model polymers: novel aspects of mutual molecular rearrangement. Langmuir 2009;25:5602–8.

[76] Wu B, Liu G, Zhang G, Craig VSJ. Stiff chains inhibit and flexible chains promote protein adsorption to polyelectrolyte multilayers. Soft Matter 2014.

[77] Yang JM, Lin HT. Wettability and protein adsorption on HTPB-based polyurethane films. J Memb Sci 2001;187:159–69.

[78] Yamasaki A, Imamura Y, Kurita K, Iwasaki Y, Nakabayashi N, Ishihara K. Surface mobility of polymers having phosphorylcholine groups connected with various bridging units and their protein adsorption-resistance properties. Colloids Surfaces B Biointerfaces 2003;28:53–62.

[79] Ilagan BG, Amsden BG. Surface modifications of photocrosslinked biodegradable elastomers and their influence on smooth muscle cell adhesion and proliferation. Acta Biomater 2009;5:2429–40.

[80] Vyner MC, Liu L, Sheardown HD, Amsden BG. The effect of elastomer chain flexibility on protein adsorption. Biomaterials 2013;34:9287–94.

[81] Storck M, Orend K-H, Schmitz-Rixen T. Absorbable suture in vascular surgery. Vasc Endovascular Surg 1993;27:413–24.

[82] Zhang Z, Kuijer R, Bulstra SK, Grijpma DW, Feijen J. The in vivo and in vitro degradation behavior of poly(trimethylene carbonate). Biomaterials 2006;27:1741–8.

[83] Pêgo AP, Van Luyn MJA, Brouwer LA, van Wachem PB, Poot AA, Grijpma DW, et al. In vivo behavior of poly(1,3-trimethylene carbonate) and copolymers of 1,3-trimethylene carbonate with D,L-lactide or epsilon-caprolactone: Degradation and tissue response. J Biomed Mater Res A 2003;67:1044–54.

[84] Vyner MC, Li A, Amsden BG. The effect of poly(trimethylene carbonate) molecular weight on macrophage behavior and enzyme adsorption and conformation. Biomaterials 2014;35:9041–8.

[85] Dalton SL, Scharf E, Briesewitz R, Marcantonio EE, Assoian RK. Cell adhesion to extracellular matrix regulates the life cycle of integrins. Mol Biol Cell 1995;6:1781–91.

[86] Gallant ND, Michael KE, García AJ. Cell adhesion strengthening: contributions of adhesive area, integrin binding, and focal adhesion assembly. Mol Biol Cell 2005;16:4329–40.

[87] Plows LD, Cook RT, Davies AJ, Walker AJ. Integrin engagement modulates the phosphorylation of focal adhesion kinase, phagocytosis, and cell spreading in molluscan defence cells. Biochim Biophys Acta - Mol Cell Res 2006;1763:779–86.

[88] Horbett TA, Schway MB. Correlations between mouse 3T3 cell spreading and serum fibronectin adsorption on glass and hydroxyethylmethacrylate-ethylmethacrylate copolymers. J Biomed Mater Res 1988;22:763–93.

[89] Massia SP, Stark J. Immobilized RGD peptides on surface-grafted dextran promote biospecific cell attachment. J Biomed Mater Res 2001;56:390–9.

[90] Webb K, Hlady V, Tresco PA. Relative importance of surface wettability and charged functional groups on NIH 3T3 fibroblast attachment, spreading, and cytoskeletal organization. J Biomed Mater Res 1998;41:422–30.

[91] Georges PC, Janmey PA. Cell type-specific response to growth on soft materials. J Appl Physiol 2005;98:1547–53.

[92] Ghosh K, Pan Z, Guan E, Ge S, Liu Y, Nakamura T, et al. Cell adaptation to a physiologically relevant ECM mimic with different viscoelastic properties. Biomaterials 2007;28:671–9.

[93] Wang HB, Dembo M, Wang YL. Substrate flexibility regulates growth and apoptosis of normal but not transformed cells. Am J Physiol Cell Physiol 2000;279:C1345–50.

[94] Gray DS, Tien J, Chen CS. Repositioning of cells by mechanotaxis on surfaces with micropatterned Young's modulus. J Biomed Mater Res A 2003;66:605–14.

[95] Lu X, Howard MD, Mazik M, Eldridge J, Rinehart JJ, Jay M, et al. Nanoparticles containing anti-inflammatory agents as chemotherapy adjuvants: optimization and in vitro characterization. AAPS J 2008;10:133–40.

[96] Pamula E, Dobrzynski P, Szot B, Kretek M, Krawciow J, Plytycz B, et al. Cytocompatibility of aliphatic polyesters - In vitro study on fibroblasts and macrophages. J Biomed Mater Res - Part A 2008;87:524–35.

[97] Scislowska-Czarnecka A, Pamula E, Tlalka A, Kolaczkowska E. Effects of Aliphatic Polyesters on Activation of the Immune System: Studies on Macrophages. J Biomater Sci Polym Ed 2012;23:715–38.

[98] Lee SH, Gupta MK, Bang JB, Bae H, Sung H-J. Current Progress in Reactive Oxygen Species (ROS)-Responsive Materials for Biomedical Applications. Adv Healthc Mater 2013;2:908–15.

[99] Lyle DB, Shallcross JC, Durfor CN, Hitchins VM, Breger JC, Langone JJ. Screening biomaterials for stimulation of nitric oxide-mediated inflammation. J Biomed Mater Res - Part A 2009;90:82–93.

[100] Sridharan R, Cameron AR, Kelly DJ, Kearney CJ, O'Brien FJ. Biomaterial based modulation of macrophage polarization: a review and suggested design principles. Mater Today 2015;18:313–25.

[101] Patel NR, Bole M, Chen C, Hardin CC, Kho AT, Mih J, et al. Cell Elasticity Determines Macrophage Function. PLoS One 2012;7:1–10.

[102] Banquy X, Suarez F, Argaw A, Rabanel J-M, Grutter P, Bouchard J-F, et al. Effect of mechanical properties of hydrogel nanoparticles on macrophage cell uptake. Soft Matter 2009;5:3984.

[103] Chapanian R, Tse MY, Pang SC, Amsden BG. The role of oxidation and enzymatic hydrolysis on the in vivo degradation of trimethylene carbonate based photocrosslinkable elastomers. Biomaterials 2009;30:295–306.

[104] Wang H, Wong C, Chin A, Kennedy J, Zhang Q, Hanash S. Quantitative Serum Proteomics Using Dual Stable Isotope coding and nano LC-MS / MSMS. J Proteome Res 2009:5412–22.

[105] Amsden B. Curable, biodegradable elastomers: emerging biomaterials for drug delivery and tissue engineering. Soft Matter 2007;3:1335.

[106] Chen H, Yuan L, Song W, Wu Z, Li D. Biocompatible polymer materials: Role of protein–surface interactions. Prog Polym Sci 2008;33:1059–87.

[107] Bajpai AK. Fibrinogen adsorption onto macroporous polymeric surfaces: correlation with biocompatibility aspects. J Mater Sci Mater Med 2008;19:343–57.

[108] Smith ML, Gourdon D, Little WC, Kubow KE, Eguiluz RA, Luna-Morris S, et al. Force-induced unfolding of fibronectin in the extracellular matrix of living cells. PLoS Biol 2007;5:e268.

[109] Parhi P, Golas A, Vogler EA. Role of proteins and water in the initial attachment of mammalian cells to biomedical surfaces: a review. J Adhes Sci Technol 2010;24:853–88.

[110] Amsden BG, Misra G, Gu F, Younes HM. Synthesis and characterization of a photo-cross-linked biodegradable elastomer. Biomacromolecules 2004;5:2479–86.

[111] Robertson C, Bogoslovov R, Roland C. Effect of structural arrest on Poisson's ratio in nanoreinforced elastomers. Phys Rev E 2007;75:051403.

[112] Weeks A, Boone A, Luensmann D, Jones L, Sheardown H. The effects of hyaluronic acid incorporated as a wetting agent on lysozyme denaturation in model contact lens materials. J Biomater Appl 2012;0:1–11.

[113] Sheardown H, Cornelius R, Brash J. Measurement of protein adsorption to metals using radioiodination methods: a caveat. Colloids Surfaces, B Biointerfaces 1997;10:29–33.

[114] Delgado-Rodríguez M, Medina-Cuadros M, Gómez-Ortega A, Martínez-Gallego G, Mariscal-Ortiz M, Martinez-Gonzalez MA, et al. Cholesterol and serum albumin levels as predictors of cross infection, death, and length of hospital stay. Arch Surg 2002;137:805–12.

[115] Kimber I, Stonard MD, Gidlow DA, Niewola Z. Influence of chronic low-level exposure to lead on plasma immunoglobulin concentration and cellular immune function in man. Int Arch Occup Environ Health 1986;57:117–25.

[116] Stathakis NE, Fountas A, Tsianos E. Plasma fibronectin in normal subjects and in various disease states. Br Med J 1981;34:504.

[117] Morioka S, Makino H, Shikata K, Ota Z. Changes in plasma concentrations of vitronectin in patients with diabetic nephropathy. Acta Med Okayama 1994;48:137–42.

[118] Voinova M V, Rodahl M, Jonson M, Kasemo B. Viscoelastic acoustic response of layered polymer films at fluid-solid interfaces: continuum mechanics approach. Phys Scr 1999;59:391–6.

[119] Fischer H, Polikarpov I, Craievich AF. Average protein density is a molecular-weight-dependent function. Protein Sci 2004;13:2825–8.

[120] Holly FJ, Refojo MF. Wettability of hydrogels. I. Poly (2-hydroxyethyl methacrylate). J Biomed Mater Res 1975;9:315–26.

[121] Armstrong JK, Wenby RB, Meiselman HJ, Fisher TC. The hydrodynamic radii of macromolecules and their effect on red blood cell aggregation. Biophys J 2004;87:4259–70.

[122] Vermeer AW, Norde W. The thermal stability of immunoglobulin: unfolding and aggregation of a multi-domain protein. Biophys J 2000;78:394–404.

[123] Tooney NM, Mosesson MW, Amrani DL, Hainfeld JF, Wall JS. Solution and surface effects on plasma fibronectin structure. J Cell Biol 1983;97:1686–92.

[124] Lynn GW, Heller WT, Mayasundari A, Minor KH, Peterson CB. A model for the three-dimensional structure of human plasma vitronectin from small-angle scattering measurements. Biochemistry 2005;44:565–74.

[125] García AJ, Vega MD, Boettiger D. Modulation of cell proliferation and differentiation through substrate-dependent changes in fibronectin conformation. Mol Biol Cell 1999;10:785–98.

[126] Holmberg M, Hou X. Competitive protein adsorption of albumin and immunoglobulin G from human serum onto polymer surfaces. Langmuir 2010;26:938–42.

[127] Reimhult E, Larsson C, Kasemo B, Höök F. Simultaneous surface plasmon resonance and quartz crystal microbalance with dissipation monitoring measurements of biomolecular adsorption events involving structural transformations and variations in coupled water. Anal Chem 2004;76:7211–20.

[128] Malmström J, Agheli H, Kingshott P, Sutherland DS. Viscoelastic modeling of highly hydrated laminin layers at homogeneous and nanostructured surfaces: quantification of protein layer properties using QCM-D and SPR. Langmuir 2007;23:9760–8.

[129] Roach P, Farrar D, Perry CC. Interpretation of protein adsorption: surface-induced conformational changes. J Am Chem Soc 2005;127:8168–73.

[130] Jordan JL, Fernandez EJ. QCM-D sensitivity to protein adsorption reversibility. Biotechnol Bioeng 2008;101:837–42.

[131] Wang K, Cai L, Hao F, Xu X, Cui M, Wang S. Distinct cell responses to substrates consisting of poly(ε-caprolactone) and poly(propylene fumarate) in the presence or absence of cross-links. Biomacromolecules 2010;11:2748–59.

[132] Zheng X, Baker H, Hancock WS, Fawaz F, McCaman M, Pungor E. Proteomic analysis for the assessment of different lots of fetal bovine serum as a raw material for cell culture. Part IV. Application of proteomics to the manufacture of biological drugs. Biotechnol Prog 2006;22:1294–300.

[133] Magnani A, Barbucci R, Lamponi S, Chiumento A, Paffetti A, Trabalzini L, et al. Two-step elution of human serum proteins from different glass-modified bioactive surfaces: A comparative proteomic analysis of adsorption patterns. Electrophoresis 2004;25:2413–24.

[134] Yu K, Lai BFL, Foley JH, Krisinger MJ, Conway EM, Kizhakkedathu JN. Modulation of Complement Activation and Amplification on Nanoparticle Surfaces by Glycopolymer Conformation and Chemistry. ACS Nano 2014:7687–703.

[135] Boersema PJ, Raijmakers R, Lemeer S, Mohammed S, Heck AJR. Multiplex peptide stable isotope dimethyl labeling for quantitative proteomics. Nat Protoc 2009;4:484–94.

[136] Brown WM, Saunders NR, Møllgård K, Dziegielewska KM. Fetuin--an old friend revisited. Bioessays 1992.

[137] Boersema PJ, Aye TT, Van Veen TAB, Heck AJR, Mohammed S. Triplex protein quantification based on stable isotope labeling by peptide dimethylation applied to cell and tissue lysates. Proteomics 2008;8:4624–32.

[138] Sakwe AM, Koumangoye R, Goodwin SJ, Ochieng J. Fetuin-A (alpha-2-HS-glycoprotein) is a major serum adhesive protein that mediates growth signaling in breast tumor cells. J Biol Chem 2010;285:41827–35.

[139] Kundranda MN, Ray S, Saria M, Friedman D, Matrisian LM, Lukyanov P, et al. Annexins expressed on the cell surface serve as receptors for adhesion to immobilized fetuin-A. Biochim Biophys Acta 2004;1693:111–23.

[140] Chen NX, O'Neill KD, Chen X, Duan D, Wang E, Sturek MS, et al. Fetuin-A uptake in bovine vascular smooth muscle cells is calcium dependent and mediated by annexins. Am J Physiol Renal Physiol 2007;292:F599–606.

[141] Hynes RO. Integrins: versatility, modulation, and signaling in cell adhesion. Cell 1992;69:11–25.

[142] Linscott WD, Triglia RP. The bovine complement system. Adv Exp Med Biol 1981;137:413–30.

[143] Williams MR, Maxwell DA, Spooner RL. Quantitative studies on bovine immunoglobulins, normal plasma levels of IgG2, IgG1, IgM and IgA. Res Vet Sci 1975;18:314–21.

[144] Henning A-K, Groschup MH, Mettenleiter TC, Karger A. Analysis of the bovine plasma proteome by matrix-assisted laser desorption/ionisation time-of-flight tandem mass spectrometry. Vet J 2014;199:175–80.

[145] Malan-Shibley L, Iype PT. A serum-free medium for clonal growth and serial subculture of diploid rat liver epithelial cells. In Vitro 1983;19:749–58.

[146] Wang S, Haslam S. Serum-free primary culture of normal mouse mammary epithelial and stromal cells. Vitr Cell Dev Biol 1994:859–66.

[147] Rizzino A, Sato G. Growth of embryonal carcinoma cells in serum-free medium. Proc Natl Acad Sci U S A 1978;75:1844–8.

[148] Kwon MS, Park CS, Choi K, Ahnn J, Kim JI, Eom SH, et al. Calreticulin couples calcium release and calcium influx in integrin-mediated calcium signaling. Mol Biol Cell 2000;11:1433–43.

[149] Maher P. Copper and calcium binding motifs in the extracellular domains of fibroblast growth factor receptors. J Biol Chem 1996;271:3343–6.

[150] Boynton A, Whitfield J, Isaacs R, Morton H. Control of 3T3 cell proliferation by calcium. In Vitro 1974;10:12–7.

[151] Hou Q, Grijpma DW, Feijen J. Porous polymeric structures for tissue engineering prepared by a coagulation, compression moulding and salt leaching technique. Biomaterials 2003;24:1937–47.

[152] Song Y, Wennink JWH, Kamphuis MMJ, Sterk LMT, Vermes I, Poot AA, et al. Dynamic culturing of smooth muscle cells in tubular poly(trimethylene carbonate) scaffolds for vascular tissue engineering. Tissue Eng Part A 2011;17:381–7.

[153] Nair LS, Laurencin CT. Biodegradable polymers as biomaterials. Prog Polym Sci 2007;32:762–98.

[154] Franco L, Bedorin S, Puiggalí J. Comparative thermal degradation studies on glycolide/trimethylene carbonate and lactide/trimethylene carbonate copolymers. J Appl Polym Sci 2007;104:3539–53.

[155] Jansen J, Koopmans SA, Los LI, van der Worp RJ, Podt JG, Hooymans JMM, et al. Intraocular degradation behavior of crosslinked and linear poly(trimethylene carbonate) and poly(D,L-lactic acid). Biomaterials 2011;32:4994–5002.

[156] Kluin OS, van der Mei HC, Busscher HJ, Neut D. A surface-eroding antibiotic delivery system based on poly-(trimethylene carbonate). Biomaterials 2009;30:4738–42.

[157] Kaihara S, Fisher JP, Matsumura S. Chemo-enzymatic synthesis of degradable PTMC-b-PECA-b-PTMC triblock copolymers and their micelle formation for pH-dependent controlled release. Macromol Biosci 2009;9:613–21.

[158] Albertsson A, Eklund M. Influence of molecular structure on the degradation mechanism of degradable polymers: in vitro degradation of poly(trimethylene carbonate), poly(trimethylene carbonate-co-caprolactone), and poly(adipic anhydride). J Appl Polym Sci 1995;57:87–103.

[159] Anderson JM. Biological responses to materials. Annu Rev Mater Res 2001;31:81–110.

[160] Acemoglu M, Nimmerfall F, Bantle S, Stoll GH. Poly(ethylene carbonate)s, part I: syntheses and structural effects on biodegradation. J Control Release 1997;49:263–76.

[161] Bat E, van Kooten TG, Feijen J, Grijpma DW. Resorbable elastomeric networks prepared by photocrosslinking of high-molecular-weight poly(trimethylene carbonate) with photoinitiators and poly(trimethylene carbonate) macromers as crosslinking aids. Acta Biomater 2011;7:1939–48.

[162] Zhang Z, Zou S, Vancso GJ, Grijpma DW, Feijen J. Enzymatic surface erosion of poly(trimethylene carbonate) films studied by atomic force microscopy. Biomacromolecules 2005;6:3404–9.

[163] Stoll GH, Nimmerfall F, Acemoglu M, Bodmer D, Bantle S, Müller I, et al. Poly(ethylene carbonate)s, part II: degradation mechanisms and parenteral delivery of bioactive agents. J Control Release 2001;76:209–25.

[164] Dadsetan M, Christenson EM, Unger F, Ausborn M, Kissel T, Hiltner A, et al. In vivo biocompatibility and biodegradation of poly(ethylene carbonate). J Control Release 2003;93:259–70.

[165] Nathan C. Secretory products of macrophages. J Clin Invest 1987;79:319–26.

[166] Chapanian R, Amsden BG. Osmotically driven protein release from photo-cross-linked elastomers of poly(trimethylene carbonate) and poly(trimethylene carbonate-co-d,l-lactide). Eur J Pharm Biopharm 2010;74:172–83.

[167] Labow RS, Meek E, Santerre JP. Differential synthesis of cholesterol esterase by monocyte-derived macrophages cultured on poly(ether or ester)-based poly(urethane)s. J Biomed Mater Res 1998;39:469–77.

[168] Li F, Hui DY. Modified low density lipoprotein enhances the secretion of bile salt-stimulated cholesterol esterase by human monocyte-macrophages. J Biol Chem 1997;272:28666–71.

[169] Chait A, Iverius PH, Brunzell JD. Lipoprotein lipase secretion by human monocyte-derived macrophages. J Clin Invest 1982;69:490–3.

[170] Tang YW, Labow RS, Santerre JP. Enzyme-induced biodegradation of polycarbonate-polyurethanes: dependence on hard-segment chemistry. J Biomed Mater Res 2001;57:597–611.

[171] Sammon C, Mura C, Yarwood J, Everall N, Swart R, Hodge D. FTIR−ATR studies of the structure and dynamics of water molecules in polymeric matrixes. A comparison of PET and PVC. J Phys Chem B 1998;102:3402–11.

[172] Hayes W, Keer L, Herrmann G, Mockros L. A mathematical analysis for indentation tests of articular cartilage. J Biomech 1972;5:541–51.

[173] Carrillo F, Gupta S, Balooch M, Marshall SJ, Marshall GW, Pruitt L, et al. Nanoindentation of polydimethylsiloxane elastomers: effect of crosslinking, work of adhesion, and fluid environment on elastic modulus. J Mater Res 2011;20:2820–30.

[174] Ping Z., Nguyen Q., Chen S., Zhou J., Ding Y. States of water in different hydrophilic polymers — DSC and FTIR studies. Polymer (Guildf) 2001;42:8461–7.

[175] Guy O, Lombardo D, Brahms JG. Structure and conformation of human pancreatic carboxyl-ester hydrolase. Eur J Biochem 1981;117:457–60.

[176] Teichroeb JH, Forrest JA, Jones LW, Chan J, Dalton K. Quartz crystal microbalance study of protein adsorption kinetics on poly(2-hydroxyethyl methacrylate). J Colloid Interface Sci 2008;325:157–64.

[177] Alf ME, Hatton TA, Gleason KK. Insights into thin, thermally responsive polymer layers through quartz crystal microbalance with dissipation. Langmuir 2011;27:10691–8.

[178] Giamblanco N, Yaseen M, Zhavnerko G, Lu JR, Marletta G. Fibronectin conformation switch induced by coadsorption with human serum albumin. Langmuir 2011;27:312–9.

[179] Höök F, Kasemo B, Nylander T, Fant C, Sott K, Elwing H. Variations in coupled water, viscoelastic properties, and film thickness of a Mefp-1 protein film during adsorption and cross-linking: a quartz crystal microbalance with dissipation monitoring, ellipsometry, and surface plasmon resonance study. Anal Chem 2001;73:5796–804.

[180] Fischer B. Isolation and characterization of the extracellular lipase of acinetobacter calcoaceticus 69 V. J Basic Microbiol 1987;27:427–32.

[181] Mueller R-J. Biological degradation of synthetic polyesters—enzymes as potential catalysts for polyester recycling. Process Biochem 2006;41:2124–8.

[182] Zhu KJ, Hendren RW, Jensen K, Pitt CG. Synthesis, properties, and biodegradation of poly(1,3-trimethylene carbonate). Macromolecules 1991;24:1736–40.

[183] Krsko P, Kaplan JB, Libera M. Spatially controlled bacterial adhesion using surface-patterned poly(ethylene glycol) hydrogels. Acta Biomater 2009;5:589–96.

[184] Ravi S, Qu Z, Chaikof EL. Polymeric Materials for Tissue Engineering of Arterial Substitutes. Vascular 2009;17:S45–54.

[185] Jia Y, Shen X, Gu X, Dong J, Mu C, Zhang Y. Synthesis and characterization of tercopolymers derived from e-caprolactone, trimethylene carbonate, and lactide. Polym Adv Technol 2008:159–66.

[186] Chapanian R, Tse MY, Pang SC, Amsden BG. Long term in vivo degradation and tissue response to photo-cross-linked elastomers prepared from star-shaped prepolymers of poly(ε-caprolactone-co- D,L-lactide). J Biomed Mater Res - Part A 2010;92:830–42.

[187] Sung H-J, Meredith C, Johnson C, Galis ZS. The effect of scaffold degradation rate on three-dimensional cell growth and angiogenesis. Biomaterials 2004;25:5735–42.

[188] Kao WJ. Evaluation of protein-modulated macrophage behavior on biomaterials: designing biomimetic materials for cellular engineering. Biomaterials 1999;20:2213–21.

[189] Battiston KG, Ouyang B, Honarparvar E, Qian J, Labow RS, Simmons C a., et al. Interaction of a block-co-polymeric biomaterial with immunoglobulin G modulates human monocytes towards a non-inflammatory phenotype. Acta Biomater 2015;24:35–43.

[190] Shen M, Garcia I, Maier R V, Horbett TA. Effects of adsorbed proteins and surface chemistry on foreign body giant cell formation, tumor necrosis factor alpha release and procoagulant activity of monocytes. J Biomed Mater Res A 2004;70:533–41.

[191] Sudhakaran PR, Radhika A, Jacob SS. Monocyte macrophage differentiation in vitro: Fibronectin-dependent upregulation of certain macrophage-specific activities. Glycoconj J 2007;24:49–55.

[192] McNally AK, Jones JA, MacEwan SR, Colton E, Anderson JM. Vitronectin is a critical protein adhesion substrate for IL- 4- induced foreign body giant cell formation. J Biomed Mater Res Part A 2008;86A:535–43.

[193] Jones JA, Dadsetan M, Collier TO, Ebert M, Stokes KS, Ward RS, et al. Macrophage behavior on surface-modified polyurethanes. J Biomater Sci Polym Ed 2004;15:567–84.

[194] Jones JA, Chang DT, Meyerson H, Colton E, Kwon IK, Matsuda T, et al. Proteomic analysis and quantification of cytokines and chemokines from biomaterial surface-adherent macrophages and foreign body giant cells. J Biomed Mater Res Part A 2007;83A:585–96.

[195] McBane JE, Ebadi D, Sharifpoor S, Labow RS, Santerre JP. Differentiation of monocytes on a degradable, polar, hydrophobic, ionic polyurethane: Two-dimensional films vs. three-dimensional scaffolds. Acta Biomater 2011;7:115–22.

[196] Amsden BG, Tse MY, Turner ND, Knight DK, Pang SC. In vivo degradation behavior of photo-cross-linked star-poly(epsilon-caprolactone-co-D,L-lactide) elastomers. Biomacromolecules 2006;7:365–72.

[197] Radmacher M, Fritz M, Cleveland JP, Walters DA, Hansma PK. Imaging adhesion forces and elasticity of lysozyme adsorbed on mica with the atomic force microscope. Langmuir 1994;10:3809–14.

[198] Lee KH, Chu CC. The role of superoxide ions in the degradation of synthetic absorbable sutures. J Biomed Mater Res 2000;49:25–35.

[199] Mantovani A, Sica A, Sozzani S, Allavena P, Vecchi A, Locati M. The chemokine system in diverse forms of macrophage activation and polarization. Trends Immunol 2004;25:677–86.

[200] Battiston KG, Labow RS, Santerre JP. Protein binding mediation of biomaterial-dependent monocyte activation on a degradable polar hydrophobic ionic polyurethane. Biomaterials 2012;33:8316–28.

[201] Fadok VA, Savill JS, Haslett C, Bratton DL, Doherty DE, Campbell PA, et al. Different populations of macrophages use either the vitronectin receptor or the phosphatidylserine receptor to recognize and remove apoptotic cells. J Immunol 1992;149:4029–35.

[202] Parker CJ, Frame RN, Elstad MR. Vitronectin (S protein) augments the functional activity of monocyte receptors for IgG and complement C3b. Blood 1988;71:86–93.

[203] Blystone SD, Graham IL, Lindberg FP, Brown EJ. Integrin alpha v beta 3 differentially regulates adhesive and phagocytic functions of the fibronectin receptor alpha 5 beta 1. J Cell Biol 1994;127:1129–37.

[204] Sakagami H, Kishino K, Amano O, Kanda Y, Kunii S, Yokote Y, et al. Cell death induced by nutritional starvation in mouse macrophage-like RAW264.7 cells. Anticancer Res 2009;29:343–7.

[205] Moeslinger T, Friedl R, Volf I, Brunner M, Baran H, Koller E, et al. Urea induces macrophage proliferation by inhibition of inducible nitric oxide synthesis. Kidney Int 1999;56:581–8.

[206] Chin BY, Petrache I, Choi a M, Choi ME. Transforming growth factor beta1 rescues serum deprivation-induced apoptosis via the mitogen-activated protein kinase (MAPK) pathway in macrophages. J Biol Chem 1999;274:11362–8.

[207] He Z, Zhang H, Yang C, Zhou Y, Zhou Y, Han G, et al. The interaction between different types of activated RAW 264.7 cells and macrophage inflammatory protein-1 alpha. Radiat Oncol 2011;6:86.

[208] Goettsch C, Kliemt S, Sinningen K, von Bergen M, Hofbauer LC, Kalkhof S. Quantitative proteomics reveals novel functions of osteoclast-associated receptor in STAT signaling and cell adhesion in human endothelial cells. J Mol Cell Cardiol 2012;53:829–37.

[209] Tarasova NK, Ytterberg AJ, Lundberg K, Zhang X-M, Harris RA, Zubarev RA. Proteomics Reveals a Role for Attachment in Monocyte Differentiation into Efficient Proinflammatory Macrophages. J Proteome Res 2015;14:3940–7.

[210] Dinnes DLM, Marçal H, Raftery MJ, Labow RS, Mahler SM. The macrophage–biomaterial interface: a proteomic analysis of the conditioned medium environment. J Chem Technol Biotechnol 2008;83:482–95.

[211] Schiller HB, Friedel CC, Boulegue C, Fässler R. Quantitative proteomics of the integrin adhesome show a myosin II-dependent recruitment of LIM domain proteins. EMBO Rep 2011;12:259–66.

[212] Battiston KG, McBane JE, Labow RS, Santerre JP. Differences in protein binding and cytokine release from monocytes on commercially sourced tissue culture polystyrene. Acta Biomater 2012;8:89–98.

[213] Berghaus LJ, Moore JN. Innate immune responses of primary murine macrophage-lineage cells and RAW 264.7 cells to ligands of Toll-like receptors 2, 3, and 4. … Infect Dis 2010;8335:1–13.

[214] Denlinger LC, Fisette PL, Garis K a, Kwon G, Vazquez-Torres a, Simon a D, et al. Regulation of inducible nitric oxide synthase expression by macrophage purinoreceptors and calcium. J Biol Chem 1996;271:337–42.

[215] Chan ED, Riches DW. IFN-gamma + LPS induction of iNOS is modulated by ERK, JNK/SAPK, and p38(mapk) in a mouse macrophage cell line. Am J Physiol Cell Physiol 2001;280:C441–50.

[216] Hwang JS, Choi HS, Ham SA, Yoo T, Lee WJ, Paek KS, et al. Deacetylation-mediated interaction of SIRT1-HMGB1 improves survival in a mouse model of endotoxemia. Sci Rep 2015;5:15971.

[217] Huang H, Park P-H, McMullen MR, Nagy LE. Mechanisms for the anti-inflammatory effects of adiponectin in macrophages. J Gastroenterol Hepatol 2008;23 Suppl 1:S50–3.

[218] Fogh-Andersen N, Altura BM, Altura BT, Siggaard-Andersen O. Composition of interstitial fluid. Clin Chem 1995;41:1522–5.

Appendix

Supplemental Data and Figures

A.1 Representative NMR Spectra:

A.1.1 Acrylated *star* poly(D,L lactide-*co*-ϵ-caprolactone) (ASCP)

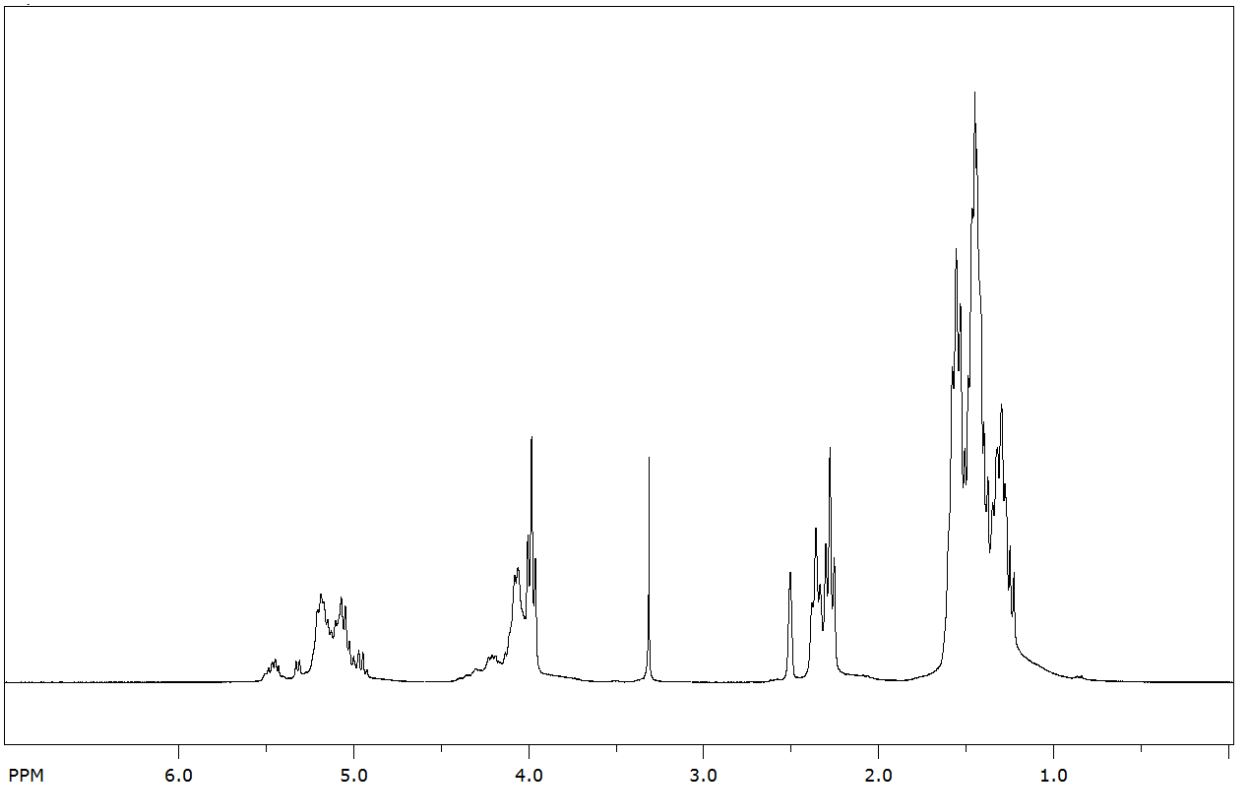

Figure A.1: Representative NMR spectrum of star poly(D,L lactide-co-ϵ-caprolactone) (SCP) in dDMSO

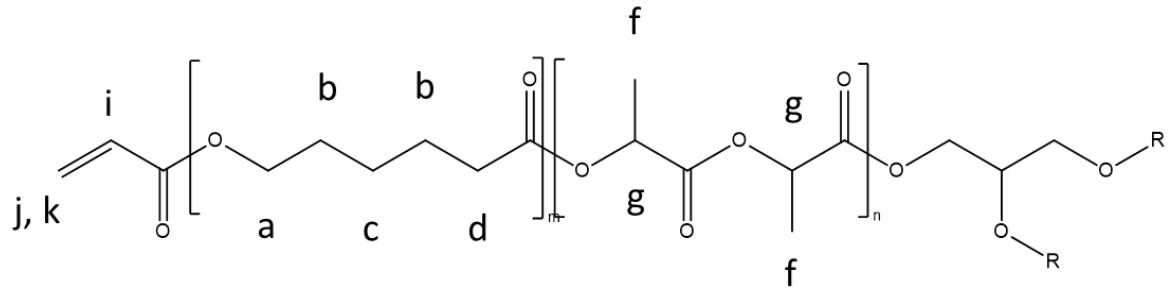

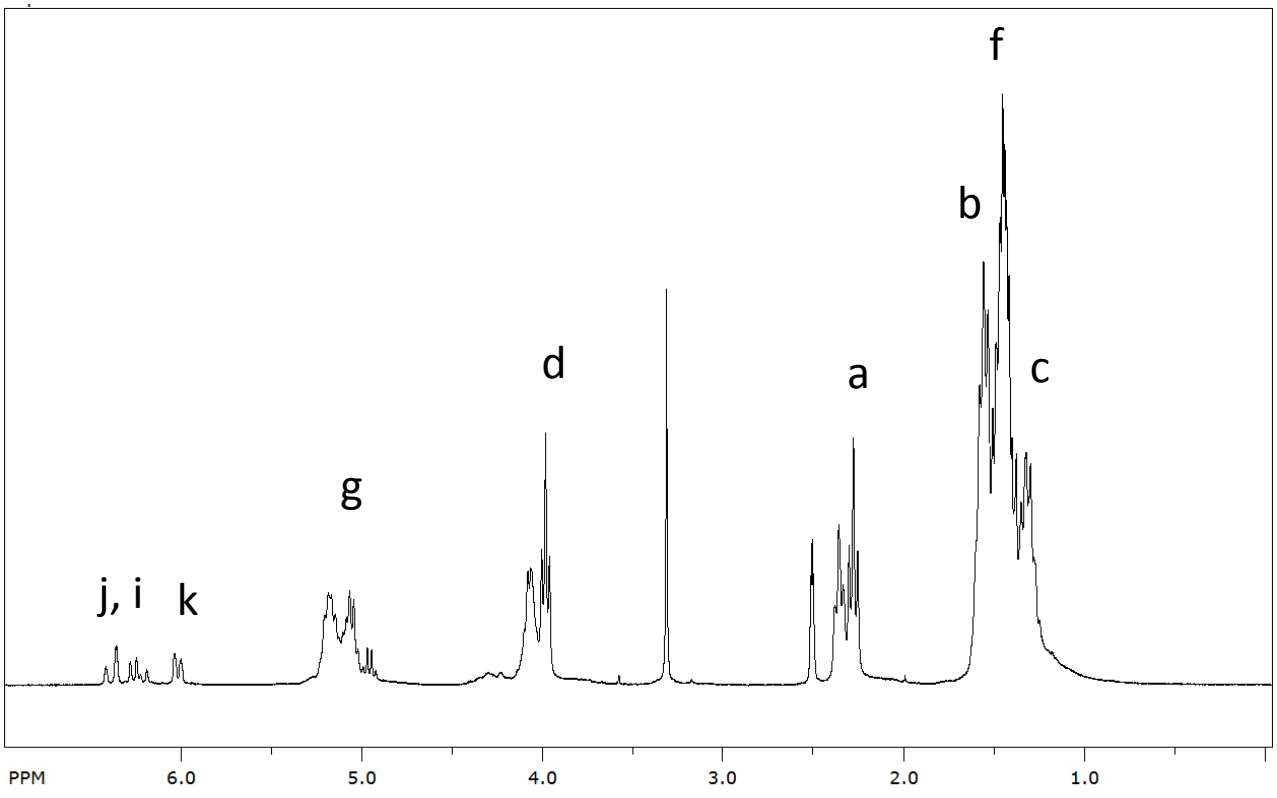

Figure A.2: Representative NMR spectrum of acrylated *star* poly(D,L lactide-*co*-ϵ-caprolactone) (ASCP) in dDMSO with peak assignments

A.1.2 Poly(trimethylene carbonate)

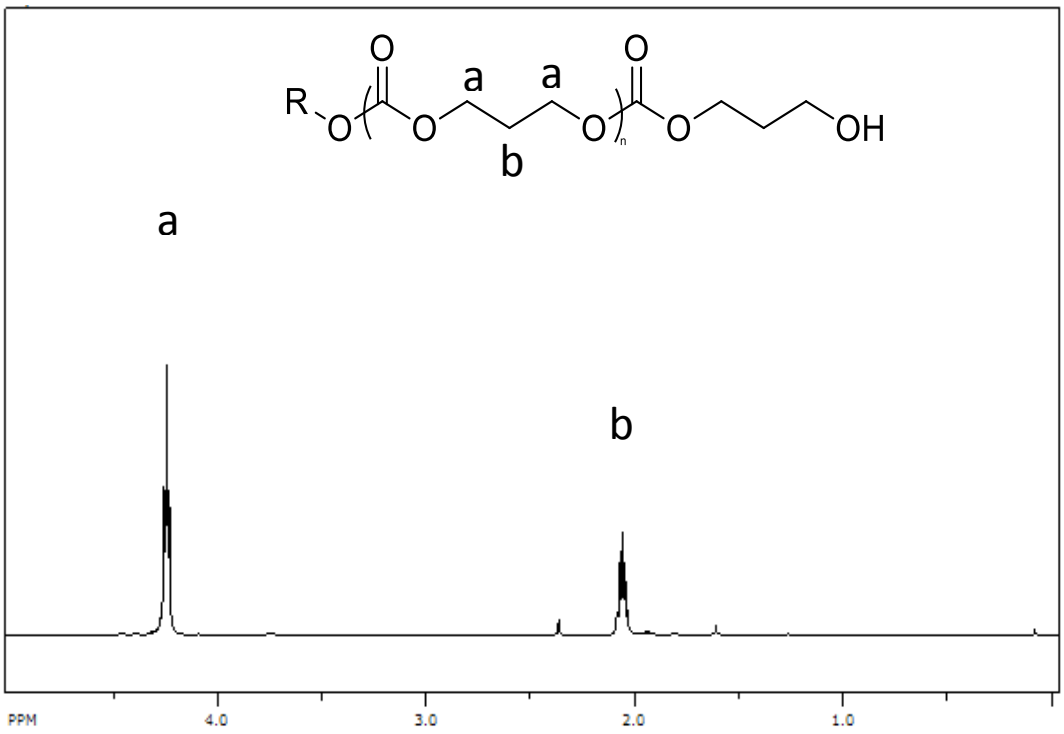

Figure A.3: Representative NMR spectrum of poly(trimethylene carbonate) in $CDCl_3$

A.2 Atomic Force Microscopy Nano-indentation

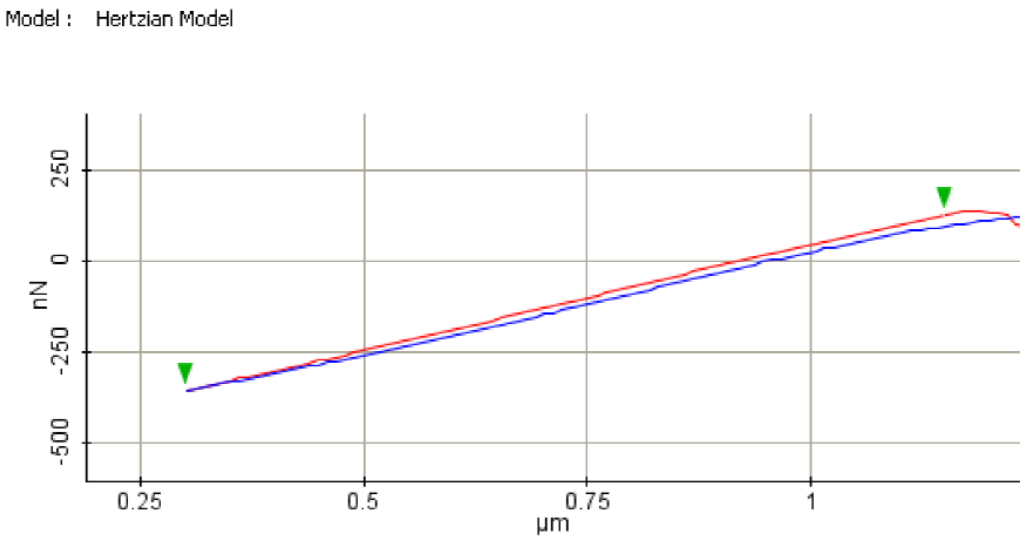

Figure A.4: Representative force-displacement curve for nanoindentation of PTMC

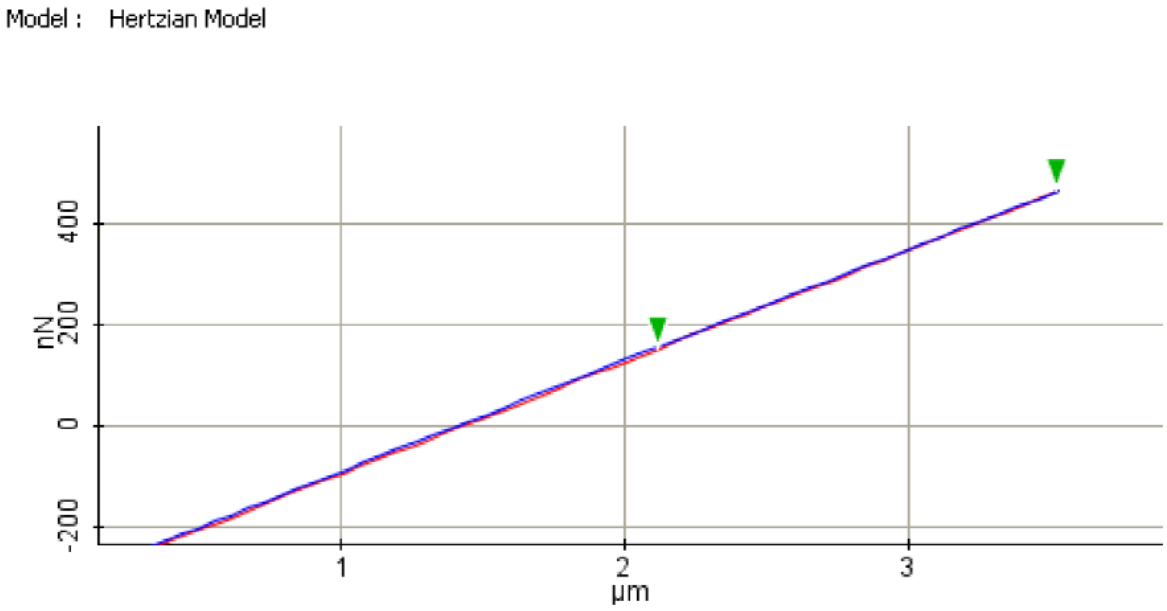

Figure A.5: Representative force-displacement curve for nanoindentation of ELAS

Table A.1: Bulk and surface moduli of dry and hydrated ELAS and PTMC

	Bulk Modulus (MPa)	Surface Modulus (MPa)
ELAS 2000 (dry)	**7.6 ± 0.3**	**7.6 ± 0.4**
ELAS 2000 (hydrated)	**7.8 ± 0.5**	**6.3 ± 0.2**
ELAS 5000 (dry)	**1.00 ± 0.04**	**1.22 ± 0.09**
ELAS 5000 (hydrated)	**1.22 ± 0.09**	**0.81 ± 0.02**
60 PTMC (dry)	**1.1 ± 0.4**	**1.17 ± 0.04**
60 PTMC (hydrated)	**1.1 ± 0.2**	**0.82 ± 0.02**
100 PTMC (dry)	**1.3 ± 0.2**	**1.4 ± 0.1**
100 PTMC (hydrated)	**1.34 ± 0.05**	**1.09 ± 0.06**

A.3 SEM Micrographs of microspheres fabricated from ELAS 2000, ELAS 5000, and 100PTMC

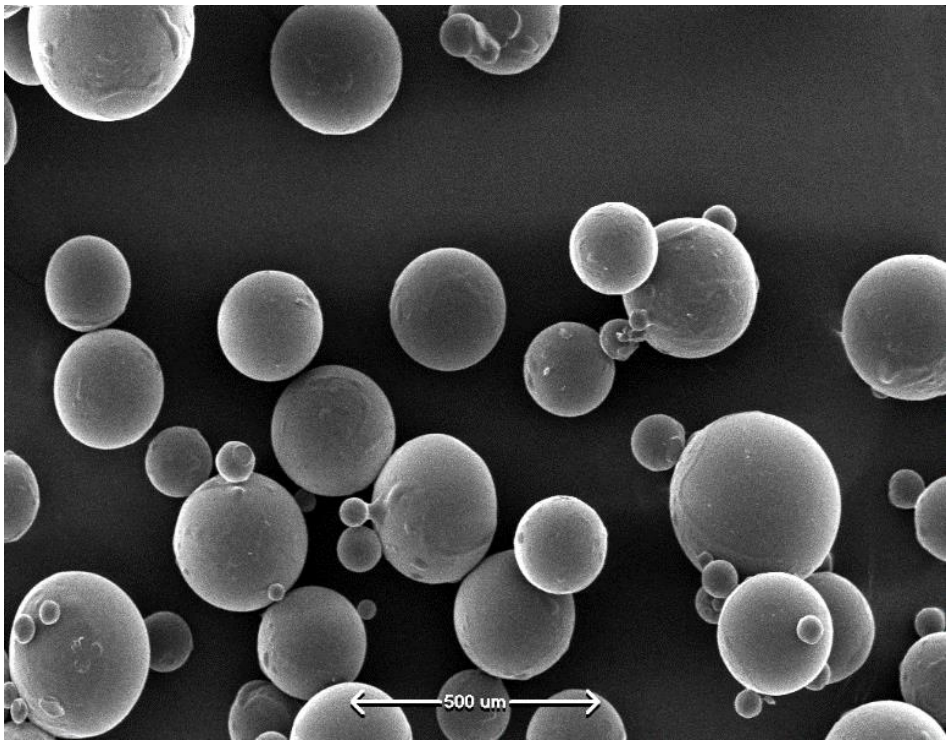

Figure A.6: SEM micrographs of ELAS 2000 microspheres

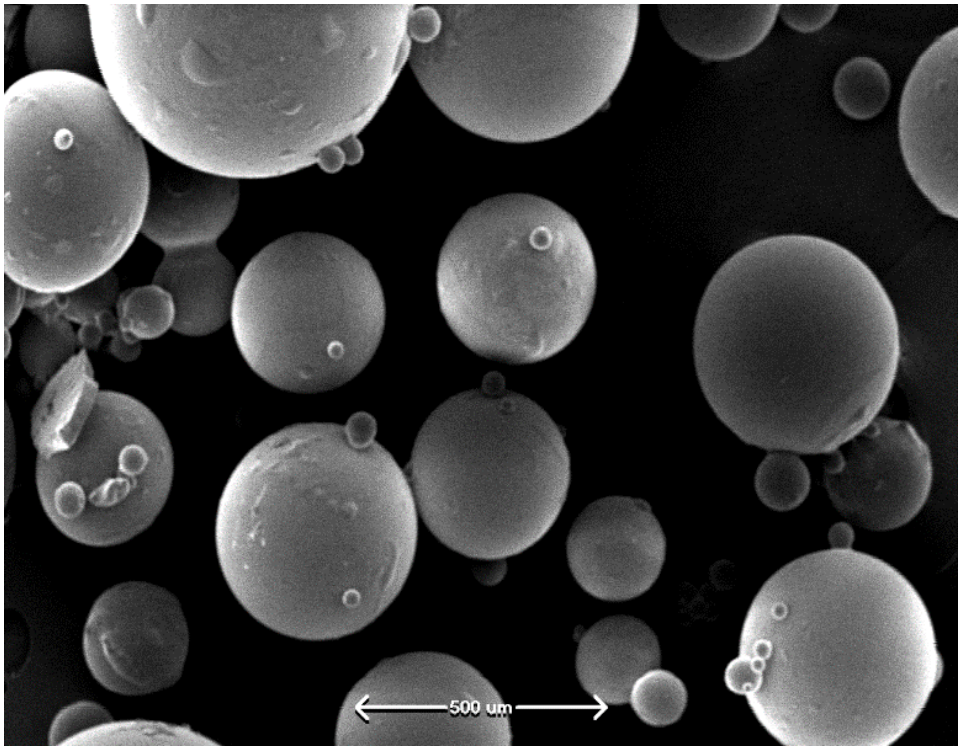

Figure A.7: SEM micrograph of ELAS 5000 microspheres

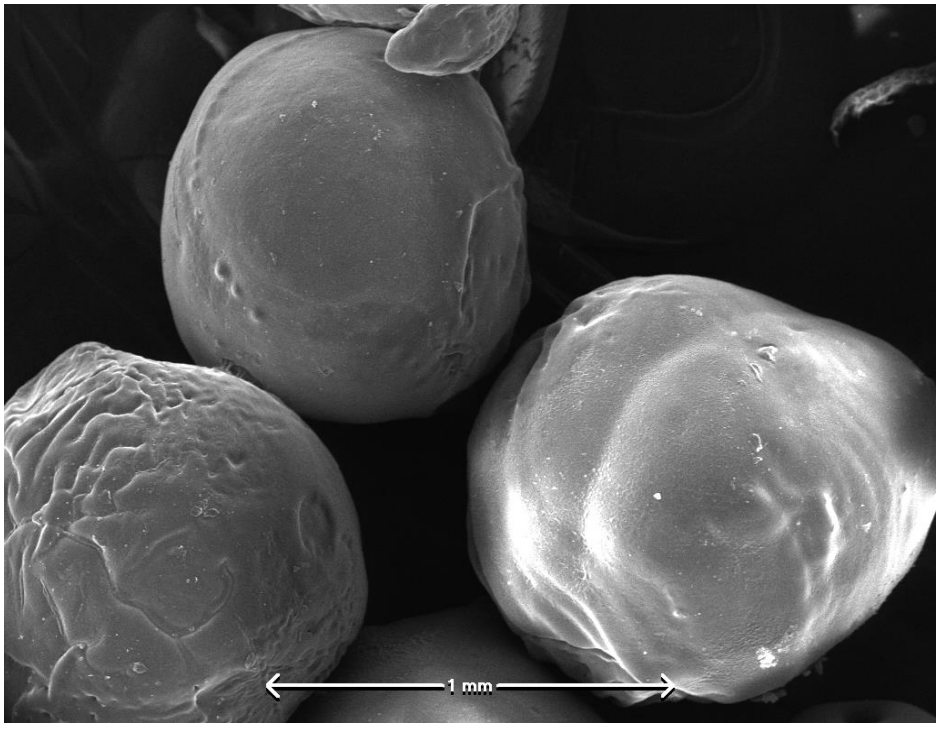

Figure A.8: SEM micrograph of 100PTMC microspheres